

LASP1, a newly identified melanocytic protein with a possible role in melanin release, but not in melanoma progression

LASP1, ein neu identifiziertes melanozytischen Protein mit einer möglichen Rolle bei der Freisetzung von Melanin, jedoch nicht in Melanomprogression



In partial fulfilment of the requirements for the degree of Doctor of Philosophy
in Biomedicine submitted to the Graduate School of Life Sciences,
Julius–Maximilians–University, Würzburg, Germany

Submitted by

ANJANA VAMAN V. S.

(From Kerala, India)

Würzburg, 2015

Submitted on :

Office stamp

Members of the Promotion committee

Chairperson : **Professor Dr. rer. nat. Thomas Müller**

Primary Supervisor : **Professor Dr. rer. nat. Elke Butt**

Second Supervisor : **Professor Dr. rer. nat. Thomas Dandekar**

Third Supervisor : **Dr. rer. nat. Erik Henke**

Date of Public Defence :

Date of Receipt of Certificates :

Affidavit

I hereby confirm that my thesis entitled "LASP1, a newly identified melanocytic protein with a possible role in melanin release, but not in melanoma progression" is the result of my own work. I did not receive any help or support from commercial consultants. All sources and / or materials applied are listed and specified in the thesis.

Furthermore, I confirm that this thesis has not yet been submitted as part of another examination process neither in identical nor in similar form.

Place, Date

Signature

TABLE OF CONTENTS

DEDICATION	i
ACKNOWLEDGEMENT	ii
ABSTRACT	iii
English	iii
German	iv
LIST OF ABBREVIATIONS	v
LIST OF FIGURES	vii
LIST OF TABLES	ix
I. CHAPTER – INTRODUCTION AND REVIEW OF LITERATURE	1
Section I – Cell physiology	2
1. Introduction	2
2. Review of literature	3
2. 1. LIM and SH3 protein 1 (LASP1)	3
2. 2. Melanocytes – the pigment producing cells	9
Section II – Cell oncology	15
1. Introduction	15
2. Review of literature	16
2. 1. LASP1 impact on human cancer	16
2. 2. Melanoma and melanocytic nevi	18
II. CHAPTER – MATERIALS AND EXPERIMENTAL PROCEDURES	22
1. List of reagents and equipments	23
2. Formulations and preparations of Reagents	33
3. Methodology	40
A. Cell culture methods	40
B. Immunohistochemistry	41
C. SDS–PAGE and Western blotting	42
D. p53 status	42
E. siRNA transfection	42
F. Cell based assays	43
G. Immunofluorescence	44
H. Determination of intracellular melanin content	45
I. Expression and purification of GST proteins	45
J. Pull-down using GST fusion proteins	46
K. Melanosome isolation by sucrose density gradient centrifugation	46
L. Preparation of nuclear and cytosolic cell fractions	47

III. CHAPTER – RESULTS	48
A. Melanocyte – specific function of LASP1	49
1. LASP1 protein expression pattern in tissue samples and in different cell lines	49
1.1. LASP1 is present in stratum basale of normal skin and is highly expressed in melanocytic nevi	49
1.2. LASP1 protein expression level in melanoma cell lines and NHEM	51
2. LASP1 knockdown influences cell migration and proliferation	54
3. LASP1 – dynamin interaction at melanocyte dendrite tips facilitate melanosome vesicle release	55
3.1 LASP1 depletion elevates intracellular melanin levels in MaMel2 cells independently of melanogenesis	55
3.2. LASP1 co-localizes with tyrosinase and dynamin at the dendrite tips of the cells	57
4. Vesicle trafficking protein dynamin – a novel binding partner of LASP1 in melanocytes	60
4.1. GST – LASP1 production	60
4.2. Pull-down assay	61
5. LASP1 and dynamin – two novel proteins associated with mature late stage melanosomes	62
5.1. Isolation and purification of melanosomal fractions by sucrose density gradient centrifugation	62
5.2. Distribution of melanosomal proteins by immunoblotting	63
5.3. LASP1 and dynamin co-localizes with tyrosinase in peripheral melanosomes	66
B. LASP1 protein impact on human melanoma cancer	69
1. LASP1 protein expression pattern in melanoma	69
1.1. LASP1 expression decreases with melanoma cancer progression	69
1.2. No correlation of LASP1 to the clinicopathological features in melanoma patients	71
2. LASP1 nuclear localization is absent in melanoma cell lines and NHEM	73
2.1. LASP1 is not localized within the nucleus in melanoma cell lines	73
2.2. LASP1 interacting partners assisting in nuclear shuttling are absent in melanocytes	74
IV. CHAPTER – DISCUSSION	75
References	85
Annexure	93
Publication and posters	94
Funding source	95
Curriculum vitae	96

DEDICATION

For my loving husband

Sooraj K. Nair

*Without whose undying support, patience and kindness
I wouldn't have been able to achieve what I have today*

ACKNOWLEDGEMENT

I would like to express my heartfelt gratitude to all of them who helped, supported and motivated me all the way for the successful completion of this doctoral dissertation.

My immense and deepest appreciation to my supervisor Prof. Dr. rer. nat. Elke Butt for all the valuable guidance, consistent encouragement, innovative and prudential suggestions during the course and also for permitting me to carry out this research in the Institute of Clinical Biochemistry and Pathobiochemistry. I am also thankful to her for helping and making me comfort in Würzburg. I would like to thank my committee members, Prof. Dr. rer. nat. Thomas Dandekar and Dr. rer. nat. Erik Henke, for conveying valuable ideas and constructive feedbacks. A big thank you to Dr. Roland Houben and Heiko Poppe for the continuous support and advices given throughout the progress of the project.

I also owe a huge thank to Mrs. Petra Thalheimer, Mrs. Petra Hönig-Lidl and Mrs. Claudia Siedel for the excellent technical assistance. No words shall suffice in thanking Mr. Prasad Prabhakaran for his dedicated support and time spend in molding my dissertation. I would like to take this opportunity to express my sincere thanks to Dr. Hariharan Subramanian for the constant and everlasting motivation and support given to me during the course of the project.

I gratefully acknowledge the funding source, Ministry of Social Justice and Empowerment, Government of India, which made my Ph.D. work possible and also would like to thank Indian embassy, Munich for all provided supports. I would like to give special appreciation to Graduate School of Life Science, University of Würzburg, Germany for the guidance's and for the offered structured doctoral training program. I have immense pleasure in expressing my deepest and jovial gratitude to the Honorable Collector Mr. K. V. Mohan Kumar I.A.S and late Mr. Pramod for the official validations.

I also express my sincere thanks to Prof. Dr. Alma Zerneck-Madsen, Head of Institute and all my colleagues for their help and encouragement and also for making my life ease in Würzburg. I am greatly indebted from my heart to my parents, in-laws, siblings and relatives for their affection, blessings and encouragement. I especially thank my friends for their helps, supports and advices. Finally, a special thanks to my beloved husband Mr. Sooraj who supported me in every possible way to see the successful completion of this work. Above all, I applaud the almighty God for giving me the strength and blessings for the successful achievement of this undertaken research task.

Anjana Vaman V S

ABSTRACT

English

LIM and SH3 protein 1 (LASP1) is a nucleocytoplasmic scaffolding protein. LASP1 interacts with various cytoskeletal proteins via its domain structure and is known to participate in physiological processes of cells. In the present study, a detailed investigation of the expression pattern of LASP1 protein in normal skin, melanocytic nevi and melanoma was carried out and the melanocyte-specific function of LASP1 was analyzed. LASP1 protein was identified in stratum basale of skin epidermis and a very high level was detected in nevi, the benign tumor of melanocyte. In the highly proliferative basal cells, an additional distinct nuclear localization of the protein was noted. In different tumor entities, an elevated LASP1 expression and nuclear localization, correlated positively with malignancy and tumor grade. However, LASP1 level was determined to be very low in melanoma and even reduced in metastases. Melanoma is distinguished as the first tumor tested to date – that displayed an absence of elevated LASP1 expression. In addition no significant relation was observed between LASP1 protein expression and clinicopathological parameters in melanoma.

The epidermal melanin unit of skin comprises of melanocytes and keratinocytes. Melanocytes are specialized cells that synthesize the photo protective coloring pigment, melanin inside unique organelles called melanosomes. The presence of LASP1 in melanocytes is reported for the first time through this study and the existence was confirmed by immunoblotting analysis in cultured normal human epidermal melanocyte (NHEM) and in melanoma cell lines, along with the immunohistostaining imaging in normal skin and in melanocytic nevi. LASP1 depletion in MaMel2 cells revealed a moderate increase in the intracellular melanin level independently of *de novo* melanogenesis, pointing to a partial hindrance in melanin release. Immunofluorescence images of NHEM and MaMel2 cells visualized co-localization of LASP1 with dynamin and tyrosinase concomitant with melanosomes at the dendrite tips of the cells. Melanosome isolation experiments by sucrose density gradient centrifugation clearly demonstrated the presence of LASP1 and the melanosome specific markers tyrosinase and TRP1 in late stage melanosomes.

The study identified LASP1 and dynamin as novel binding partners in melanocytes and provides first evidence for the existence of LASP1 and dynamin (a protein well-known for its involvement in vesicle formation and budding) in melanosomes. Co-localization of LASP1 and dynamin along the dendrites and at the tips of the melanocytes indicates a potential participation of the two proteins in the membrane vesicle fission at the plasma membrane.

In summary, a possible involvement of LASP1 in the actin–dynamin mediated membrane fission and exocytosis of melanin laden melanosome vesicles into the extracellular matrix is suggested.

German

LIM und SH3 protein 1 (LASP1) ist ein nukleozytoplasmatisches Gerüstprotein. LASP1 interagiert über seine Domänenstruktur mit verschiedenen Zytoskelettproteinen und ist an physiologischen Prozessen wie Migration und Zellproliferation beteiligt. In der vorliegenden Studie wurde eine detaillierte Untersuchung des Expressionsmusters von LASP1 in normaler Haut, Nävi und Melanom durchgeführt und die Melanozyten-spezifische Funktion des Proteins analysiert.

LASP1 konnte durch immunhistologische Färbungen im Stratum basale der Epidermis und in hoher Konzentration in Nävi (gutartige Tumore der Melanozyten) nachgewiesen werden, während die Expression in Melanom und Metastasen sehr gering ist. Auch wurde kein signifikanter Zusammenhang zwischen der LASP1 Proteinexpression in Melanomen und den klinisch-pathologischen Parametern bei 58 Patienten festgestellt. Dies steht im Gegensatz zu allen bisher getesteten Tumoren (u.a. Brust, HCC und Medulloblastom), bei denen eine erhöhte LASP1 Expression in den Tumoren beobachtet wurde, die mit dem Tumorgrad korrelierte.

Die hochproliferativen Basalzellen der Epidermis bestehen aus Keratinozyten und Melanozyten und weisen, im Gegensatz zu Nävi und Melanomzellen, eine deutliche Kernlokalisierung des LASP1 Proteins auf. Melanozyten sind spezialisierte Zellen, die das UV-Schutzfarbpigment Melanin in einzigartigen Organellen, genannt Melanosomen, synthetisieren. Die Expression von LASP1 in diesen Melanozyten konnte zum ersten Mal in dieser Studie nachgewiesen werden. Immunfluoreszenzaufnahmen und Western Blots mit kultivierten normalen menschlichen epidermalen Melanozyten (NHEM) und Melanom-Zelllinien bestätigen die LASP1 Expression. Funktionelle Experimente mit LASP1 depletierten Zellen zeigen eine erhöhte Melaninkonzentration, die unabhängig von der *de novo* Melanogenese ist. Immunfluoreszenzaufnahmen visualisieren eine Ko-Lokalisation von LASP1 mit Tyrosinase an den Melanosomen in den Zellausläufern von pigmentierten MaMel2 Zellen. Eine Auftrennung der einzelnen Melanosomenstadien durch Saccharose-Dichtegradienten-Zentrifugation erlauben die Detektion von LASP1 mit Dynamamin, TRP1 und Tyrosinase in spätem Stadium IV Melanosomen.

Die vorliegende Studie liefert den ersten Beweis für die Existenz von Dynamamin (einem für die Vesikelbildung essentiellen Protein) in Melanosomen und identifiziert Dynamamin als neuartigen Bindungspartner von LASP1 in Melanozyten. Die Ko-Lokalisierung LASP1 und Dynamamin entlang der Dendriten und in den Spitzen der Melanozyten weist auf eine mögliche Beteiligung beider Proteine an der Melanosomen-Vesikel-Abspaltung an der Plasmamembran hin.

Zusammenfassend lässt sich sagen, dass LASP1 an der Actin-Dynamamin vermittelten Exocytose von Melanin-beladenen Melanosomvesikeln in die Extrazellulärmatrix beteiligt ist.

LIST OF ABBREVIATIONS

Expansions	Abbreviations
1.4-Diazabicyclo-(2.2.2) octan	DABCO
4-(2-hydroxyethyl)-1-piperazineethanesulfonic acid	HEPES
4',6-diamidino-2-phenylindole	DAPI
Adenylyl cyclase	AC
Ammonium persulphate	APS
Binding Immunoglobulin Protein	BIP
Bovine serum albumin	BSA
Concentration	Conc
Dimethyl sulfoxide	DMSO
Enhanced chemiluminescence	ECL
Escherichia coli	<i>E.coli</i>
Ethylene diamine tetra acetic acid	EDTA
Foetal calf serum	FCS
Glutathione S-transferase	GST
Hydrochloric acid	HCl
Hydrogen peroxide	H ₂ O ₂
Immunoreactive Score	IRS
Immunofluorescence	IF
Isopropyl β-D-1-thiogalactopyranoside	IPTG
LIM and SH3 protein 1	LASP1
Lipoma Preferred Partner	LPP
Luria-Bertani	LB
Microtubules	MT
Normal human epidermal melanocyte	NHEM
Paraformaldehyde	PFA
Phosphate buffered saline	PBS
Polyacrylamide gel electrophoresis	PAGE

Protein Kinase A	PKA
Roswell Park Memorial Institute medium	RPMI
Serine-146	Ser-146
Small interfering RNA	siRNA
Sodium chloride	NaCl
Sodium dodecyl sulphate	SDS
Src homology 3	SH3
Tetra methyl ethylene diamine	TEMED
Tris (hydroxymethyl) amino methane	TRIS
Tris Buffered Saline with Tween 20	TBST
Tyrosine-171	Y-171
Ultraviolet	UV
Western blot	WB
Wild type	wt
Zona Occludens 2	ZO2

LIST OF FIGURES

Figure 1: Schematic representation of LASP1 protein domain structure	3
Figure 2: LASP1 distribution and PKA–induced trans-localization	7
Figure 3: Diagrammatic presentation of melanosome maturation	11
Figure 4: Melanosomes transport from perinuclear area to the cell periphery	12
Figure 5: Different melanosome transfer mechanisms	13
Figure 6: Depicted a typical nevus and a nevus–associated melanoma	18
Figure 7: Melanoma progression from melanocytes	19
Figure 8: Schematic representation of the protocol for differently oriented sucrose density gradients	47
Figure 9: Human skin	49
Figure 10: Consecutive sections of normal skin stained with LASP1 and MART1 antibodies	50
Figure 11: LASP1 nuclear positive basal cells in the epidermis	50
Figure 12: Depicted images of melanocytic nevi	51
Figure 13: Nuclear LASP1–positivity is absent in melanocytic nevi	51
Figure 14: LASP1 expression in melanoma cell lines and in normal human epidermal melanocyte (NHEM)	52
Figure 15: Bright field image of pigmented MaMel2 cells	52
Figure 16: Passage–dependent pigmentation difference in MaMel2 cell pellets	53
Figure 17: LASP1 depletion in melanocyte and melanoma cell	53
Figure 18: The effect of LASP1 silencing on proliferation, adhesion and migration	54
Figure 19: LASP1 depletion increases intracellular melanin in MaMel2 cells	56
Figure 20: Subcellular distribution of LASP1 and tyrosinase in different cell lines	58
Figure 21: Co-localization of LASP1 and dynamin in different cell lines	59
Figure 22: Screening of the expression level of proteins in GST overexpression experiments	60

Figure 23: Dynamin a novel binding partner of LASP1 in melanocytes	61
Figure 24: Layout of sucrose density gradient centrifugation protocol for melanosome isolation	63
Figure 25: Immunoblot analysis of sucrose density gradient purified fractions	64
Figure 26: Ultracentrifuge tube with dark melanosome in 1.8 M sucrose fraction	65
Figure 27: Co-localization of LASP1 and dynamin with peripheral melanosomes in MaMel2 cells	66
Figure 28: LASP1 co-localization with tyrosinase (melanosomes) in NHEM dendrite tips	67
Figure 29: Subcellular distribution of dynamin and tyrosinase	68
Figure 30: Immunohistochemical staining of LASP1 in normal skin, melanocytic nevi, primary and metastatic melanoma	70
Figure 31: Immunoblot analysis of nuclear and cytosolic fractions for LASP1 distribution	73
Figure 32: Western blot analysis of binding partners of LASP1 in cell lines	74
Figure 33: Schematic presentation of skin structure	76
Figure 34: LASP1 immunostaining in tissue samples	77
Figure 35: Illustrated the epidermal melanin unit of skin	79
Figure 36: Proposed model for LASP1 involved actin – dynamin mediated melanosome vesicle scission at melanocyte dendrite tips	82
Figure 37: Representation of the domain organization of dynamin	83

LIST OF TABLES

Table 1: List of cell culture reagents	23
Table 2: List of chemicals	23
Table 3: List of apparatus and instruments	26
Table 4: List of disposables	28
Table 5: List of antibodies, origin and dilutions	30
Table 6: List of siRNA	32
Table 7: Plasmid and manufacturer	32
Table 8: List of kits	32
Table 9: List of softwares, websites and databases	32
Table 10: Distribution of marker proteins by Western blotting	65
Table 11: LASP1 expression in melanocytic nevi, primary melanoma, and melanoma metastases specimens	71
Table 12: Correlation of LASP1 expression to clinicopathological characteristics in 58 melanoma patients	72

I. CHAPTER

INTRODCUTION AND REVIEW OF LITERATURE

Section I – Cell physiology

1. Introduction

Periodic exposure of human skin to ultraviolet radiation (UVR) is regarded as the main causative factor in the induction of skin cancer. The most important photo protective factor— melanin serves as a barrier against UVR induced DNA damage of skin cells and also acts as an antioxidant and has radical scavenging properties. Melanin granules are produced by specialized cells called melanocytes and are synthesized and packaged inside unique membrane bound organelles termed melanosomes.

Melanosome biogenesis occurs through four morphologically different stages and the mature melanosomes are transported towards the cell dendrite tips and eventually released into the extracellular matrix. The melanosome vesicles are then phagocytized by keratinocytes and the melanin forms a nuclear cap and protects the DNA of the cell. The progression of melanosomes through the different stages and the excision of melanin laden melanosome vesicles at the plasma membrane are regulated by interdependent interactions of molecular motor proteins, multi–protein assemblies and cytoskeletal rearrangements.

A single melanocyte is responsible to deliver melanin to a large number of keratinocytes (~40) through extensive and elaborated cytoplasmic extensions or dendrites, which spread throughout the intracellular spaces of the lower epidermis. On account of the less number of melanocytes, the transfer of melanosomes from melanocytes to keratinocytes is considered as the crucial step in the whole process.

LIM and SH3 protein 1 (LASP1) has been recently identified as a novel protein expressed in cells of the epidermal basal layer of skin. It is a cytoskeletal scaffolding protein preferentially localized at focal contacts and along the membrane edges of the cell. Moreover, studies have shown LASP1 binding to various cytoskeletal proteins and also demonstrated its participation in various secretory processes, for instance secretory HCl response in gastric parietal cells.

Although the biogenesis of melanosomes and the synthesis and release of melanin granules have been studied extensively, the mechanisms are still less characterized. The expression of LASP1 in the epidermal basal layer of skin, comprising of melanocytes and keratinocytes together with previous reports describing LASP1 protein participation in granula release prompted us to investigate the expression pattern of LASP1 in skin tissue samples as well as in cultured melanocyte specific cell lines and also to research its contribution in melanogenesis.

2. Review of literature

2. 1. LIM and SH3 protein 1 (LASP1)

(a). General description of human LASP1

LASP1 was initially identified as pp40, a phosphoprotein that migrates on SDS-PAGE gels with an apparent molecular mass of ~40 kDa (Chew and Brown 1987). Later, pp40 was isolated, partially sequenced and cloned by the same group and shown to be homologous to the predicted protein product of the human gene, metastatic auxiliary lymph nodes (MLN50). Northern blot analysis revealed an approximately 4.0 kb long mRNA of MLN50 that is ubiquitously expressed at basal levels in normal tissues. Sequence analysis showed that MLN50 encoded a putative protein with a LIM motif at its amino terminus and a Src homology 3 (SH3) domain at its C-terminal part. This domain organization defined a new LIM protein subfamily characterized by the combined presence of LIM and SH3 domains. Thereupon, MLN50 is termed accordingly: LIM and SH3 Protein 1 – in short: LASP1 (Tomasetto, Moog-Lutz et al. 1995; Schreiber, Masson et al. 1998). LASP1 gene was mapped to chromosomal region 17q11–q21.3, a region altered in 20–30% of all breast cancers suggesting that it could play a role in tumor development and metastases. A schematic representation of the domain organization of LASP1 protein is depicted in Figure 1. It encodes a protein of 261 amino acids. (Chew, Chen et al. 2002; Keicher, Gambaryan et al. 2004).

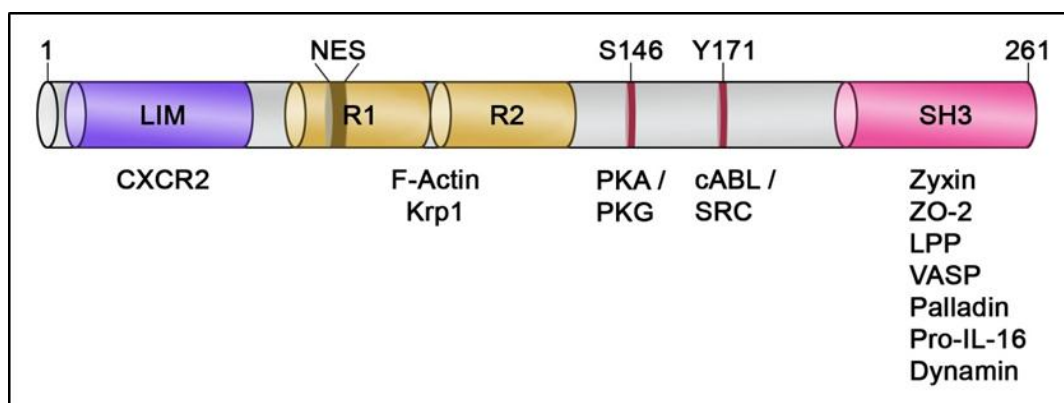


Figure 1: Schematic representation of LASP1 protein domain structure. Linear representation of the domain organization of LASP1 based on its three-dimensional structure, as revealed by crystallographic studies (numbers indicate amino acid position within the primary sequence of human LASP1). It contains an amino terminal cysteine-rich, zinc finger LIM domain and a carboxyl terminal Src homology 3 (SH3) domain. LASP1 interacts to the proline-rich motifs of other proteins through the SH3 domain. It has two short nebulin-like repeats (R1 and R2), each comprised of 35 residues that allow binding to F-Actin, a Nuclear Export Signal (NES) and two specific kinase phosphorylation sites at serine 146 (PKA and PKG) and tyrosine 171 (SRC and cABL).

LASP1 is ubiquitously expressed, albeit differentially distributed, in tissues including platelets, brain, heart, kidneys, lung, liver, endothelial cells, smooth muscle cells, and fibroblasts (Butt, Gambaryan et al. 2003). In brain, LASP1 is expressed in cortex, hippocampus and cerebellum and also densely concentrated at the postsynaptic membrane of dendritic spines (Grunewald and Butt 2008). Studies have also revealed a particularly prominent expression of this protein among various secretory tissues and in other F-Actin rich ion transporting cells e.g. gastric parietal cells, salivary duct cells, certain distal tubule and collecting duct cells in the kidney and in ductal cells of the exocrine pancreas (Chew, Chen et al. 2002).

The actin-binding protein LASP1 is predominantly found at multiple sites of cytoplasmic dynamic actin assembly such as focal contacts, lamellipodia, membrane ruffles, pseudopodia and podosomes where it interacts with a number of motility-associated proteins (Grunewald, Kammerer et al. 2007; Stolting, Wiesner et al. 2012; Mihlan, Reiss et al. 2013).

Comparing with normal tissues, tumor cells display an elevated level of LASP1 expression and also a LASP1-positive nuclei hypothesising a role of the protein in transcription or serving as a transcriptional cofactor. Recently several data's have published that substantiates LASP1 function as a signal transducer and mediates the functions of various other genes like insulin-like growth factor-I receptor (IGF-IR) in cancer progression [reviewed in (Orth, Cazes et al. 2015)].

(b). Domain structure and interacting partners of LASP1

LIM domain:

The three-dimensional structure of the domain at the N-terminal half of LASP1 is superimposable with the zinc modules of the chicken CRP and rat CRIP LIM proteins, confirming that this cysteine-rich motif present in LASP1 is literally a LIM domain (Schreiber, Masson et al. 1998). The LIM domain is comprised of two zinc-binding modules and highly conserved eight cysteine and histidine residues (C-X₂-C-X_{16/23}-H-X₂-C-X₂-C-X₂-C-X_{16/21}-C-X_{2/3}-C/D/H) and functions as a modular molecular binding interface to mediate protein-protein interactions. The chemokine receptors (CXCR) 1-4 have been demonstrated to interact with LASP1 via its LIM domain (Raman, Sai et al. 2010; He, Yin et al. 2013). The presence of LIM domains is considered as a hallmark of proteins that can associate with actin cytoskeleton and are predicted to link with the transcription machinery (Kadmas and Beckerle 2004).

SH3 domain:

LASP1 participates in protein–protein interaction by binding to the proline–rich SH3 motifs of other proteins. The SH3 domain regulates protein–protein interaction and facilitates cellular localization during signal transduction (Keicher, Gambaryan et al. 2004). Investigations have proved LASP1 specially interacts with a number of motility–associated, focal adhesion proteins including zyxin (Li, Zhuang et al. 2004), palladin (Rachlin and Otey 2006), LPP (Keicher, Gambaryan et al. 2004), pro-interleukin-16 (Pro-IL-16), vasodilator stimulated phosphoprotein (VASP) and dynamin via SH3 domain (Grunewald, Kammerer et al. 2007; Zhang, Chen et al. 2009; Tang, Kong et al. 2012; He, Yin et al. 2013) and most of them are involved in actin filament dynamics and pseudopodial elongation. Mutation analysis of LASP1 demonstrates that its SH3 domain is necessary for pseudopodial extension and invasion (Spence, McGarry et al. 2006).

Zyxin, a focal adhesion protein is a prime candidate in the list of binding partners of LASP1 (Li, Zhuang et al. 2004). It is predominantly localized at focal adhesion plaques but also has the ability to shuttle into the nucleus and is crucial for actin filament polymerization in mammalian cells (Grunewald and Butt 2008). Interaction of the C–terminal SH3 domain of LASP1 with the proline rich region of zyxin has been confirmed using the two–hybrid system (Li, Zhuang et al. 2004). Under normal conditions, zyxin is mainly associated with the plasma membrane and with focal contacts by interacting to LASP1. Silencing of LASP1 dramatically influences zyxin distribution and also demonstrated that the phosphorylation of LASP1 at Ser–146 modulates the interaction with zyxin (Mihlan, Reiss et al. 2013).

ZO2 is a multidomain scaffolding protein that interacts with several cell signalling proteins, to the actin cytoskeleton and to gap, tight and adherens junction protein (Gonzalez-Mariscal, Bautista et al. 2012). LASP1 lacks a known nuclear import signal and it was reported recently that ZO2 regulates nuclear transport of LASP1 (Mihlan, Reiss et al. 2013).

LPP, a shuttle protein and transcription factor that is ubiquitously expressed in all tissues, transduces signals from focal contacts to the nucleus, and interacts with LASP1 through proline rich motifs (Grunewald and Butt 2008; Grunewald, Pasedag et al. 2009; Zhang, Chen et al. 2009; Frietsch, Grunewald et al. 2010). Pro-IL-16 is present in the cytoplasm as well as in the nucleus of T–cells. Binding of LASP1 to Pro-IL-16 by means of SH3 domain indicates a potential role of LASP1 in modifying T–lymphocyte proliferation since it is highly expressed in T–lymphocytes as well (Grunewald and Butt

2008). LASP1 interacts with palladin via the SH3 domain and this interaction is known to mediate the binding of LASP1 to actin stress fibres. Palladin knockdown results in the loss of LASP1 at actin stress fibres and redirection of the protein to focal contacts without changing actin filaments (Rachlin and Otey 2006).

Nebulin repeats:

The N-terminal LIM domain is followed by two nebulin-like repeats called R1 and R2, each containing 35 residues that enable protein binding to F-Actin (Schreiber, Masson et al. 1998). Furthermore, the presence of nebulin-like actin binding repeats along with the co-immunoprecipitation of actin with GST-LASP1 fusion protein confirms the interaction of LASP1 with the actin cytoskeleton (Chew, Parente et al. 2000). Even though LASP1 seems to be the most distantly related nebulin family member, the protein still participates in the stabilization of cytoskeletal structures like actin filaments and focal adhesions and is also found to be essential for other cellular activities (Chew, Chen et al. 2002). LASP1 by means of nebulin repeats also binds to Krp1, a focal adhesion protein involved in pseudopodial elongation and cell migration (Spence, McGarry et al. 2006; Gray, McGarry et al. 2009).

Linker region:

The actin-binding motifs are followed by a linker-region with distinguished precise phosphorylation residues at serine/threonine and tyrosine. Various researches have demonstrated that the subcellular distribution and physiological activity of LASP1 is controlled by phosphorylation at several sites. For example, LASP1 phosphorylation in fibroblasts prevents protein localization at focal contacts and promotes its perinuclear enrichment (Keicher, Gambaryan et al. 2004).

(c). LASP1 phosphorylation

Human LASP1 is phosphorylated by cyclic adenosine monophosphate- and cyclic guanosine monophosphate- dependent protein kinase (PKA and PKG) at serine-146 (Ser-146) (Butt, Gambaryan et al. 2003). Studies in pancreas, intestine and gastric mucosa have manifested, LASP1 as a signalling molecule that gets phosphorylated upon elevation of cAMP (Chew, Chen et al. 2002). Moreover, phosphorylation of LASP1 at Ser-146 by PKA and PKG resulted in translocation of the protein from membrane to cytosol (Grunewald, Kammerer et al. 2007; Mihlan, Reiss et al. 2013). Figure 2 demonstrates the localization and shuttling of LASP1 protein after phosphorylation in cells.

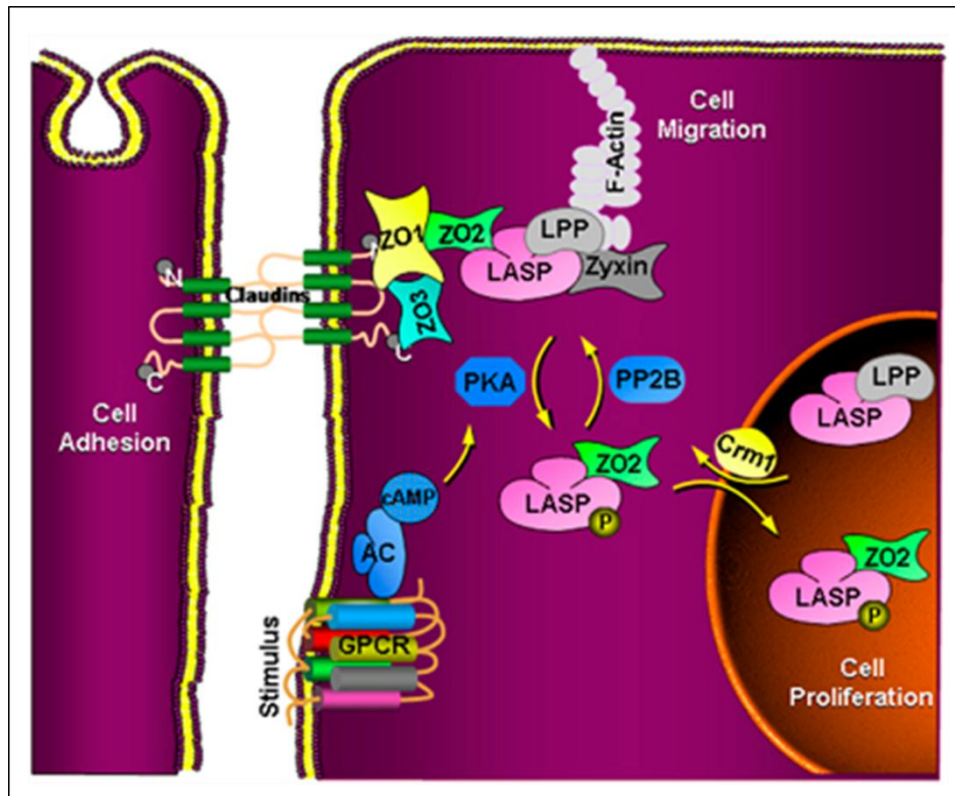


Figure 2: LASP1 distribution and PKA– induced trans-localization. Under basal conditions, LASP1 localized at the plasma membrane and focal contacts binding with F-Actin, zyxin and ZO2 and also partially shuttles between the cytoplasm and the nucleus. Upon phosphorylation at Ser-146, LASP1 forms a complex with ZO2 and translocate into the nucleus.

Source: <http://www.nature.com/onc/journal/v32/n16/full/onc2012216a.html>

Investigations in gastric parietal cells demonstrate histamine and forskolin mediated LASP1 phosphorylation by PKA and concomitant a partial redistribution of LASP1 from the cortical membrane to the intracellular canalicular region, a site of active HCl secretion, thus indicating a regulatory role of LASP1 in actin cytoskeleton plasticity and vesicle trafficking (Chew, Chen et al. 2002). Moreover, experiments have shown LASP1 associates with F-Actin in a phosphorylation–dependent manner and also binds to and co-localizes with endocytosis–associated proteins like dynamin2 (Okamoto, Li et al. 2002) to regulate HCl secretion.

In 2003, *Butt et al.* determined LASP1 as a novel substrate of PKG in human platelets. Studies with human LASP1 mutants identified Ser–146 as the specific phosphorylation site for PKA and PKG *in vivo* and also illustrated that phosphorylation of LASP1 at Ser–146 leads to a redistribution of the actin–bound protein from the tips of the cell membrane to the cytosol, accompanied with a reduced cell migration. Additionally, experiments analysing the molecular signature in neurons, suggested that after

phosphorylation, LASP1 was modified and plays a role in homocysteic acid induced neurotoxicity and also showed its involvement in neuronal differentiation and development (Grunewald and Butt 2008).

Therewithal, human LASP1 protein is phosphorylated at tyrosine-171 (Y-171) by abelson tyrosine kinase (Abl kinase) and Src kinase, two kinases strongly involved in carcinogenesis. In NIH 3T3 cells, phosphorylation of LASP1 at Y-171 is associated with loss of LASP1 protein from focal adhesion points, and initiation of cell death with no change in the dynamics of migratory processes. In platelets, LASP1 phosphorylation by Src kinase is associated with platelet activation, translocation of LASP1 to focal contacts and cytoskeleton rearrangements (Grunewald, Kammerer et al. 2007; Grunewald and Butt 2008).

Collectively, LASP1 is an extremely versatile protein because of its ubiquitous expression in normal tissues, its interaction with various binding partners and its ability to regulate cell structure, physiological processes and cells signalling.

2. 2. Melanocytes – the pigment producing cells

(a). Melanocyte origin, occurrence and function

The pigment producing melanocytes are primarily residing in the hair follicle, epidermis and eye, and are responsible for hair, skin and eye pigmentation (Goding 2007). However, the existence of melanocytes has also been confirmed in the inner ear, in the nervous system and in heart (Tachibana 1999; Brito and Kos 2008). Besides pigmentation, melanocytes are also essential for hearing. In the stria vascularis, melanocytes are required for the generation of endolymph-mediated action potentials and consequently genetic mutations that lead to loss of melanocytes in the inner ear are a major cause of deafness (Steel and Barkway 1989). There are debates that going on the chemical structure of melanin, and hence, its precise function may vary between distinct sites of melanocytes reside (Goding 2007).

During embryogenesis epidermal melanocytes derive from the neural crest and migrate towards the epidermis, where they reside in the basal layer of skin epidermis in contact with keratinocytes (Videira, Moura et al. 2013). Upon UV irradiation keratinocytes secrete α -melanocyte stimulating hormone (α -MSH) and other related proopiomelanocortin-derived peptides that bind to the melanocortin 1 receptor (MC1R) on melanocytes, which subsequently activates the cAMP-PKA pathway and the microphthalmia-associated transcription factor (MITF) – a master regulator of melanocyte function and melanogenesis, [reviewed in (Vance and Goding 2004; Garcia-Borron, Sanchez-Laorden et al. 2005)] and thereby initiate melanogenesis.

Melanogenesis involves several steps like transcription of melanogenic proteins, melanosome biogenesis, sorting of melanogenic proteins into melanosomes and melanin synthesis, transport of melanosomes to the tips of melanocyte dendrites and finally transfer into keratinocytes [reviewed in (Park, Kosmadaki et al. 2009; Sitaram and Marks 2012)]. Melanogenesis leads to the production of a high ratio of melanin and are considered as the most enigmatic pigments/biopolymers found in nature [reviewed in (d'Ischia, Wakamatsu et al. 2013; Besaratinia and Tommasi 2014)].

(b). Characteristics of melanin

Melanin is complex hetero polymers produced within specific membrane-bound organelles known as melanosomes inside melanocytes (Yamaguchi and Hearing 2006). Melanin synthesis and distribution in the epidermis comprises of several phases and is

regulated by numerous paracrine and autocrine factors in response to endogenous and exogenous stimuli, principally UV irradiation (Park, Kosmadaki et al. 2009).

In humans, melanin is subclassified into eumelanin a dark black–brown insoluble polymer and pheomelanin a light yellow–reddish sulfur containing soluble polymer (d'Ischia, Wakamatsu et al. 2013). Diversity of skin pigmentation among different ethnic groups is preserved and depends on the ratio of eumelanin to total melanin. The kind of melanin production is based on the availability of substrates and the function of melanogenesis enzymes (Cichorek, Wachulska et al. 2013). The amount of the melanin pigment varies under different pathological conditions and as well as within different species.

Investigations have reported that melanin has various features which are beneficial to the body: UV light absorption and scattering, free radical scavenging, coupled oxidation–reduction reactions and ion storage (Cichorek, Wachulska et al. 2013). Studies also have shown the role of melanin in preserving cell membrane lipids from UV–A induced peroxidation. Melanin within the melanosomes also acts as a sink for highly reactive oxygen species (ROS), efficiently filters toxic substances and protects tissues from oxidative and chemical stress (d'Ischia, Wakamatsu et al. 2013). Unfortunately, melanin intermediates as well as melanin itself can enhance UV–induced DNA damage on chronic exposures, most likely through the generation of ROS.

Since melanin has a wide variety of functions, estimation of melanin is essential to have a close look on pigment related diseases. Different methods have been used for the evaluation of melanin content of specimens from pigmented tissues or from cultured cells (Hu 2008). The most popular and relatively simple technique used for the measurement of melanin in cultured pigment cells is the spectrophotometric method. Various studies have shown the estimation of melanin by dissolving it in 1N NaOH in DMSO and incubating at 80°C (Abdel-Naser, Krasagakakis et al. 2003).

(c). Melanosome biogenesis and melanogenesis

Melanosome formation is a multiplex process and begins with trafficking of a large number of pigment cell–specific melanosomal proteins into endosomes leading to the gradual transformation into a mature pigment producing organelle. A cascade of proteins localized in melanosomes plays an active roles in the structure and function of the organelle, either as catalytic entities involved in melanin synthesis such as tyrosinase (TYR) and tyrosinase–related proteins (TRP1, TRP2) or as structural proteins important for the integrity of melanosomes like Pmel17 (GP100) (Sitaram and Marks 2012). When

the processes of melanogenesis gets disturbed, it may lead to different types of pigmentation defects, which can be congenital or acquired, permanent or temporary, systemic or skin-restricted and has a significant impact on patient's quality of life (Fistarol and Itin 2010).

Classical electron microscopy studies revealed that melanosomes mature through four morphologically distinct stages. The mechanism of melanosome biogenesis is schematically illustrated in Figure 3. Stage I melanosomes or pre-melanosomes are round, vacuolar domains harboring intraluminal vesicles and irregular arrays of amyloid fibrils composed of pigment cell-specific protein Pmel17 (gp100) (Raposo and Marks 2007; Sitaram and Marks 2012). In stage II melanosomes the fibrils are structured into organized striations and the crucial melanosome enzyme, tyrosinase is expressed. Stage III melanosomes is characterized by melanin production and deposition onto the protein fibrils, giving rise to thick striations while stage IV melanosomes are fully melanized and melanin deposits mask the internal matrix. Eventually, fully melanized melanosomes are transported to surrounding keratinocytes by elements of the cytoskeletal system [reviewed in (Park, Kosmadaki et al. 2009; Cichorek, Wachulka et al. 2013)].

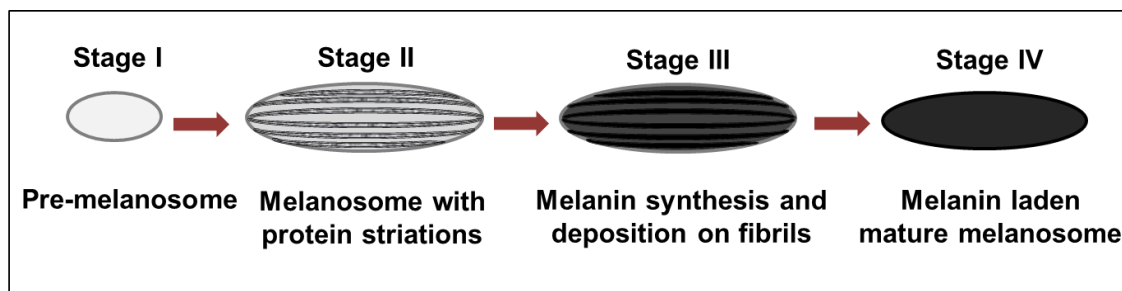


Figure 3: Diagrammatic presentation of melanosome maturation. Melanogenesis takes place inside melanosomes through four morphologically different stages. Pre-melanosome first develops as a vesicle (Stage I), followed by a fibrillar glycoprotein matrix formation and expression of tyrosinase and other enzymes of melanogenesis (Stage II). Melanosomes start producing melanin that polymerizes and settles on the internal fibrils (Stage III). In the last stage, (Stage IV) melanosomes are filled up with melanin.

Sucrose density gradient centrifugation has been known as a successful method to prepare highly purified melanin-laden melanosomes (Watabe, Kushimoto et al. 2005). Ultracentrifugation of cellular homogenates layered on top of a 1.0 – 2.0 M sucrose gradient allows separation of melanosome stages in different molar zones according to the sedimentation rate. Previous analysis showed that 1.0 and 1.2 M sucrose fractions contain the early stages while the late stages are present in the 1.6 and 1.8 M gradients

(Kushimoto, Basrur et al. 2001; Basrur, Yang et al. 2003). The purified fractions can be used for enzymatic and/or proteomic analyses or for structural characterization.

(d). Melanosome transport from cell center to periphery

Melanosomes are transferred from the site of synthesis in melanocyte perikaryon along the dendrite tips to the periphery and released into the extracellular matrix (Jordens, Westbroek et al. 2006). The transport occurs with the help of microtubules (MT) that are arranged parallel to the long axis of the dendrite and is regulated by two MT-associated motor proteins: kinesins and cytoplasmic dyneins, both forming cross-bridge structures and connecting the organelle to the microtubules. The melanosome transport machinery is depicted in Figure 4. Studies examining melanosomal transport suggest that MT-dependent movement is bidirectional: centrifugal anterograde organelle movement is mediated primarily by kinesin (Hara, Yaar et al. 2000), whereas centripetal movement is controlled by cytoplasmic dynein (Byers, Yaar et al. 2000).

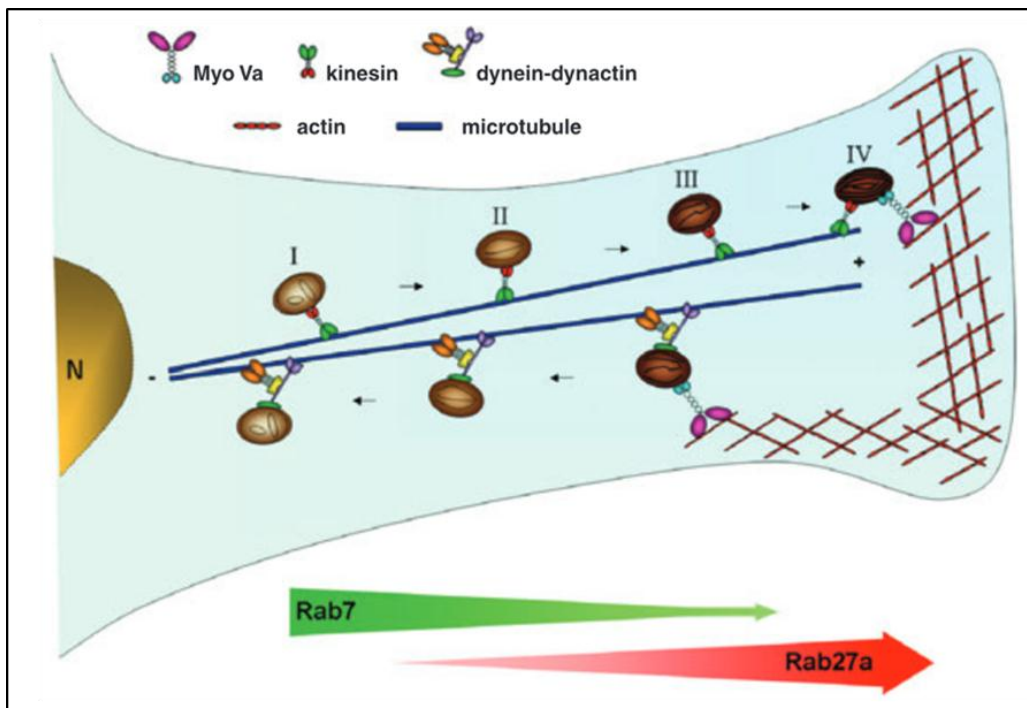


Figure 4: Melanosomes transport from perinuclear area to the cell periphery. Melanosomes are transported bi-directionally during the process of maturation. Microtubules, cortical actin network along with molecular motor proteins enables the movement of vesicle.

Source: <http://onlinelibrary.wiley.com/doi/10.1111/j.1600-0749.2006.00329.x/pdf>

It has been reported that, the small GTPase Rab27a recruits effector proteins to the melanosome membrane in conjunction with the modular adaptor protein – melanophilin and thereby regulating intracellular trafficking events. Rab27a recruits melanophilin and myosin Va, a molecular motor, to the melanosome membrane resulting in a tripartite

capture complex, which mediates the MT to actin organelle transport. Accordingly, melanosomes integrated to the dense cortical actin shell facilitated by myosin Va-dependent coupling, thus get dispersed and retained in the peripheral dendrites. Thence MT and actin track and motor systems jointly foster melanosome transport and retention in peripheral dendrites (Raposo and Marks 2007; Hume and Seabra 2011).

There are several hypotheses describing the transfer of mature melanosomes from melanocytes to neighboring keratinocytes: exocytosis, cytophagocytosis, fusion of plasma membranes and transfer by membrane vesicles (Figure 5).

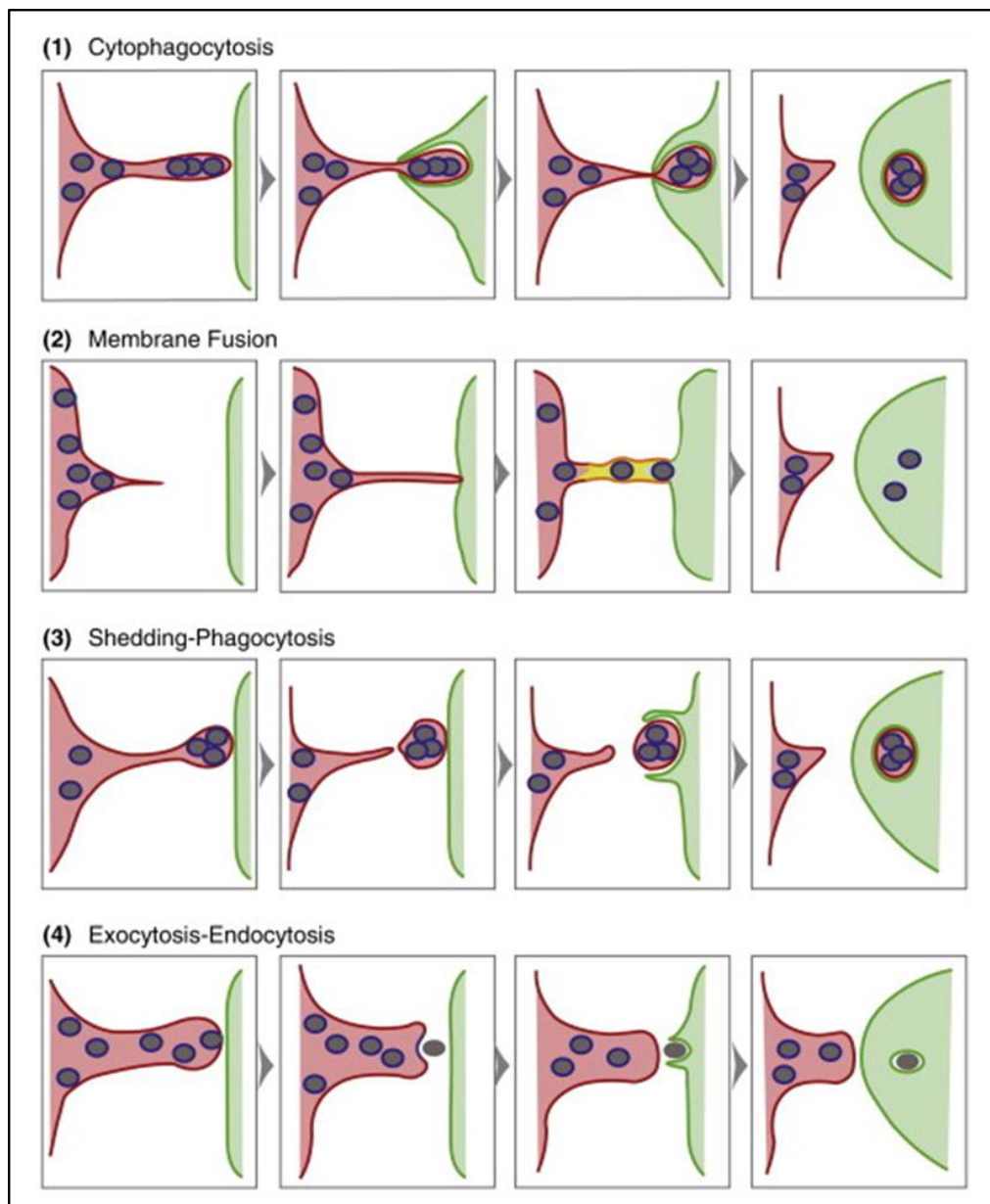


Figure 5: Different melanosome transfer mechanisms. Demonstrated four possible mechanisms of intercellular melanosome transfer to keratinocytes.

Source: <http://www.sciencedirect.com/science/article/pii/S0955067414000234>

In the cytophagocytosis model, keratinocyte phagocytizes the melanocyte's melanosome-rich dendritic tip, whereas in the membrane fusion model the melanosome moves through a transient membrane conduit connecting the cytoplasm of the melanocyte and keratinocyte. In the third model, melanosome-rich vesicles shed from the melanocyte and are subsequently internalized by the keratinocyte via phagocytosis or by membrane fusion. In the fourth mode of transfer, melanocyte releases the melanosomes melanin core into the extracellular space via exocytosis, and the keratinocyte then internalizes this 'melanocore' via phagocytosis (Van Den Bossche, Naeyaert et al. 2006; Wu and Hammer 2014). Researches have given strong evidences for three and four mechanisms.

Concluding that melanocytes are cells responsible for the synthesis of melanin inside specific organelles termed as melanosomes and the production and dispersion is essential for the photoprotection of cells.

Section II – Cell oncology

1. Introduction

Metastasis is a hallmark of malignant tumors and is responsible for as much as 90% of cancer-associated mortality, yet this process remains one of the most baffling facets of the cancer pathogenesis. It is well established that metastasis is a complex, multistep process, in which malignant cells spread from the tumor of origin to colonize distant organs. Tumor cells thus populate and flourish in new tissue habitats and, eventually, cause organ dysfunction and cell death. Prevention and management of metastases by understanding the voluminous molecular contributors and processes are entailed, and are therefore among the key goals in basic and clinical cancer research.

Cutaneous melanoma ('henceforth referred to as melanoma') is a highly malignant neoplasm originating from the pigment producing melanocytes in the basal layer of epidermis. Melanocytic nevi are benign neoplasms of melanocytic lineage and provide a roadway to melanoma. Malignant cutaneous melanoma develops through well-distinguished phases of tumor progression, including cell growth, invasion and metastasis. The worldwide incidence of melanoma has increased over the past few decades, with a growing fraction of patients possessing advanced metastatic melanoma or being at a high risk of for the disease for which prognosis remains poor despite advances in therapies. Under these circumstances, it is essential to discover new melanoma therapeutic targets, which would be an over-and-above advantage for the adjuvant treatments.

There are quite a few new molecules involved in carcinogenesis and cancer progression that have been discovered in the past few years, and one such protein is LIM and SH3 protein 1 (LASP1). Whilst LASP1 is expressed at low basal levels virtually in all normal tissues, an up-regulation of the protein has been noticed in various cancer entities studied hitherto. Besides, researches have shown the involvement of this protein in tumor cell proliferation and migration. Moreover, an elevated LASP1 level together with nuclear localization positively correlated with malignancy, higher tumor grade and metastatic lymph node status [reviewed in (Orth, Cazes et al. 2015)]. LASP1 also serves as a prognostic tumor marker.

Recently LASP1 was identified in human breast epidermal basal cells (Grunewald, Kammerer et al. 2007). Therefore, it was of great interest to investigate the influence of LASP1 in the development and progression of melanoma.

2. Review of literature

2. 1. LASP1 impact on human cancer

Decade ago, LASP1 was initially identified from a cDNA library of metastatic axillary lymph nodes (MLN) from human breast cancer (Tomasetto, Moog-Lutz et al. 1995). Since then, LASP1 was pinpointed in multiple microarray studies that peruse genes associated with tumor development and cancer progression [reviewed in (Orth, Cazes et al. 2015)]. LASP1 is upregulated in a range of cancers, including breast (Grunewald, Kammerer et al. 2006; Grunewald, Kammerer et al. 2007; Frietsch, Grunewald et al. 2010; Wang, Zheng et al. 2012), prostate (Nishikawa, Goto et al. 2014), ovarian (Grunewald, Kammerer et al. 2007), colorectal (Zhao, Wang et al. 2010; Wang, Li et al. 2013; Wang, Li et al. 2014), medulloblastoma (Traenka, Remke et al. 2010), hepatocellular carcinoma (Wang, Feng et al. 2009; Tang, Kong et al. 2012; Wang, Li et al. 2013) and oral carcinoma (Shimizu, Shiiba et al. 2013).

In the past few years various researches demonstrated the massive influence of LASP1 in tumor development such as cell proliferation and migration, exploiting different strategies including transient overexpression or knockdown of the protein. Several studies exhibited a decreased cell migration and a reduced proliferation followed by siRNA-dependent depletion of LASP1 in different cell lines – including breast, ovarian, prostate and hepatoma cancer cell lines, concomitant with cell cycle arrest in G₂/M-phase (Grunewald and Butt 2008; Frietsch, Grunewald et al. 2010). On the other hand, up-regulation of LASP1 increased the migratory activity of non-transformed PTK2 cells but had no significant effect on primary human umbilical vein endothelial cell migration (Grunewald, Kammerer et al. 2007; Zhang, Chen et al. 2009) with cell cycle arrest in G₂/M-phase (Grunewald and Butt 2008; Frietsch, Grunewald et al. 2010).

Interestingly, a prominent nuclear localization of LASP1 protein is noticed in the immunohistochemical analysis of breast cancer and medulloblastoma, which correlated significantly with tumor size, nodal positivity and a poor long-term survival of the patients (Frietsch, Grunewald et al. 2010; Traenka, Remke et al. 2010). The existence of nuclear LASP1 was detected and confirmed by confocal microscopy and Western blots of cytosolic and nuclear preparations in various breast cancer cell lines. In malignant breast cancer, the concentration of PKA is four times higher than in normal cells, therefore the up-regulation of LASP1 in breast cancer cells in combination with LASP1 hyper phosphorylation by PKA at Ser-146 and subsequent nuclear import might be crucial for its oncogenic potential (Mihlan, Reiss et al. 2013).

In several studies, an up-regulation of LASP1 has been shown to promote cell migration and proliferation. In HCC, LASP1 overexpression contributes to the aggressive phenotype of cells and is proposed as an independent novel prognostic indicator (Wang, Li et al. 2013). In colorectal cancer (CRC) tissues, LASP1 level is high and has a significant relationship with lymph node metastasis and the overall survival of the patients (Zhao, Wang et al. 2010). Moreover, LASP1 unveiled effects on metastatic dissemination and disease progression with high potential in medulloblastoma (Traenka, Remke et al. 2010) and is also reported to have an influence on cell proliferation, migration and invasion of the esophageal squamous cell carcinoma (ESCC) (He, Yin et al. 2013). *Yang et al.* validated an increased LASP1 expression in a series of 216 clear cell renal cell carcinoma (ccRCC) tissues and also stated this up-regulation is significantly associated with large tumor size and worse TNM stage (Yang, Zhou et al. 2014).

Recent research in our group identified LASP1 as a novel and overexpressed protein in chronic myeloid leukemia (CML) and as a direct substrate of the oncogenic BCR–ABL tyrosine kinase in CML. LASP1 is specifically phosphorylated by BCR–ABL at tyrosine–171. Contradictory to other tumor entities, no nuclear localization is observed in CML patients (Frietsch, Kastner et al. 2014).

2. 1. 1. LASP1 expression regulation in human cancer

To date, several studies have been carried out to investigate the regulatory mechanisms of LASP1 expression, such as the potential tumor suppressor prostate–derived ETS factor (PDEF) (Frietsch, Grunewald et al. 2010), urokinase–type plasminogen activator (uPA) (Tang, Kong et al. 2012), HBx, a protein encoded by the X gene of HBV genome (Tang, Kong et al. 2012), and HIF1 α (Zhao, Ren et al. 2015).

Furthermore, an association between elevated nuclear LASP1 levels and mutations of the p53 tumor–suppressor gene is detected in hepatocellular carcinoma. It has been shown that LASP1 was repressed by wild–type p53 at the transcriptional level and a functional negative p53 mutations led to increased LASP1 expression and to a more aggressive HCC phenotype (Wang, Feng et al. 2009; Tang, Kong et al. 2012).

MicroRNAs (miRNAs), small non-coding RNA molecules– can suppress the expression of target genes and are thought to regulate various malignancies. LASP1 expression was proven to be regulated by miR–203 (Takeshita, Mori et al. 2012; Wang, Zheng et al. 2012), miR–133a (Wang, An et al. 2013) and miR–218 (Nishikawa, Goto et al. 2014).

2. 2. Melanoma and melanocytic nevi

Melanoma arises from the malignant transformation of melanocytes, the coloring pigment producing cells and in many countries melanoma has become a serious public health problem. The key triggers leading to this malignant transformation are considered to be multi-factorial and include UV radiation damage and genetic susceptibility (Bastian 2014). Cutaneous malignant melanoma accounts for 3 to 5 percent of all skin cancers, still is responsible for approximately 75 percent of all deaths from skin cancer (Shenenberger 2012).

The steady increase in the incidence of melanoma worldwide is thought to be due to the periodic exposure of fair-skinned individuals to intense sunlight and the outspread is faster than any other type of cancer (Thompson, Scolyer et al. 2005; Tronnier and Mitteldorf 2014). Episodic exposure of skin to ultraviolet radiation can lead to malignancy through a sequence of alterations in the skin by direct mutagenic effects on DNA or indirectly by stimulating cellular constituents like promoting growth factor production or formation of reactive oxygen species of melanin that cause DNA damage and suppress apoptosis (Meyskens, Farmer et al. 2004).

(a). The progression from melanocytes to melanoma

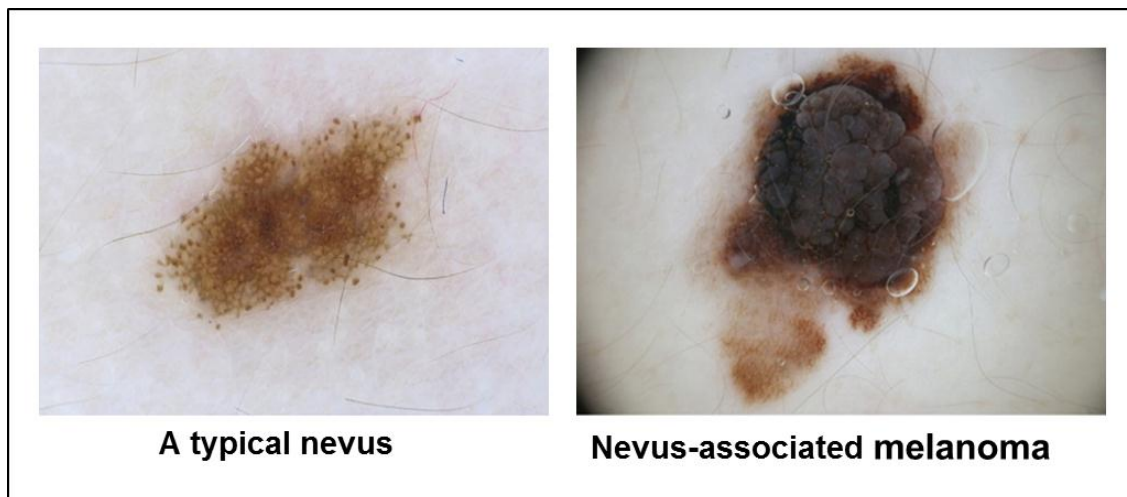


Figure 6: Depicted a typical nevus and a nevus-associated melanoma.

Source: <http://www.ncbi.nlm.nih.gov/pubmed/?term=The+Morphologic+Universe+of+Melanocytic+Nevi>

Melanoma can develop *de novo* or in a pre-existing nevus and tumor risk increases with size and cellularity of the nevus. A melanocytic nevus and a nevus derived melanoma are shown in Figure 6. Melanocytic nevi are benign neoplasms or hamartomas, composed of melanocytes that constitutively colonize in the epidermis. They categorized

namely into congenital nevi – showing up at birth or within the first few months of life – and acquired nevi – arises during an individual’s life time (Krengel, Hauschild et al. 2006; Zalaudek, Manzo et al. 2009).

Melanoma progression from normal melanocytes involves a series of steps as presented in Figure 7. About 20–30% of melanomas are thought to arise in association with a nevus precursor. In a first step, the proliferation and aggregation of melanocytes into nests occurs, leading to nevus generation. The next step comprises progression from nevus to melanoma and cells grow into the dermis with physical access to lymphatics and blood vessels. In a final step, in metastatic melanoma, tumor cells have spread from the primary site and established foci of disease at distant sites [reviewed in (Damsky, Rosenbaum et al. 2010)].

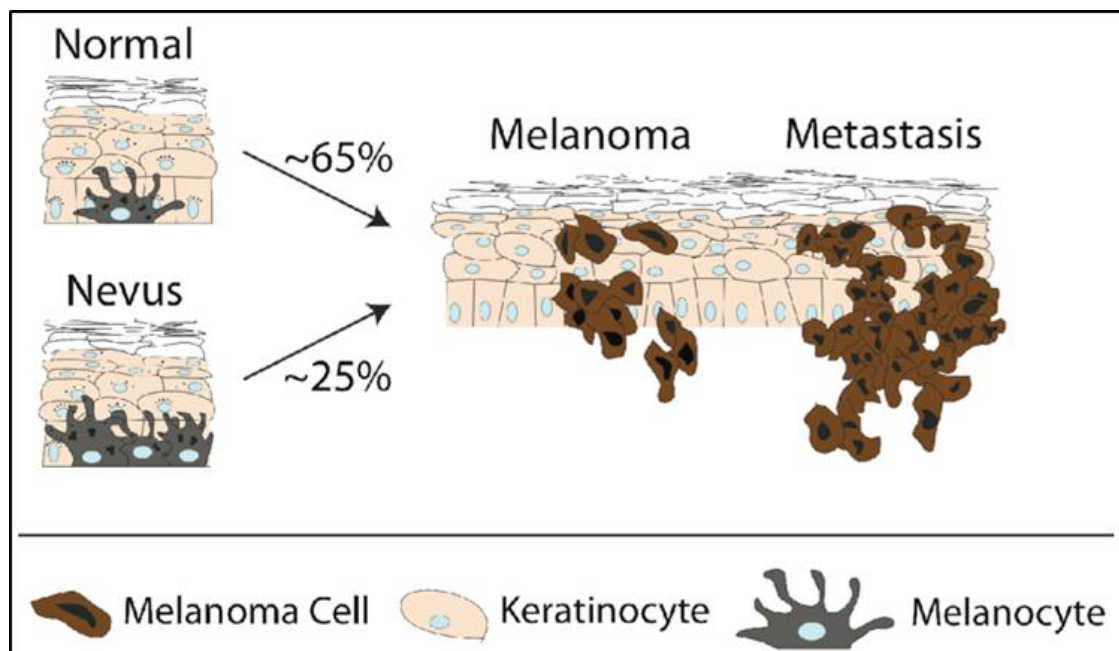


Figure 7: Melanoma progression from melanocytes. Melanoma can develop either from a pre-existing melanocytic nevus (mole) (25%) or de novo (65%).

Source: <http://www.ncbi.nlm.nih.gov/pmc/articles/PMC3756353/>

Furthermore, melanoma develops due to mutations in genes involved in the MAPK pathway, which is one of the most important pathways in melanoma tumor development. Important oncogenes in this pathway are BRAF, NRAS, HRAS, GNAQ, GNA11 and KIT and specific mutations in any of these genes lead to different subtypes of benign and malignant melanoma [reviewed in (Fecher, Amaravadi et al. 2008; Yajima, Kumasaka et al. 2012)]. p53, which is essential for the protection of DNA against damage is rarely mutated early in melanoma, could be one of several adaptations to permit survival of cells responsible for generating sun-protective pigment (Eller, Maeda et al. 1997).

Except KIT mutations, all of the above-mentioned mutations can also be found in melanocytic nevi and in common nevi. For instance, BRAF and NRAS mutations are present in 60–87.5% and 20%, respectively of all nevi (Bastian 2014; Van Engen-van Grunsven, Kusters-Vandeveldel et al. 2014). The symmetric distribution of the neoplastic cells in most nevi, the monotony of their constituent melanocytes, and the presence of identifiable mutations in bulk populations of nevus cells suggest that nevi result from the clonal expansion of a single cell (Bastian 2014). Furthermore, recent immunohistochemistry studies analyzing the BRAF status describe BRAFV600E mutations in the majority of neoplastic cells in melanocytic nevi and suggest that BRAF mutant nevi are clonal (Busam 2013; Bastian 2014; Van Engen-van Grunsven, Kusters-Vandeveldel et al. 2014).

Persons with an increased number of moles, dysplastic (also called atypical) nevi, or having a family history of the disease are at high risk (Slominski, Wortsman et al. 2001; Thompson, Scolyer et al. 2005; Shenemberger 2012). Histopathological analysis of hematoxylin and eosin-stained tissue sections and correlation with the clinical context remains the gold standard for the diagnosis of melanoma and experienced dermatopathologists can make a definitive, reliable, and reproducible distinction (Busam 2013). The American Joint Committee on Cancer (AJCC) approved a new staging system for melanoma, based on factors including tumor thickness, ulceration, mitotic rate, and sentinel lymph node status, as well as sex and age of the patients, and tumor site (Homsy, Kashani-Sabet et al. 2005).

Non-cutaneous melanocytes lining the choroidal layer of the eye, the respiratory, gastrointestinal, and genitourinary mucosal surfaces, or the meninges can occasionally also undergo malignant transformation, and develop melanoma, albeit at a low frequency (Tsao, Chin et al. 2012). However, comparative studies are suggesting a better prognosis for nevus-associated melanoma (Lin, Luo et al. 2015).

Summing up, melanoma can develop from *de novo* or in pre-existing melanocytic nevi. The prognosis of advanced melanomas is still challenging, although thin melanomas have an excellent prognosis, there is great need for the identification of additional therapeutics targets.

In view of all these facts, I endeavor to investigate the involvement of LASP1 in melanogenesis and to study how the existence of LASP1 reflects on human melanoma cancer. Immunohistochemical slides with dermal tissues, kindly provided from the Department of Dermatology, University Hospital Würzburg, Würzburg, Germany were analyzed for LASP1 expression pattern. LASP1 protein expression in cultured normal human epidermal melanocyte (NHEM) and in various melanoma cell lines were analysed by Western blotting and the subcellular localization of the proteins was examined by immunofluorescence. Knockdown as well as melanosome isolation experiments were carried out to further scrutinize the function of LASP1 in melanocytes. Additionally, cell based assays were performed to examine LASP1 involvement in cell proliferation, adhesion and migration.

In the following sections of this dissertation the experimental methods and results obtained are discussed in detail.

II. CHAPTER

MATERIALS AND EXPERIMENTAL PROCEDURES

1. List of reagents and equipments

Table 1: List of cell culture reagents

Reagents	Catalogue Number	Manufacturer
Cholera toxin	C8052	Sigma–Aldrich, St. Louis, MO, USA
DPBS	14190 – 094	Gibco® Life Technologies GmbH, Darmstadt, Germany
FCS	10270 – 109	Gibco® Life Technologies GmbH, Darmstadt, Germany
IBMX	I5879	Sigma–Aldrich, St. Louis, MO, USA
ITS	BD 354351	Sigma–Aldrich, St. Louis, MO, USA
Nutrient Mixture F–10 Ham	N6908	Sigma–Aldrich, St. Louis, MO, USA
Penicillin/streptomycin	P0781	Sigma–Aldrich, St. Louis, MO, USA
RPMI	61870 – 010	Gibco® Life Technologies GmbH, Darmstadt, Germany
TPA	P8139	Sigma–Aldrich, St. Louis, MO, USA
Trypsin–EDTA	T3924	Sigma–Aldrich, St. Louis, MO, USA

Table 2: List of chemicals

Reagents	Catalogue Number	Manufacturer
Acetic acid	33209	Sigma–Aldrich, St. Louis, MO, USA
Ampicillin	A9393	Sigma–Aldrich, St. Louis, MO, USA
APS	21, 558–9	Sigma–Aldrich, St. Louis, MO, USA
Bromophenol blue	B – 0126	Sigma–Aldrich, St. Louis, MO, USA
BSA	A2153–	Sigma–Aldrich, St. Louis, MO, USA
Collagen	C9791	Sigma–Aldrich, St. Louis, MO,

List of reagents and equipments

		USA
Complete mini protease inhibitors	11 836 153 001	Roche, Basel, Switzerland
Coomassie brilliant blue R	B7920	Sigma–Aldrich, St. Louis, MO, USA
Crystal violet	C0775	Sigma–Aldrich, St. Louis, MO, USA
DAPI	D9564	Sigma–Aldrich, St. Louis, MO, USA
DMSO	D2650	Sigma–Aldrich, St. Louis, MO, USA
Ethanol	32205	Sigma–Aldrich, St. Louis, MO, USA
Fibronectin	F4759	Sigma–Aldrich, St. Louis, MO, USA
Forskolin	1099	BIOZOL Diagnostics, Eching, Germany
Glycerol	3783.2	Carl Roth GmbH & Co. KG, Karlsruhe, Germany
Glycine	A3707	Sigma–Aldrich, St. Louis, MO, USA
Goat serum	G9023	Sigma–Aldrich, St. Louis, MO, USA
H ₂ O ₂	H1009	Sigma–Aldrich, St. Louis, MO, USA
HCl	HC309594	Merck Millipore, Darmstadt, Germany
HEPES	H – 7006	Sigma–Aldrich, St. Louis, MO, USA
IPTG	I6758	Sigma–Aldrich, St. Louis, MO, USA
Luminol sodium salt	A4685	Sigma–Aldrich, St. Louis, MO, USA
Metafectene	T020 – 1.0	Biontix Laboratories GmbH, Munich, Germany
Methanol	322.13	Merck Millipore, Darmstadt, Germany
Mowiol 4–88	0713.1	Carl Roth GmbH & Co. KG, Karlsruhe, Germany
NAOH solution	HC273287	Merck Millipore, Darmstadt,

List of reagents and equipments

		Germany
Non-fat Dry milk	170 – 6404	Bio–Rad Laboratories GmbH, Munich, Germany
Page ruler protein marker	P – 26616	Thermo Scientific, Rockford, IL, USA
p–Coumaric acid	C9008	Sigma–Aldrich, St. Louis, MO, USA
PFA	P – 6148	Sigma–Aldrich, St. Louis, MO, USA
Ponceau S	P3504	Sigma–Aldrich, St. Louis, MO, USA
Rotiphorese® GEL 30 (37.5:1) Acrylamide A. Bisacrylamide stock solution	3029.1	Carl Roth GmbH & Co. KG, Karlsruhe, Germany
SDS	L3771	Sigma–Aldrich, St. Louis, MO, USA
Sepharose beads	71024800	GE Healthcare Bio Sciences, Uppsala, Sweden
Sodium bicarbonate	S5761	Sigma–Aldrich, St. Louis, MO, USA
Sodium chloride	31434	Sigma–Aldrich, St. Louis, MO, USA
Sodium hydroxide	30620	Sigma–Aldrich, St. Louis, MO, USA
Sodium phosphate	S0751	Sigma–Aldrich, St. Louis, MO, USA
Sucrose	S0389	Sigma–Aldrich, St. Louis, MO, USA
Synthetic melanin	M8631	Sigma–Aldrich, St. Louis, MO, USA
TEMED	T9281	Sigma–Aldrich, St. Louis, MO, USA
Tris Buffer grade	A1379	AppliChem GmbH, Darmstadt, Germany
Triton X–100	X – 100	Sigma–Aldrich, St. Louis, MO, USA
Trypan blue	T8154	Sigma–Aldrich, St. Louis, MO, USA
Tween–20	P1379	Sigma–Aldrich, St. Louis, MO, USA

β-mercaptoethanol	M6250	Sigma–Aldrich, St. Louis, MO, USA
-------------------	-------	-----------------------------------

Table 3: List of apparatus and instruments

Instruments	Model Number	Manufacturer
Automatic flake ice machine	AF 100	Scotsman Ice Systems, Milan – Italy
Class II Type A2 Biosafety Cabinet	SterilGARD® e3	The Baker Company, Sanford, Maine USA
Electronic balance	1801	Sartorius AG, Göttingen, Germany
Fedegari Steam sterilizer	22657	Integra Biosciences GmbH, Fernwald, Germany
Gel dryer	583	Bio–Rad Laboratories GmbH, Munich Germany
Haemocytometer	ZK13	A. Hartenstein, Society for laboratory and medical mbH, Würzburg, Germany
Microplate reader	VMAX	Molecular Devices, Sunnyvale, USA
pH meter	PHM82	Radiometer Analytical, Lyon, France
PowerPac™ HC Power Supply	164–5052	Bio–Rad Laboratories GmbH, Munich, Germany
Scepeter™ handheld automated cell counter	PHCC00000	Millipore corporation, Billerica, MA, USA
SDS-PAGE electrophoretic apparatus	165–3189	Bio–Rad Laboratories GmbH, Munich, Germany
Sonicator	Sonifier 250–102C	Branson Ultrasonics, Danbury, CT, USA
Stirrer/hot plate	PC–420D	Corning Incorporated, NY, USA
Test tube shaker Vibro Shaker	L46 V427	A. Hartenstein, Society for laboratory and medical mbH, Würzburg, Germany
ThermoMixer® compact	5350	Eppendorf Biotech Company, Hamburg, Germany
Trans–Blot® Turbo™ Blotting	M1703910	Bio–Rad Laboratories

List of reagents and equipments

System		GmbH, Munich, Germany
UV/visible spectrophotometer	Ultra Spec 2000	Amersham Pharmacia Biotech Inc., Piscataway, USA
Vacuum Pump Systems	04943239	KNF Neuberger Inc., Trenton, USA
Vortex–Genie	K–550–GE	Bender & Hobein AG, Zurich, Switzerland
Wallac 1420 VICTOR 2™ plate reader	1420–018	Perkin Elmer, Baesweiler Germany
Water bath	GFL 1083	Gesellschaft für Labortechnik GmbH, Willich, Germany
X–OMAT X–Ray Film Processor	RT–KP–M35A	Eastman Kodak Company, Rochester, N.Y, USA
List of Incubators		
CERTOMAT® R Benchtop Shaker CERTOMAT ® H Incubation Hood	BBI–886 3024 BBI–886 3202	B. Braun Melsungen AG, Tuttlingen, Germany
CO ₂ incubator	336	Labor–Technik–Göttingen, Rosdorf, Germany
List of centrifuges		
Bench top centrifuge	Universal 320R	Hettich Lab Technology GmbH, Tuttlingen, Germany
Picofuge™	HF 120	Stratagene, United States
Refrigerated microcentrifuge	5417R	Eppendorf Biotech Company, Hamburg, Germany
Super speed centrifuge	Sorvall RC–5B	Du Pont Instruments, Newtown, CT, USA
Ultra centrifuge	L 80	Beckman coulter GmbH, Krefeld, Germany
List of Microscopes		
Fluorescent microscope	Axioskop	Zeiss, Oberkochen, Germany
Fluorescent Microscope	BZ 9000	Keyence, Osaka, Japan
Inverted microscope	Axiovert 25	Zeiss, Oberkochen, Germany

List of pipettes		
Single channel pipettes	0.0 – 2.0 µl 0.5 – 10.0 µl 2.0 – 20.0 µl 20 – 200.0 µl 1000 µl	Gilson, Inc., Middleton, Wisconsin
Multichannel pipettes Multipette® Plus	3122000051 022260201	Eppendorf Biotech Company, Hamburg, Germany
Pasteur pipettes	202303	A. Hartenstein, Society for laboratory and medical mbH, Würzburg, Germany
Serological Pipettes	5.0 ml 10.0 ml 25.0 ml	Greiner Bio–One GmbH, Frickenhausen, Germany
Accu–jet® pro pipette Controller	26330	BrandTech® Scientific, Essex, CT, USA
Pipette stand	F161401	Gilson, Inc., Middleton, Wisconsin
List of refrigerators and freezers		
4°C	Kirch GmbH, Offenberg, Germany	
–20°C	Liebherr MediLine, Newport Pagnell, MK, UK	
–80°C	–86°C ULT	Thermo Scientific Inc., Waltham, MA USA
Glass homogeniser	HOG3	A. Hartenstein, Society for laboratory and medical mbH, Würzburg, Germany

Table 4: List of disposables

Items	Item Numbers	Manufactures
Combitips advanced®	2.5 ml – 0030 089.448 5.0 ml – 0030 089.456	Eppendorf Biotech Company, Hamburg, Germany
Biosphere® Pipette Tips	0–10 µl 20–200 µl 100–1000 µl	Sarstedt AG & Co, Nümbrecht, Germany
X–50 scepter sensors (60µM)	PHCC60050	Merck Chemicals GmbH, Schwalbach am Taunus, Germany
Glass slides	Duran Group GmbH, Wertheim/Main, Germany	

List of reagents and equipments

X-ray film	47410.19236	Fujifilm corporation, Tokyo, Japan
Nitrocellulose membrane	10401 196	GE Healthcare Bio Sciences, Uppsala, Sweden
Cover slips 24mm Cell scraper Whatsmann filter paper	DKR5 C25B F859	A. Hartenstein Society for laboratory and medical mbH, Würzburg, Germany
List of cell culture plates and flasks		
Tissue culture plates Cell suspension plate White Lumitrac 200 plate Cell culture flasks	6 well – 657 160 12 well – 665 180 48 well – 677 180 96 well – 655 180 48 well – 677 102 96 well – 655086 T 25 – 690 175 T75 – 658 170 T150 – 660 160	Greiner Bio–One GmbH Frickenhausen, Germany
Transwell® Inserts	3458	Corning Incorporated, NY, USA
Cryovials	710522	Biozym Scientific GmbH, Oldendorf, Germany
List of tubes		
Microcentrifuge tubes	1.5 ml – 2.0 ml –	Eppendorf Biotech Company, Hamburg, Germany
Falcon tubes	15.0ml 50.0 ml	Greiner Bio–One GmbH, Frickenhausen, Germany
14 ml PP tubes	187 261	Greiner Bio–One GmbH, Frickenhausen, Germany
Ultra centrifuge tubes	344057	Beckman Instruments, CA, U.S.A
List of miscellaneous items		
SensiCare® Ice gloves	486802	Medline Industries, Inc., Mundelein, Illinois, USA
Terralin®	Z11091	Schülke & Mayr GmbH, Norderstedt, Germany
Microliter™ syringe	MH 03	Hamilton Bonaduz AG,

		Bonaduz, GR, Switzerland
Omnican® Insulin syringe (30G X ½")	U – 40	B. Braun Melsungen AG, Tuttlingen, Germany
Filtropur S 0.45 µm syringe filter	83.1826	Sarstedt AG & Co, Nümbrecht, Germany
Disposable syringes	2 ml – 300928 5 ml – 309050 10 ml – 309110	Becton Dickinson, New Jersey, USA
Aqua Ad Iniectionabilia	3170/1	DeltaSelect GmbH, Munich, Germany
Surgical disposable scalpel	2019–10	B. Braun Melsungen AG, Tuttlingen, Germany
Hand held counters Table stopwatch Digital timer Parafilm® M Test tube stand	KM13 KM14 KM10 PF10 GR07; GRE3; GR25	A. Hartenstein Society for laboratory and medical mbH, Würzburg, Germany
Scanner	CanoScan 5200F	Canon, Tokyo, Japan,

Table 5: List of antibodies, origin, and dilutions

List of primary antibodies				
Antibody	Type	Purpose/ Dilution	Cata. No./ Conc.	Manufacturer
Actin (I–19)	Rabbit Polyclonal	WB (1:5000)	sc–1616–R 200 µg/ml	Santa Cruz Biotechnology, Inc., Heidelberg, Germany
Dynamin (E–11)	Mouse Monoclonal	WB (1:200) IF (1:20)	sc–17807 200 µg/ml	Santa Cruz Biotechnology, Inc., Heidelberg, Germany
GAPDH (V–18)	Goat Polyclonal	WB (1:2000)	sc–20357 200 µg/ml	Santa Cruz Biotechnology, Inc., Heidelberg, Germany
Histone H2B (N–20)	Rabbit Polyclonal	WB (1:2000)	sc–8650 200 µg/ml	Santa Cruz Biotechnology, Inc., Heidelberg, Germany
Lamin A/C (N–18)	Rabbit Polyclonal	WB (1:2000)	sc–3216 200 µg/ml	Santa Cruz Biotechnology, Inc., Heidelberg, Germany
LASP1	Rabbit	WB (1:5000)	380 µg/ml	ImmunoGlobe GmbH,

List of reagents and equipments

	Polyclonal	IF (1:250)	1.6 mg/ml	Himmelstadt, Germany
PKA	Rabbit Polyclonal	WB	(Lohmann, Walter et al. 1980)	
pLASP1	Rabbit Polyclonal	WB (1:5000)	55 µg/ml	ImmunoGlobe GmbH, Himmelstadt, Germany
TRP1 (H-90)	Rabbit Polyclonal	WB (1:200)	sc-25543 200 µg/ml	Santa Cruz Biotechnology, Inc., Heidelberg, Germany
Tyrosinase (T311)	Mouse Monoclonal	WB (1:200) IF (1:20)	sc-20035 200 µg/ml	Santa Cruz Biotechnology, Inc., Heidelberg, Germany
Tyrosinase	Rabbit Polyclonal	IF (1:20)	ab58450 1 mg/ml	Abcam, Biotech company, Cambridge, United Kingdom
ZO2	Rabbit Polyclonal	WB (1:1000)	2847S 100 µl	Cell Signaling, Beverly, U.S.A
Zyxin	Mouse Monoclonal	WB (1:2000)	307 011 100 µg	Synaptic Systems, Goettingen, Germany
Rab27A	Mouse Monoclonal	WB (1:200)	MABN446 100 µg	EMD Millipore Bioscience, Billerica, MA, USA
BIP	Rabbit Polyclonal	WB (1:1000)	3183 100 µl	Cell Signaling, Beverly,U.S.A
List of secondary antibodies				
Cyanine 3 anti- rabbit		IF (1:250)	111-165-045 1.5 mg/ml	Dianova, Hamburg, Germany
Cyanine 2 anti- mouse		IF (1:250)	115-225-146 1.5 mg/ml	Dianova, Hamburg, Germany
Goat anti-mouse HRP conjugate		WB (1:5000)	170-6516 2ml	Bio-Rad Laboratories GmbH, Munich, Germany
Goat anti-rabbit HRP conjugate		WB (1:5000)	170-6515 2ml	Bio-Rad Laboratories GmbH, Munich, Germany
Donkey anti-goat HRP conjugate		WB (1:5000)	sc-2020 200 µg/0.5 ml	Santa Cruz Biotechnology, Inc., Heidelberg, Germany

Table 6: List of siRNA

siRNA	Target sequence	Manufactures
Control siRNA	5'AATTCTCCGAACGTGTCACGT-3'	Qiagen company Hilden, Germany
LASP1 siRNA	5'-AAG CAT GCT TCC ATT GCG AGA -3'	Qiagen company Hilden, Germany

Table 7: Plasmid and manufacturer

Plasmid	Catalogue No.	Manufacture
pGEX – 4T – 1	27-4580-01	GE Healthcare Bio Sciences, Uppsala, Sweden

Table 8: List of kits

Kits	Catalogue No.	Manufactures
Pierce™ BCA Protein Assay Kit	23223	Pierce Biotechnology, Rockford, IL, USA
CellTiter–Glo® Luminescent Cell Viability Assay kit	G7571	Promega Corporation, Madison, WI, USA
NE – PER Nuclear and Cytoplasmic Extraction Reagents	78833	Pierce Biotechnology, Rockford, IL, USA

Table 9: List of softwares, websites and databases

Wallac software	Wallac 1420 explorer
Elisa software	Softmax version 3.32
BZ 9000 software	BZ II viewer
Adobe photoshop	Photoshop CS2
Microsoft office	Office 2013
Graph pad	http://www.graphpad.com/
Statistical test calculator	http://www.socscistatistics.com/Default.aspx

2. Formulations and preparations of Reagents

ECL Home-made

Stock solutions

Solution A	:	100 ml 0.1 M Tris/HCl (pH 8.6) and 25 mg luminol (stored at 4°C).
Solution B	:	11 mg para-hydroxy coumarin acid in 10 ml DMSO (stored at room temperature).
Solution C	:	H ₂ O ₂ (30%) (Stored at 4°C).

Working solution – The above listed solutions were mixed in a proportion – 3 ml reagent A + 300 µl reagent B + 0.9 µl H₂O₂.

Crystal violet (1%, 50 ml)

Crystal violet	:	0.5 g
Ethyl alcohol	:	2%

Working solution – 0.5 g of crystal violet was dissolved in 50 ml of 2% ethyl alcohol. The solution was filtered using 0.45 µm filter before use.

Transfer buffer for tank blotting

Tris-glycine buffer (Towbin buffer) – (1X, 10 L)

(A) 25 mM TRIS (Base)	:	30 g
192 mM glycine	:	144 g
NaOH pellet	:	56 g
(B) 20% methanol	:	2 L

Working solution – All the above listed reagents (A) were dissolved in distilled water and pH was adjusted to 10.0. To this solution, 2 L of methanol was added and made up to 10 L. Transfer buffer was stored in cold room.

Collagen

Collagen	:	1 mg
Acetic acid	:	0.1 M

Stock Solution – 1 mg of collagen was dissolved in 1 ml of 0.1 M acetic acid, mixed 2–3 hr in magnetic stirrer and was stored at 4°C.

Working Solution (50 µg / mL) – 1 ml of stock solution was mixed with 9 ml of ice cold PBS.

Blocking medium (3%, 100 ml)

3% non-fat Dry milk : 3 g

Working solution – 3 g of milk powder was dissolved in 100 ml of 1X TBST and the solution was stored at 4°C.

Ammonium persulphate (10%, 10 ml)

APS : 1 g

Working solution – 1 g of APS was dissolved in 10 ml of distilled water and stored at 4°C.

Ampicillin (0.1%, 10 ml)

0.1% ampicillin : 1 g

50% ethyl alcohol : 10 ml

Working solution – 1 g of ampicillin was dissolved in 10 ml of 50% ethyl alcohol. The solution was stored at –20°C.

Staining and destaining solution

Coomassie brilliant Blue

Coomassie brilliant blue : 0.8 g

Isopropanol absolute : 200 ml

Acetic acid : 200 ml

Working solution – All the above listed reagents were dissolved in distilled water and made up to 2 L. The solution was filtered before use.

Destaining solution

Acetic acid : 10%

Ethyl alcohol : 10%

Working solution – The two solutions were mixed together and made up to 1 L and kept at room temperature.

IPTG (1 M)

IPTG : 238 mg

Working solution – 2.38 g of IPTG was dissolved in 10 ml of distilled water and stored at –20°C.

Sodium Dodecyl Sulphate (10%, 100 ml)

SDS : 10 g

Working solution – 10 g of SDS was dissolved in 50 ml deionized water with gentle stirring and brought to 100 ml. Stored at room temperature.

Luria Broth (LB medium) (1 L)

(A) Tryptone : 10 g

Yeast extract : 5 g

NaCl : 5 g

(B) Ampicillin

Stock solution – All the components (A) were mixed in 1 L of deionized water and sterilized by autoclaving at 15 psi, from 121–124°C for 15 min. Stored at room temperature.

Working solution – To the above solution ampicillin was added.

Ponceau S solution (0.5%, 100 ml)

Ponceau S : 0.5 g

Acetic acid : 10%

Working solution – 0.5 g of Ponceau S was dissolved in 100 ml 10% acetic acid and stored at room temperature.

Laemmli sample buffer (3X, 100 ml)

(A) Tris/HCl (pH–6.7) : 200 mM

SDS : 6 g

Glycerin : 15%

Bromophenol blue : 3 mg

(B) β -Mercaptoethanol : 10%

Stock solution – All reagents (A) were dissolved in 100 ml of distilled water and stored at room temperature.

Working solution – To 9 ml of stock solution, 1 ml of β -mercaptoethanol was added. The solutions were kept at room temperature.

Hypotonic buffer (1X, pH 8.1, 100 ml)

- | | | |
|-----------------------------|---|------------------|
| (A) HEPES | : | 10 mM |
| KCl | : | 10 mM |
| EDTA | : | 1.5 mM |
| Sucrose | : | 200 mM |
| (B) Complete Mini proteases | : | one tablet/10 ml |

Stock solution – All the above listed reagents (A) were dissolved in 70 ml of deionized water, pH was adjusted to 8.1 and the solution was made up to 100 ml. Stored at 4°C.

Working solution – To 10 ml of the solution, one tablet of complete mini proteases was added.

E.coli lysis buffer (1X, pH 8.0, 100 ml)

- | | | |
|-------------------------|---|------------------|
| (A) Tris/HCl (pH 8.0) | : | 50 mM |
| EDTA | : | 1 mM |
| NaCl | : | 100 mM |
| (B) Triton X-100 | : | 0.1% |
| Complete Mini proteases | : | one tablet/10 ml |

Stock solution – All the above listed reagents (A) were added in 70 ml of deionized water, pH was adjusted to 8.1. To this solution, 0.1% triton X-100 was added and made up to 50 ml. Stored at 4°C.

Working solution – To 10 ml of the solution, one tablet of complete mini proteases was added.

Tris-buffered Saline (10X, pH7.5, 1 L)

- | | | |
|-------------------|---|--------|
| (A) 100 mM Tris | : | 100 mM |
| 1.5 mM NaCl | : | 1.5 mM |
| (B) 0.1% Tween 20 | : | 1 ml |

Stock solution – The reagents (A) were dissolved in 500 ml of distilled water and pH was adjusted to 7.5, made up to 1 L. Stored at room temperature.

Working solution (1X TBS-T) – To 100 ml of the stock solution, 900 ml of distilled water was added.

SDS–PAGE running buffer (10X, pH 8.9, 1 L)

(A) 250 mM TRIS (Base)	:	120 g
192 mM glycine	:	576 g
1% SDS	:	40 g

Stock solution – All reagents were dissolved in distilled water and made up to 4 L. The buffer was stored at room temperature.

Working solution (1X, 1l) – To 100 ml of the stock solution, 900 ml of distilled water was added and used for PAGE.

Bovine serum albumin (1%, 50 ml)

1% BSA	:	0.5 g
PBS	:	50 ml

Working solution – 0.5 g of BSA was dissolved in 50 ml of PBS by vortexing. The solution was then filtered in 0.45 µM filter and stored at 4°C.

Sodium hydroxide (1N, 100 ml)

NaOH	:	4 g
DMSO	:	10 ml

Working solution – 4 g of NaOH pellets were dissolved in 10 ml of DMSO solution.

HEPES buffer (10 mM, 250 ml)

HEPES	:	0.59 g
-------	---	--------

Working solution – 0.59 g of HEPES was added in 100 ml of distilled water and pH was adjusted to 7.0, and then made up to 250 ml. Stored at 4°C.

Paraformaldehyde (4%)

PFA	:	4 g
PBS	:	100 ml

Working solution – 4 g of PFA was added to 100 ml of PBS, heated to 70°C and the solution was stored at –20°C.

Western blotting Gel preparation

(A) Resolving.gel

Components	15%	13%	10%	9%
Deionized H ₂ O	14.45 ml	17.50 ml	21.15 ml	11.20 ml
30 % Acrylamide Solution	20.0 ml	17.30 ml	13.30 ml	6.0 ml
Tris Buffer (3.0 M, pH 8.9)	5.0 ml	5.0 ml	5.0 ml	5.0 ml
10% SDS	0.4 ml	0.4 ml	0.4 ml	0.40 ml
10% APS	0.4 ml	0.4 ml	0.4 ml	0.40 ml
TEMED	20.0 µl	20.0 µl	20.0 µl	20.0 µl

(B) Stacking.gel

Components	Volume
Deionized H ₂ O	14.4 ml
30% Acrylamide Solution	2.8 ml
Tris Buffer (0.5M, pH 6.7)	2.6 ml
10% SDS	0.2 ml
10% APS	0.8 ml
TEMED	20 µl

List of culture vessels and amount of medium used

Culture vessels	Area	Medium used
48 well	1.0 cm ²	250 µl
12 well	3.9 cm ²	1.0 ml
6well	9.6 cm ²	2.0 ml
T25	25 cm ²	5.0 ml
T75	75 cm ²	15.0 ml
T150	150 cm ²	30.0 ml

Volume of trypsin and medium used for trypsinization

Culture vessels	Trypsin used	Medium used
6 well	200 µl	2 ml
T25	1 ml	3 ml
T75	2 ml	3 ml
T150	4 ml	6 ml

Cell freezing medium (6 ml)

Cell culture medium	:	3.4 ml
FCS	:	2.0 ml
DMSO	:	0.6 ml

Working solution – All the components were mixed in a 15 ml greiner.

Composition of Sucrose Step Gradient solutions

Step concentration (M)	Composition of step solution		
	2 M sucrose stock solution (ml)	H ₂ O (ml)	1 M HEPES (µl)
2.0	20	–	–
1.8	18	1.8	200
1.6	16	3.8	200
1.5	15	4.8	200
1.4	14	5.8	200
1.2	12	7.8	200
1.0	10	9.8	200
0.25	2.5	17.3	200

Working solution – Complete mini proteases was added to the above solutions and step gradient was prepared in ultracentrifuge tubes.

3. Methodology

A. Cell culture methods

a. Growth medium and cell culture conditions

RPMI and HAM's nutrient medium containing L-glutamine were used for cell culturing. RPMI medium was supplemented with 10% fetal calf serum (FCS) and 1% penicillin/streptomycin (100 U ml⁻¹). Nutrient mixture F-10 HAM's media was supplemented with 20% FCS, ITS premix (a mixture of recombinant human insulin, human transferrin, and sodium selenite), (3-Isobutyl-1-methylxanthine) IBMX, and cholera toxin. 12-O-tetradecanoylphorbol-13-acetate (TPA) was freshly added to the medium. The cells were grown at 37°C and 5% CO₂ incubator.

b. Cell lines

Human melanoma cell lines: LOXIMVI, M14, M19, MaMel2, MDAMB435, SkMel2, SkMel5, UACC62 and UACC257 and breast cancer cell line: MDAMB231 were grown in RPMI growth medium. Normal human epidermal melanocyte (NHEM) was cultured in HAM's F10 nutrient medium.

c. Recovery of cryopreserved cells

Cell culture flasks and tubes were prepared with the recommended volume of the appropriate complete growth medium as mentioned in the previous section. The cryovials containing cells were thawed by gentle agitation in a water bath at 37°C and decontaminated by 70% ethanol. The cells were then transferred to the tubes containing medium and centrifuged at 160 x g for removing the cryoprotectant agent, dimethyl sulfoxide (DMSO). Supernatant was discarded and the cells were re-suspended in 1 ml of culture medium. The cell suspension was then transferred into the culture vessel containing medium and mixed thoroughly by gentle rocking.

d. Monolayer sub-culturing

All the solutions (trypsin-EDTA solution, Dulbecco's Phosphate Buffered Saline (DPBS) without calcium or magnesium, and complete growth medium) were pre-warmed at 37°C in a water bath. At 70-90% confluence, cells were subcultured up to 4-6 passages. Medium from the culture flask was removed and the monolayer was rinsed once with DPBS. 200 µl-4 ml (depending on the size of the culture vessels) of the trypsin EDTA solutions was added and incubated in the CO₂ incubator for 2-5 min. The cell

dissociation was controlled under microscope. To the detached cells, 2–6 ml of culture medium was added to inactivate the trypsin and then centrifuged at $160 \times g$. Supernatant was discarded and the cells were resuspended in 1 ml of the culture medium. Depending on the cell growth, cells were diluted and transferred to flasks and mix thoroughly by gentle rocking.

e. Cryopreservation procedure

Cell freezing medium consisting of complete growth medium, 10% FCS and 5% DMSO was prepared. The cells were collected by centrifugation at $160 \times g$ and resuspended them in the freezing medium (6 ml medium/90% fully confluent cells in T75 flask). Approximately 1.8 ml of the cell suspension was added to cryovials labelled with the name of the cell line and the date. The vials were then kept at -20°C for 2–3 days and later transferred to liquid nitrogen tank.

B. Immunohistochemistry

Immunohistochemistry slides of tissue samples stained for LASP1 and MART1 were kindly provided from the Department of Dermatology, University Hospital Würzburg. The specimens include normal skin, 29 nevi, 58 malignant melanoma and 20 metastases samples with confirmed histological diagnosis. The samples were later photographed.

Evaluation of immunohistochemical LASP1 staining and LASP1 – IRS

Immunohistological samples were evaluated by two independent scientists to define the percentage of LASP1 positive cells, and to distinguish nuclear and cytosolic immunoreactivity. Scoring of cytosolic LASP1 expression was carried out in analogy to the scoring of the hormone receptor Immunoreactive Score (IRS), ranging from 0–12. The immunohistochemical staining was scored as described below: the intensity of staining was scored as 0, 1, 2 or 3 indicating absent, weak, moderate or strong expression, respectively. The percentages of positive cells were scored as 0 for 0–19%, 1 for 20–39%, 2 for 40–59%, 3 for 60–79% and 4 for 80–100%. The multiplication of these two scores was used to identify the LASP1 expression level. For statistical discrimination, samples scored with cytosolic LASP1–IRS <3 were classified as LASP1–negative and those with LASP1–IRS >2 as LASP1–positive. Nuclear LASP1 positivity was scored by determining the percentage of positive nuclei regardless of cytosolic LASP1 immunoreactivity. Samples were considered to be nuclear–positive if 10% or more cells showed nuclear LASP1 staining.

C. SDS-PAGE and Western blotting

a. SDS-PAGE

For Western blot analysis, cells were counted, washed once in 1X PBS and lysed in appropriate volume of Laemmli sample buffer. The total cellular proteins were resolved by 9–13% polyacrylamide gel. SDS-PAGE gel was prepared in a gel-molding cassette according to the quantities of reagents listed in the above section. The gel plates were then clamped to the electrophoresis chamber, filled with 1X electrode buffer and electrophoresis was done by giving a DC supply of 70 V for running through stacking gel and 120 V for resolving gel at room temperature till the dye front reached the bottom.

b. Western blotting

The resolved proteins were transferred to nitrocellulose membrane by immunoblotting. For blotting, a transfer sandwich was assembled using Scotch-brite pads, gel-blotting paper, resolved gel and nitrocellulose membrane presoaked in transfer buffer and were transferred for 1 hr at 1.8–2.2 A at 4°C. The membrane was then incubated for 2 min in Ponceau S solution for reversible detection of bands and washed in PBS. After blocking with 3% non-fat dry milk in TBST for 30 min at room temperature, membrane was incubated overnight with specific primary antibodies at 4°C. Followed by washing three times with TBST, the blots were incubated with HRP-labelled secondary antibodies for 1 hr at room temperature. After washing, the protein bands were visualized by autoradiography using enhanced chemiluminescence. β -Actin was used as a loading control.

D. p53 status

p53 status in the cell lines used for experiments was checked in the database http://p53.free.fr/Database/Cancer_cell_lines/NCI_60_cell_lines.html and some were kindly provided from the Department of Dermatology, University Hospital Würzburg.

E. siRNA transfection

Transfections were performed according to the manufacturer's protocol for suspension culture using metafectene® transfection reagent. A siRNA molecule targeting for LASP1 (5'–AAG CAT GCT TCC ATT GCG AGA –3') (bases 80–100) and a control siRNA were used for transfection. Transfection complex was prepared by incubating a mixture of 12 μ l metafectene and 1.2 μ M of siRNA for 15 min. Suspended cells at a density of 1×10^5

cells/ml were seeded and incubated directly with transfection complex. Cells were maintained at 37°C under 5 % CO₂ atmosphere for 72 hr.

F. Cell based assays

a. Proliferation assay

For proliferation assay, cells transfected with siRNA against LASP1 and control siRNA were seeded (1×10^4 cells/200 μ l) in 48 well plates and cultured for 72 hr. The cell viability was determined by the CellTiter–Glo® Luminescent Cell Viability Assay according to the manufacturer’s instructions. Briefly, a volume of 200 μ l of CellTiter–Glo® reagent was added and cells were lysed by shaking and incubating for 10 min at room temperature. Luminescence signal was measured using Wallac 1420 microplate reader at 590 nm. The assay was performed in eight replicates and was independently repeated four times. Cell proliferation is expressed as percentage of control cells.

Cell proliferation was also performed by counting the viable cells using automatic handheld cell sceptor and by counting using haemocytometer after trypan blue staining. Experiments were repeated independently four times. LASP1 depletion was confirmed by Western blotting (WB).

b. Cell adhesion assay

Cell suspension culture plates were coated with extracellular matrix protein, collagen (50 μ g/ml), incubated for 1.30 hr and blocked with 1% BSA in 1X PBS for 30 min. These plates washed in 1X PBS were then used for the assay. 72 hr after transfection, cells were counted and seeded on collagen coated plates with a density of 4×10^4 cells/well and allowed to grow at 37°C in a humidified incubator for 4–6 hr (50% adhesion for control cells). Non-adherent cells were removed by gentle washing with PBS and the wells were refilled with 100 μ l of medium. Leftover non-washed off wells containing cells were served as 100% control. Adherent cells were counted with CellTiter–Glo® Luminescent Cell Viability Assay according to the manufacturer’s instruction. In brief, 100 μ l of the reagent mixture was added and incubated for 10 min and the luminescence signal was detected using Wallac microplate reader at 590 nm. Assays were performed in six independent experiments each with five replicates. Knockdown of LASP1 was verified by WB.

c. Transwell migration assay

Cell migration was performed in a modified Boyden chamber. Prior to the experiments, lower surface of the transwell filters (8µm pore size) was coated with a chemo-attractant, fibronectin (5 µg/ml) in 1X PBS and incubated for 15 min and the inner filter chambers were coated with 100 µl 10% FCS in medium for 30 min. Cells serum-starved overnight were trypsinized, counted and re-suspended in serum-free RPMI medium containing 0.1% BSA at a density of 1.5×10^6 cells/ml. 500 µl RPMI medium containing 0.1% BSA and 10% FCS was added to the lower chamber of each transwell and 100 µl cell suspension (1.5×10^5 cells) was placed in the upper filter chambers and were allow to transmigrate through the filter for 4–6 hr (37°C; 5% CO₂). The non-migratory cells on the upper chamber were removed with a cotton swab, and the cells that migrated through the membrane were stained using 1% (w/v) crystal violet in 2% ethanol for 30 sec and then rinsed twice in distilled water. The cell-associated crystal violet stains were extracted by incubating the membrane for 20 min in 10% acetic acid and measured the absorbance at 595 nm, using microplate reader. All samples were prepared in six replicates, and the experiment was repeated at least three times. LASP1 knockdown was checked by WB.

G. Immunofluorescence

For immunofluorescence microscopy, cells were grown to 70–80% confluency on glass coverslips. Cells were fixed in 4% (w/v) paraformaldehyde in PBS (10 min), blocked using NH₄Cl (10 min) and then permeabilized with 0.1% (w/v) Triton X-100 in PBS (10 min). After each step, cells were gently washed three times using 1X PBS. Cells were then blocked for 30 min in 5% goat serum (0.1% (w/v) Triton X-100 in PBS) and incubated with primary antibodies for 1 hr. The primary antibodies used were affinity-purified rabbit polyclonal LASP1 and rabbit polyclonal tyrosinase, in combination with either mouse monoclonal dynamin or mouse monoclonal tyrosinase. Followed by washing three times in 1X PBS, cells were incubated in Cy3-labeled anti-rabbit and/or Cy2-labeled anti-mouse antibodies for another 1 hr. Antibodies dilution are mentioned in Table 5. Afterwards, coverslips were washed in 1X PBS, then in water and counterstained for nucleus with DAPI. Coverslips were mounted with a drop of mowiol on glass slides labeled for staining and cell lines. The glass slides with mounted samples were kept at 4°C for further examination.

H. Determination of intracellular melanin content

For intracellular melanin estimation, cells were transfected (control and LASP1) with siRNA and seeded at a density of 1×10^5 cells/ml. 72 hr post transfection, cells were harvested, washed once in PBS and lysed in 1N NaOH in 10% DMSO. Cellular melanin was dissolved by incubating the homogenate at 80°C for 2 hr and then centrifuged for 5 min at $500 \times g$. Absorbance of the supernatant was measured at 405 nm using microplate reader. Synthetic melanin diluted in 1N NaOH was used as standard, ranging from 0–80 µg/ml. Three determinations were performed in duplicates and the cellular melanin content is expressed as percentage.

I. Expression and purification of GST proteins

a. Overexpression of proteins in *E.coli* cells

Inoculated a small portion of *E.coli* strain transformed with pGEX–LASP1 recombinant plasmid and pGEX control plasmid in 2 ml Luria–Bertani (LB) medium (with ampicillin). The inoculum was grown overnight at 37°C with vigorous shaking and thereafter the cultures were diluted to 1:100 in LB medium and incubated at 37°C. The optical density at 600 nm was checked periodically, setting LB medium as blank until the culture reading reached 0.7. Subsequent stimulation with IPTG, the cultures were incubated for another 3 hr at 37°C and bacterial cells were harvested by centrifugation at $3000 \times g$ at 4°C for 10 min. The cell pellets frozen at –20°C overnight were re-suspended in ice cold *E.coli* lysis buffer (containing complete mini proteases) and incubated for 10 min on ice. Then sonicated at 60% amplitude for 30 sec with an interval of 1 min and allow the solution to cool on ice for 5 min. Sonicates were later centrifuged at $20,000 \times g$ at 4°C for 15 min, and the supernatants (soluble fraction) were carefully transferred to a clean, pre–chilled tube.

b. Purification of GST proteins using Sepharose 4B beads

High affinity glutathione sepharose 4B beads were used for purification of the GST–LASP1 fusion protein and the GST protein. The bottle containing beads were mixed by gentle shaking until all the resin was completely in suspension. 20 µl of the beads in suspension (50% slurry) was transferred to a new microcentrifuge tube and washed three times in ice cold 1X PBS by centrifugation at $500 \times g$ for 30 sec. The supernatant containing either the GST–control or LASP1 fusion protein were then mixed to the beads and incubated for 1 hr at 4°C. The mixture was centrifuged at $500 \times g$ for 30 sec and

beads were re-suspended in 500 μ l of 1X PBS and stored at 4°C. From every sample a small fraction was stopped in Laemmli lysis buffer for SDS-PAGE.

c. Analysis of GST-fusion proteins

10 μ l aliquots of each sample were resolved in 9% SDS-PAGE and gels were stained with Coomassie brilliant blue at room temperature. After 1 hr, gels were incubated in destaining solution for the visualization of the band and were dried later. BSA (0.1–1.0 mg) was used as standard for checking the concentration of the bound protein.

J. Pull-down using GST fusion proteins

MaMe12 cells were harvested, counted and 1×10^6 cells were re-suspended in 500 μ l of 1X hypotonic buffer (complete mini proteases). Followed by incubation on ice for 30 min, cell disruption was done by freeze and thaw in liquid nitrogen and subsequent mechanic lysis with a 29 1/2 gauge needle. The resultant homogenate was centrifuged at $20,000 \times g$ for 15 min at 4°C and the supernatant was incubated with 50 μ l of GST-control and GST-LASP1 beads at 4°C on a rotary mixer. After 2 hr, the samples were centrifuged and beads were washed once in ice-cold lysis buffer and twice in 1X PBS. The samples were analyzed by WB for bound proteins.

K. Melanosome isolation by sucrose density gradient centrifugation

Melanosomes were purified by sucrose density gradient ultracentrifugation. Briefly, cells were harvested and washed once in 0.25 M sucrose solution by centrifugation at $160 \times g$ for 5 min at 4°C. Cells were then homogenized on ice using 20 strokes of a Dounce glass: glass homogenizer and centrifuged at $1000 \times g$ for 10 min at 4°C. The cellular supernatant containing melanosomes was layered on a discontinuous gradient of 1.0–2.0 M sucrose solution in 10mM HEPES, pH 7.0 (1.0, 1.2, 1.4, 1.5, 1.6, 1.8, and 2.0 M) and centrifuged at $100,000 \times g$ in a Beckman SW28 swinging-bucket rotor for 1 hr at 4°C. The gradients were performed in two different orientations as illustrated in Figure 8. But the reverse sucrose gradient did not work well. Melanosomes that localized at various layers of the gradient were carefully collected and analysed by immunoblotting using antibodies indicated in figure legends in the result section.

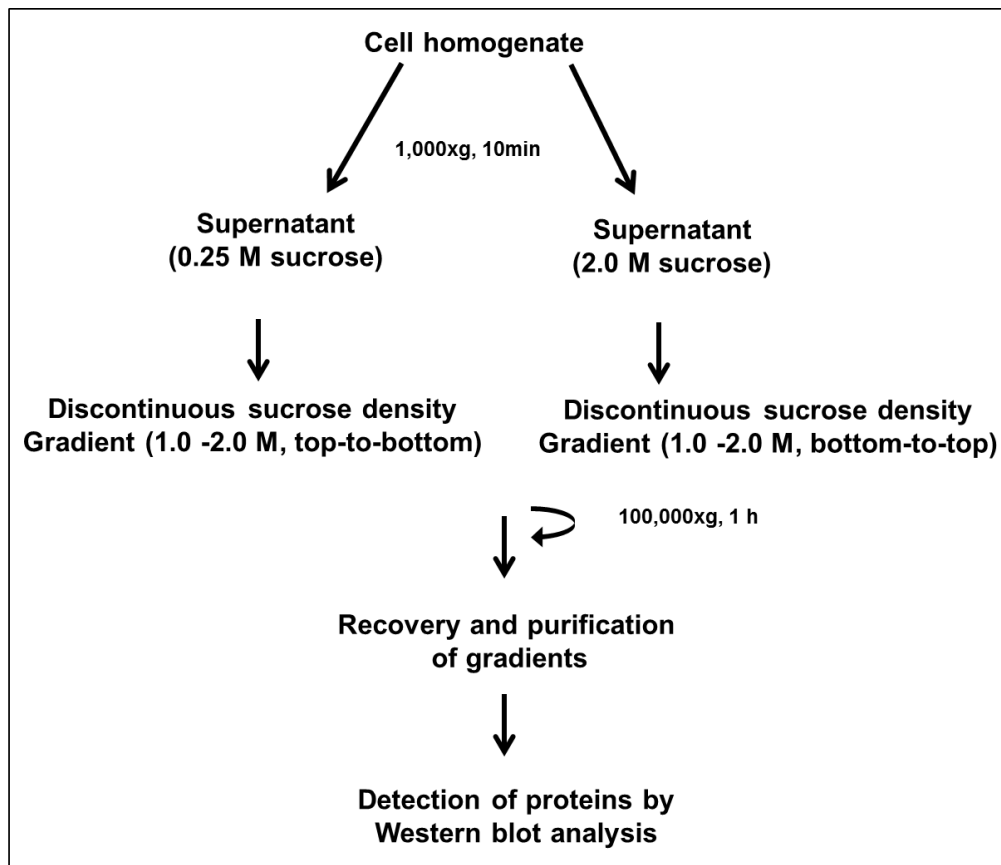


Figure 8: Schematic representation of the protocol for differently oriented sucrose density gradients.

L. Preparation of nuclear and cytosolic cell fractions

Cell lysis and centrifugal isolation of nuclear and cytoplasmic protein fractions was carried out using NE PER nuclear and cytoplasmic extraction reagents following the manufacturer's instructions. Briefly, cells were starved overnight and treated with forskolin (5 $\mu\text{M}/\text{ml}$) for 20 min for phosphorylation. Forskolin-treated, as well as untreated cells, were harvested, washed once in PBS and nuclei and cytosol was isolated using NE-PER kit. The protein concentration of the samples was estimated using BCA reagent and equal protein amount of the fractions was loaded and analysed by WB. The purity of the isolated fractions was controlled by GAPDH, lamin A/C or histone H2B.

III. CHAPTER – RESULTS

A. Melanocyte – specific function of LASP1

1. LASP1 protein expression pattern in tissue samples and in different cell lines

The tissue samples were examined by immunohistochemistry with antibodies against LASP1 and MART1 in consecutive sections. Cultured normal human epidermal melanocytes (NHEMs) and nine melanoma cell lines were analyzed by Western blotting.

1.1. LASP1 is present in stratum basale of normal skin and is highly expressed in melanocytic nevi

Skin is composed of different layers – epidermis, dermis and hypodermis. The different epidermal layers of skin are presented in Figure 9 A. The epidermis is relatively thin and the tough outer layer of skin and stratum basale is the deepest of the five epidermal layers. A representative human normal skin section immunostained for LASP1 is shown in Figure 9 B. LASP1 exhibits a distinct expression in the stratum basale (basal layer) of the epidermis of skin.

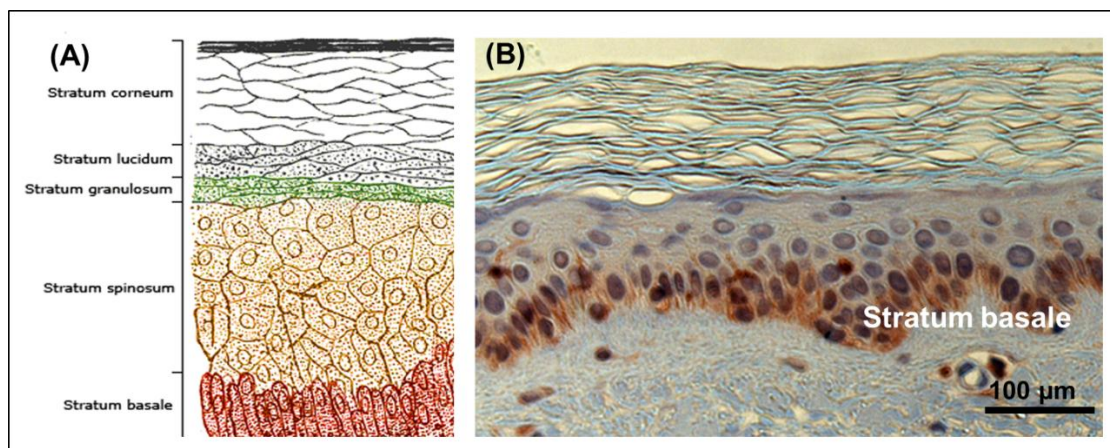


Figure 9: Human skin. (A) Diagrammatic presentation of the different layers of epidermis. **Source:** http://en.wikipedia.org/wiki/Stratum_basale#/media/File:Skinlayers.png (B) Paraffin embedded section of normal skin immunostained for LASP1. LASP1 positively stains the stratum basale of epidermis. (Magnification 20X)

The epidermal basal layer of skin consists of melanocytes, the pigment producing cells, and basal keratinocytes. Representative specimens of two consecutive sections of normal skin, immunostained for LASP1 and MART1 (a protein antigen present in the surface of melanocytes) (Sheffield, Yee et al. 2002; Prieto and Shea 2011) are depicted in Figure 10. LASP1 immunostaining is detected in both, basal melanocytes and keratinocytes (Figure 10 A). The intermittent staining of MART1 in the basal layer represents melanocytes (Figure 10 B). In the dermis, histiocytes (yellow arrow) and

blood vessels with vascular smooth muscle cells (red arrow) also exhibit LASP1–positivity (Figure 10 A).

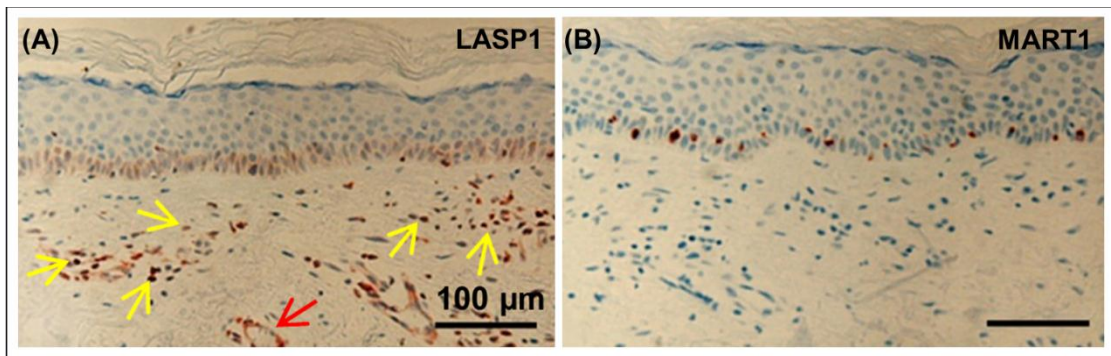


Figure 10: Consecutive sections of normal skin stained with LASP1 and MART1 antibodies. (A) LASP1 stained the basal cells in the epidermis of skin. Epidermal basal cells show distinct LASP1–positivity. In the dermis, histiocytes (yellow arrow) and cut blood vessels (red arrow) exhibit LASP1 expression. **(B)** Interspersed melanocyte cells in the consecutive section stained with MART1 antibodies. Sections were counter stained with hematoxylin and eosin. (Magnification 20X; Scale bar = 100 µm)

The cells in stratum basale divide, differentiate and migrate towards the surface (stratum spinosum) and in these cells a positive LASP1 nuclear staining is also observed (Figure 11). But the cells in the layer spinosum and granulosum are lacking LASP1 staining (Figure 11).

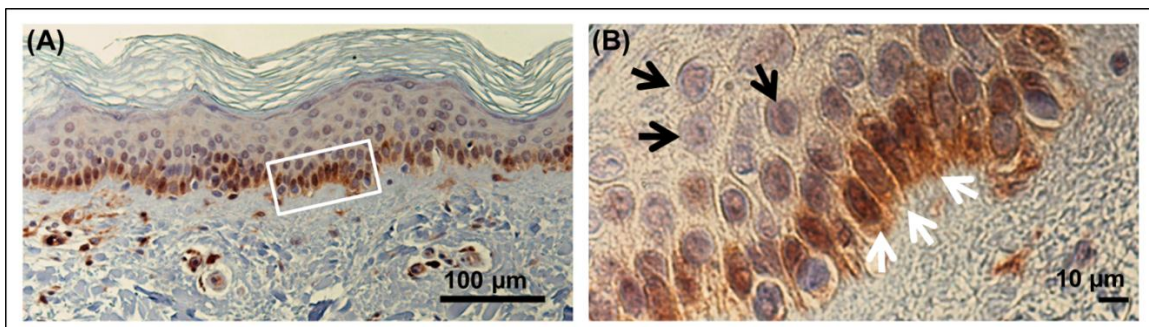


Figure 11: LASP1 nuclear positive basal cells in the epidermis. (A) Magnification 20 X; Scale bar = 100 µm **(B)** the marked section in 100 X magnification; Scale bar = 10 µm. (LASP1–positive nuclei: white arrowheads, LASP1–negative nuclei: black arrowheads). Nuclear localization of LASP1 is present in stratum basale and is absent in the upper layers (stratum spinosum and stratum granulosum).

Melanocytic nevi – the benign tumor of melanocytes are important markers for the risk of melanoma development. The analyzed samples of melanocytic nevi exhibited a very high expression of LASP1 in MART1–positive melanocytes. The consecutive sections of nevi samples stained with LASP1 and MART1 antibodies are depicted in Figure 12. In

contrast to melanocytes in the basal layer, melanocytic nevi samples are devoid for nuclear LASP1 (Figure 13).

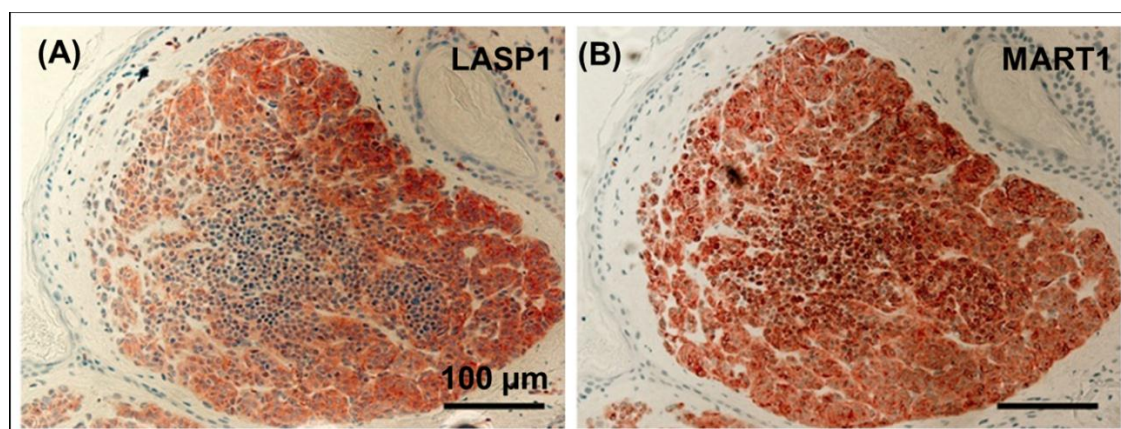


Figure 12: Depicted images of melanocytic nevi. Paraffin-embedded consecutive sections of nevi were subjected to immunohistochemistry with specific antibodies. **(A)** LASP1 immunostaining. **(B)** MART1 staining. LASP1 shows an extremely intense staining in melanocyte-positive nevus cells (Magnification 20 X; Scale bar = 100 µm).

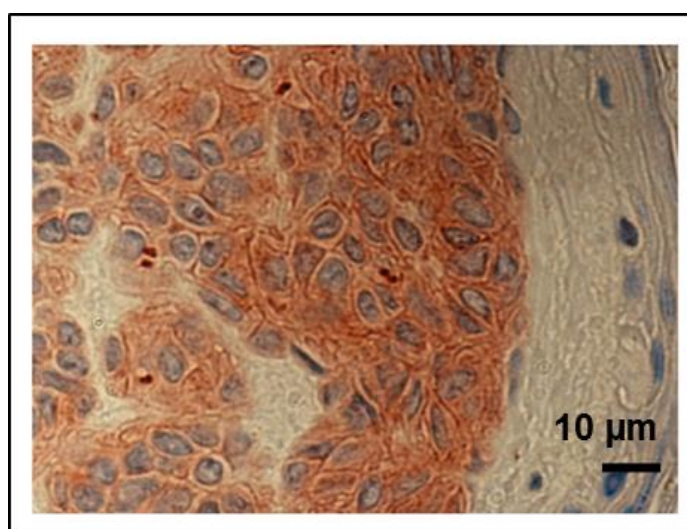


Figure 13: Nuclear LASP1-positivity is absent in melanocytic nevi. (Magnification 100 X; Scale bar = 10 µm)

1.2. LASP1 protein expression level in melanoma cell lines and NHEM

To estimate the LASP1 protein expression level, Western blotting was done in nine melanoma cell lines and in a normal human epidermal melanocytes (NHEMs) cell line. All cell lysates were immunoblotted against LASP1 and β -Actin, which serves as a loading control. Figure 14 illustrates the graphical representation of the LASP1 to actin ratio in different analyzed cell lines and the respective Western blots. All tested melanoma cell lines and the NHEMs express a distinct LASP1 level.

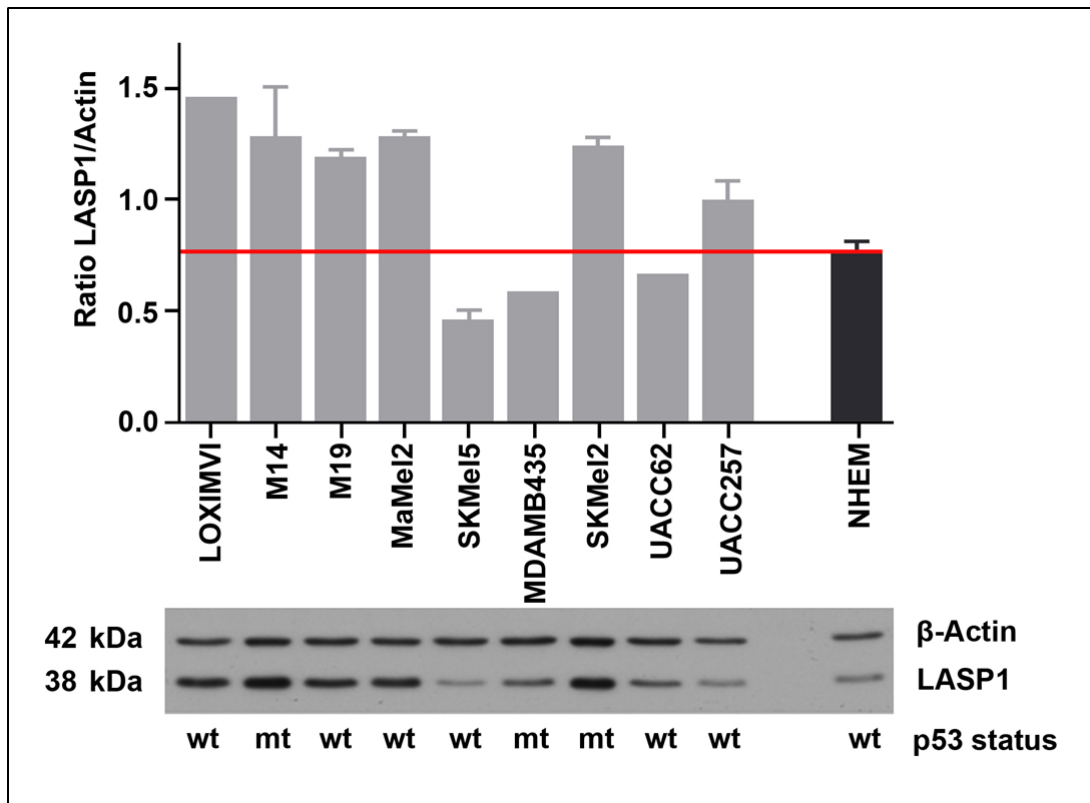


Figure 14: LASP1 expression in melanoma cell lines and in normal human epidermal melanocyte (NHEM). Graphical presentation of LASP1 to β -Actin ratio in nine melanoma cell lines and in NHEMs is shown. Representative immunoblots for LASP1 protein in each cell lines is depicted below the graph. β -Actin served as loading control. The status of tumor suppressor, p53 oncogene is also noted.

In the former studies it has been shown that the tumor suppressor p53 regulates the expression of LASP1 protein (Wang, Feng et al. 2009). Therefore validated p53 status in all these cell lines and are presented in Figure 14. However, no functional repression of LASP1 by wild type (wt) p53 is noticed.

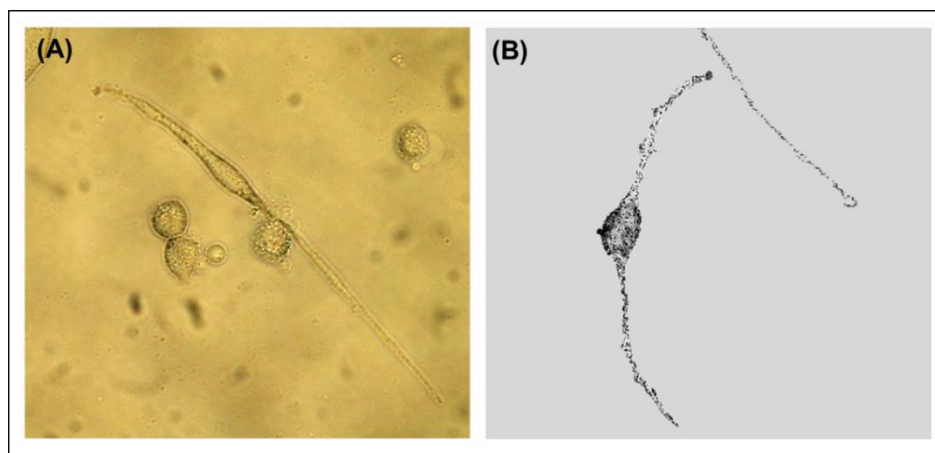


Figure 15: Bright field image of pigmented MaMel2 cells. (A) MaMel2 cell under culture condition (Magnification 32X). (B) MaMel2 cell fixed in paraformaldehyde (Magnification 60X).

For further experiments, MaMel2, a melanotic cell line derived from a subcutaneous melanoma metastasis with high LASP1 protein levels and UACC257, a slightly melanotic primary melanoma cell line, along with NHEM cells, were considered. The bright field image of a MaMel2 cell under cell culture conditions as well as a formaldehyde fixed cell are illustrated in Figure 15. The visible tiny black spots are melanosomes. The level of pigmentation in MaMel2 cells was observed to increase with cell culture passages. Pigmentation difference in MaMel2 cells in passage 1 and passage 4 is shown in Figure 16.

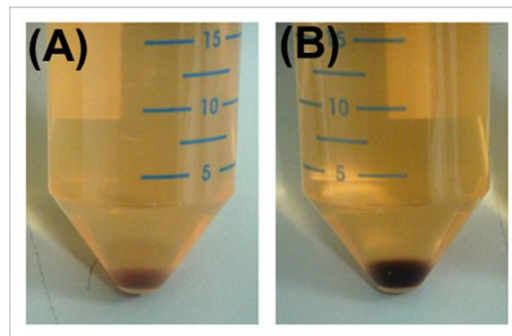


Figure 16: Passage-dependent pigmentation difference in MaMel2 cell pellets. (A) Passage 1 and (B) Passage 4 is presented. Pigmentation level in cells increases with cell culture passages.

Transfection was performed in normal human epidermal melanocytes (NHEMs) using metafectene reagent, but as shown in Figure 17 A, LASP1 depletion was not successful in NHEM cells. Knockdown experiments in melanoma cell lines were found to be perfect with cells in passage 2 to 6 (Figure 17 B). Taken together these two facts (pigmentation and LASP1 silencing) all experiments were done with cells from passage 2 to 6.

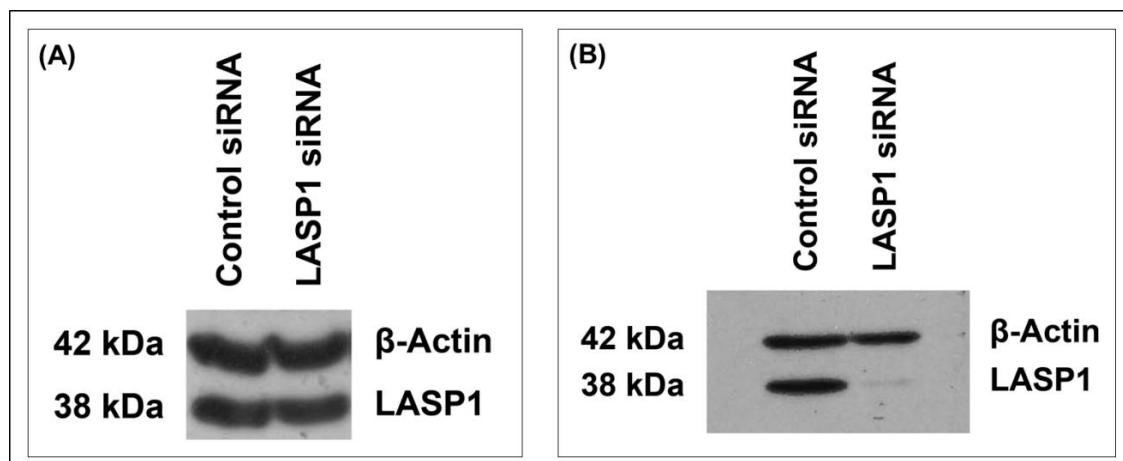


Figure 17: LASP1 depletion in melanocyte and melanoma cell. (A) Representative Western blot of LASP1 knockdown in NHEMs. Transfection of LASP1 siRNA using metafectene transfection reagent did not work in NHEMs. (B) A maximum silencing was observed in MaMel2 cells using metafectene after 72 hr of transfection. β -Actin serves as loading control.

2. LASP1 knockdown influences cell migration and proliferation

Previous studies have demonstrated that LASP1 plays an important role in cell viability, motility and tumor dissemination (Raman, Sai et al. 2010; Traenka, Remke et al. 2010; Tang, Kong et al. 2012; Zhao, Ren et al. 2015), and also nuclear localization positively correlated with aggressive, proliferative cell growth and a transcriptional function or role in cell cycle control is discussed. Since a distinct LASP1 expression and a positive LASP1–nuclear immunostaining noticed in the basal cells of the epidermis, this study focused on the functional role of LASP1 in melanocytes.

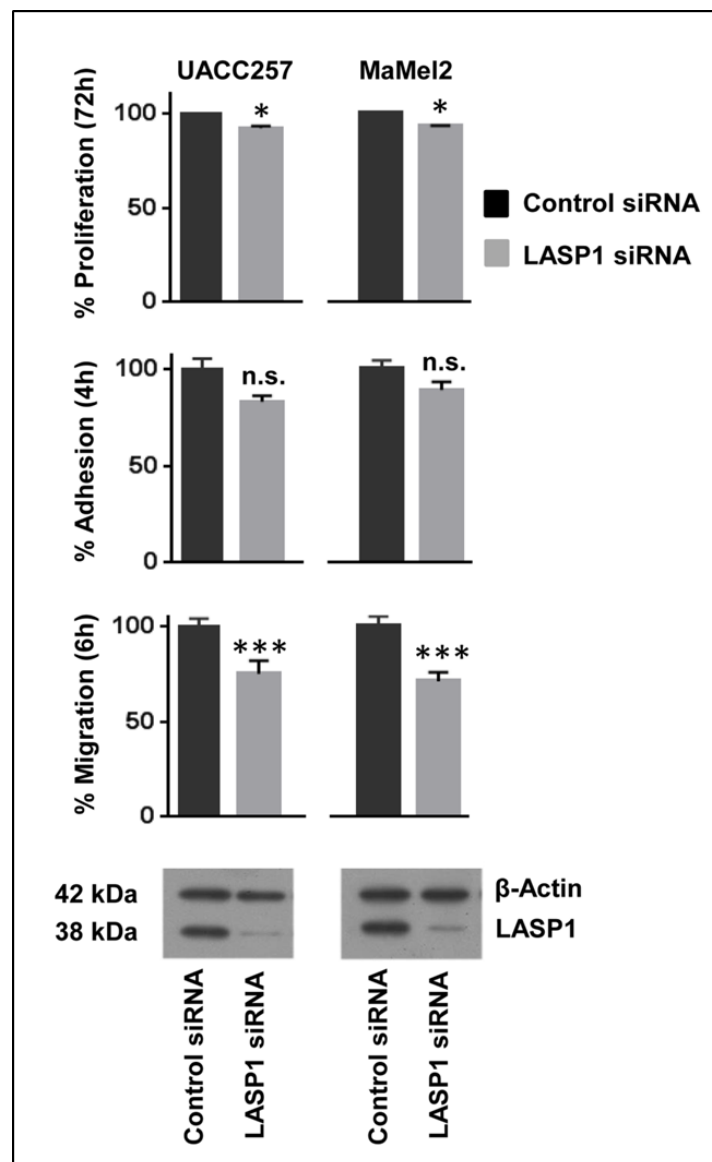


Figure 18: The effect of LASP1 silencing on proliferation, adhesion and migration. Melanoma cell lines– UACC257 and MaMel2 were transfected with siRNA against LASP1 and control siRNA and were cultured for 72 hr. Post transfection cells were harvested and assayed (protocol explained in the methods section) and the measured absorbances are presented in percentages. LASP1 depletion was confirmed by Western blot.

Therefore, in order to study LASP1 role on proliferation, adhesion and migration, melanoma cell lines – UACC257 and MaMel2 were transiently transfected with siRNA against LASP1 or control. As shown in Figure 18, an effectual reduction in the LASP1 protein level (~75%) was observed after 72 hr. The effect of LASP1 silencing on these two cell lines, examined by using a modified Boyden–chamber for migration, a fibronectin adhesion assay and the MTT viability test are furnished in Figure 18. A distinct reduction of the migratory potential (~25%, $p \leq 0.005$) in combination with a weak but significant inhibition of proliferation (~10%, $p \leq 0.001$) was observed upon LASP1 silencing (Figure 18). Although not significant, a modest decrease in adhesion (~15%; $p > 0.05$) was detected. Unlike to the studies with other cancer cells, the observed influence of LASP1 on cell division and movement in melanoma cell lines is low.

3. LASP1 – dynamin interaction at melanocyte dendrite tips facilitate melanosome vesicle release

In consideration of the presence of LASP1 in the basal cells of epidermal layer and the very high expression of LASP1 in melanocytic nevi, the investigator hypothesized about a melanocyte specific LASP1 function. The primary function of melanocytes is the production of the photo protective pigment melanin (Cichorek, Wachulka et al. 2013). Melanogenesis initiates with the pre-melanosome vesicle formation at the Golgi complex (Sitaram and Marks 2012), maturation of melanosome vesicle through four different stages with subsequent melanin synthesis and deposition on the fibrils followed by transport of the matured melanosome vesicle to the dendrite tips and finally melanin dense melanosome vesicles are released at the plasma membrane into the extracellular matrix (Costin and Hearing 2007). LASP1 can bind to various melanosome trafficking proteins like F–Actin (Chew, Chen et al. 2002; Watabe, Valencia et al. 2008) and dynamin (Chi, Valencia et al. 2006; Mihlan, Reiss et al. 2013) via its unique domain organization. Consideration binding of LASP1 to these proteins, protein depletion in melanocytes can influence intracellular melanin level by regulating either melanogenesis pathway or melanosome vesicle release processes.

3.1 LASP1 depletion elevates intracellular melanin levels in MaMel2 cells independently of melanogenesis

In order to scrutinize LASP1 involvement in melanogenesis, intracellular melanin level was measured in MaMel2 cells transiently transfected with LASP1 siRNA. Graphical presentation of melanin concentration in MaMel2 cells treated with control– or LASP1–siRNA is shown in Figure 19 A. siRNA transfection resulted in more than 90% silencing and a representative Western blot for LASP1 knockdown is depicted in Figure 19 A. In

comparison to the control cells, a moderate but significant elevation of ~10%, in the cellular melanin amount was detected in LASP1 depleted cells ($p=0.03$) (Figure 19 A and B).

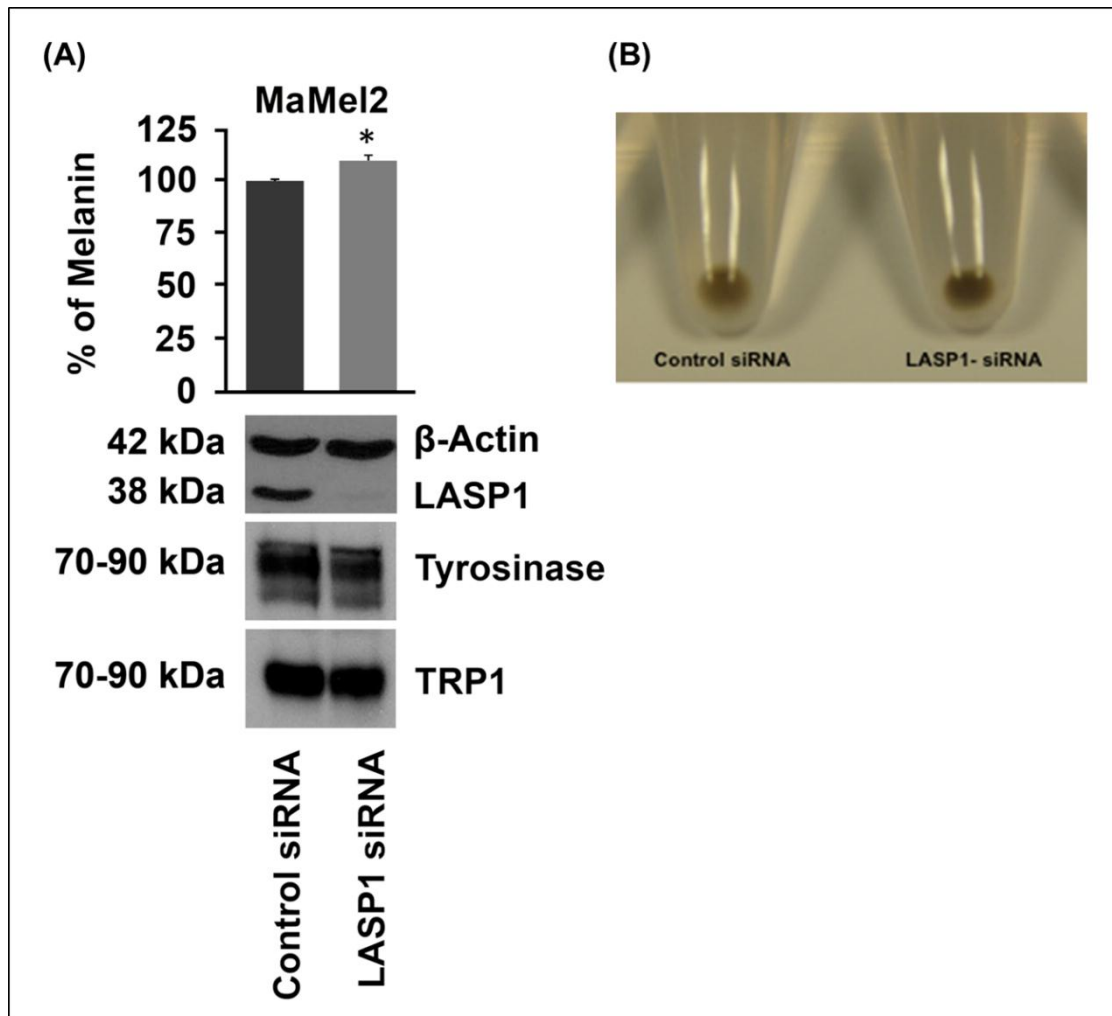


Figure 19: LASP1 depletion increases intracellular melanin in MaMel2 cells. MaMel2 cells transfected with control- and LASP1- siRNA were harvested, cellular melanin was dissolved by incubating in 1N NaOH at 80°C and measured at 450nm. **(A)** Graphical representation of the intracellular melanin level (~10% increase in LASP1 knockdown cells, $p=0.03$) in percentage and immunoblots of the corresponding samples against LASP1 and β-Actin (loading control), tyrosinase and TRP1 (melanogenesis regulators, not affected) are depicted. **(B)** Pellets from control and LASP1 knockdown MaMel2 cells after 72 hr of transfection.

Tyrosinase and tyrosinase related protein 1 (TRP1) are two important proteins for melanin synthesis and the generation of mature melanosome is highly dependent upon the cellular abundance of these two proteins (Sitaram and Marks 2012). The expression levels of these two melanogenesis regulators were examined to analyze whether the increased melanin amount is due to the cellular melanogenesis. Notably, as shown in Figure 19 A, no change is observed in the expression levels of both proteins. These data confirmed that the monitored accumulation of melanin content in LASP1 depleted cells is

not due to the *de novo* melanogenesis pathway as the melanogenesis regulators remained unaffected by these experiments, presuming a hindrance in melanin release.

3.2. LASP1 co-localizes with tyrosinase and dynamin at the dendrite tips of the cells

Immunofluorescence experiments were conducted to further check association of LASP1 with melanosomes and also to study its participation in melanin release. Tyrosinase, a melanosome specific marker was used to analyze the localization of LASP1 with melanosomes. Figure 20 presents the co-localization of LASP1 with the melanosome specific marker tyrosinase in different cell lines. Although a clear staining for tyrosinase displayed along the perinuclear vesicles and at the dendrite tips, co-localization with LASP1 was shown only at the dendrite tips of the melanocytes; assuming that LASP1 is associated with late stage melanosomes.

Next step was taken to check LASP1 involvement in melanosomes vesicle release at the dendrite tips. LASP1 co-localization with dynamin, a well-known protein for its participation in clathrin coated vesicle trafficking was studied. Immunofluorescence images in Figure 21 demonstrate a distinct presence of dynamin mainly at the Golgi around the nucleus, along the cell membrane and at the tips. In agreement with the observed localization of LASP1 with tyrosinase, dynamin and LASP1 co-localizes only at the tips of the cells but not around the nucleus. These data further confirmed that LASP1 is associated with late stage melanosomes and is involved in the melanosome vesicle release at the plasma membrane. Control experiments without primary antibodies revealed no staining with the secondary antibodies.

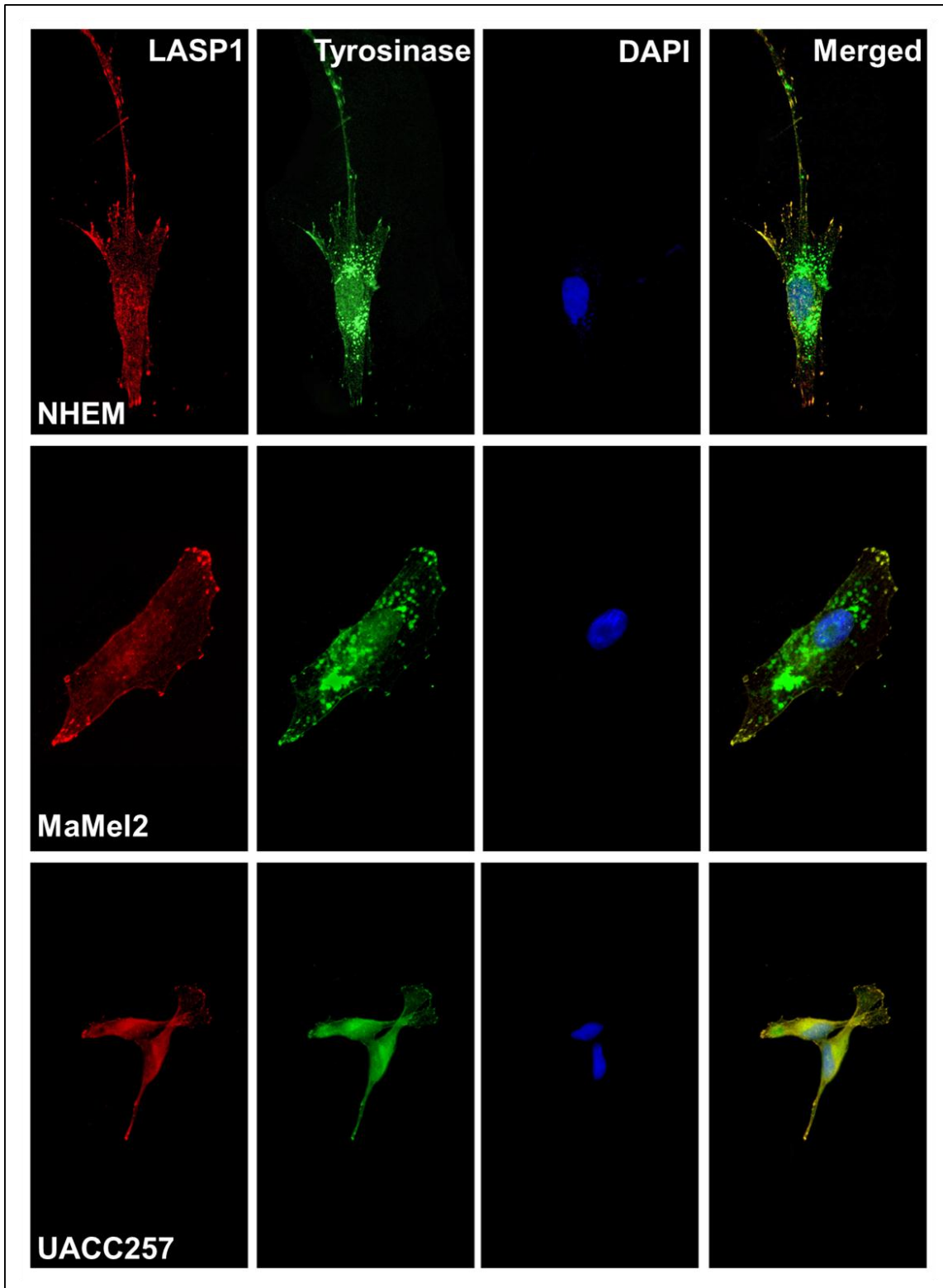


Figure 20: Subcellular distribution of LASP1 and tyrosinase in different cell lines. Cells were fixed in 4% formaldehyde, stained for indicated antibodies and counterstained with DAPI for nucleus. Immunofluorescence images showing LASP1 co-localization with tyrosinase (an enzyme that regulates melanogenesis) in NHEMs, MaMel2, and UACC257 cells. LASP1 (red), tyrosinase (green), DAPI (blue) and merged (yellow). Co-localization is observed at the dendrite tips of the cells.

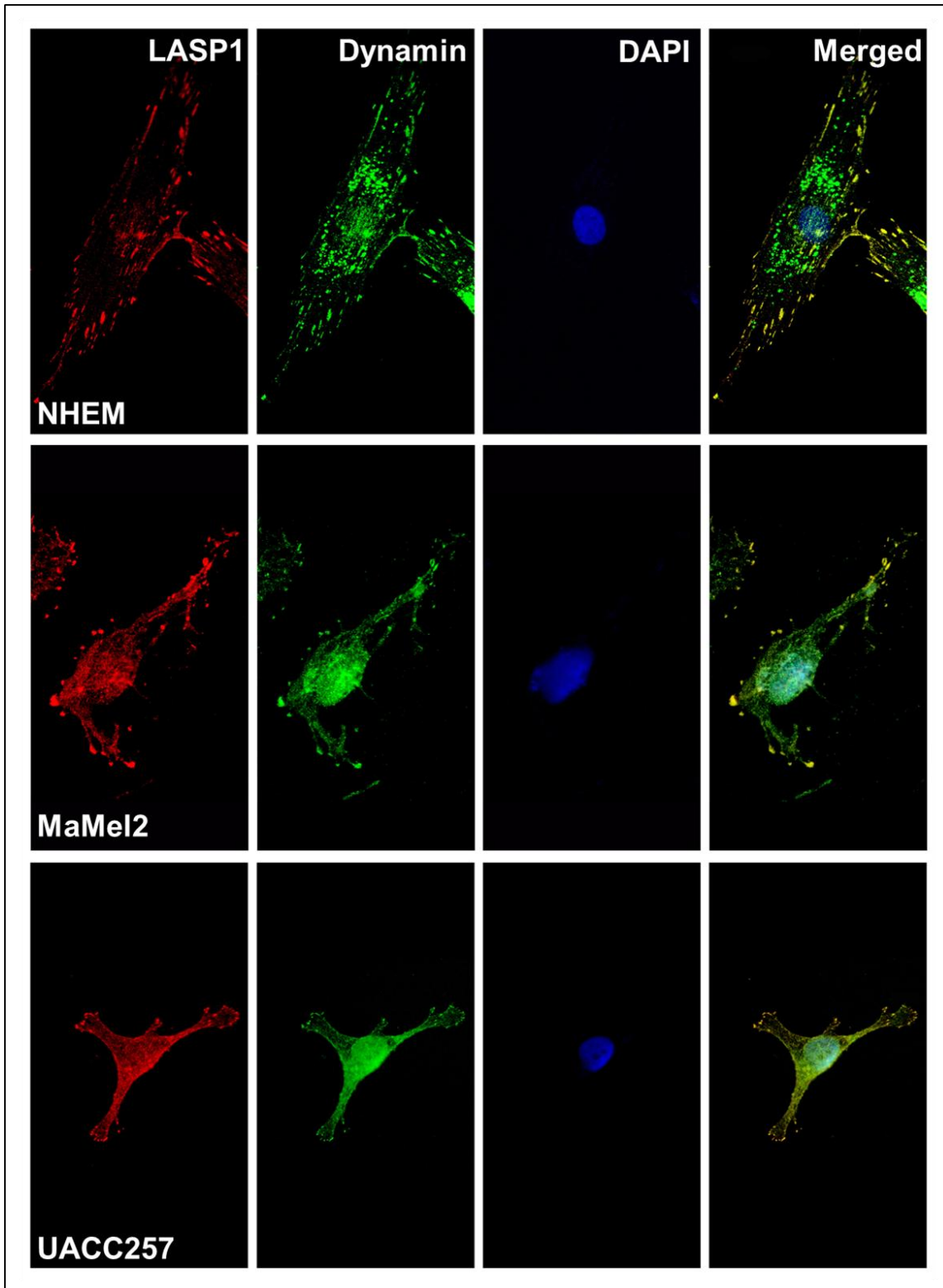


Figure 21: Co-localization of LASP1 and dynamin in different cell lines. LASP1 co-localizes with dynamin (a protein involved in vesicle formation, trafficking and budding) at the dendrite tips in NHEMs, MaMeI2, and UACC257 cells. LASP1 (red), dynamin (green), DAPI (blue) and merged (yellow).

4. Vesicle trafficking protein dynamin – a novel binding partner of LASP1 in melanocytes

Pull-down assays were carried out to further investigate the observed co-localization of dynamin and tyrosinase with LASP1 demonstrated by immunofluorescence and to analyze a possible binding interaction of the proteins.

4.1. GST–LASP1 production

The *E.coli* strains expressing GST–LASP1 fusion gene were stimulated with IPTG and the protein was purified using GST beads. To dissect the expression of the purified GST–LASP1 protein, samples from every step of preparation and purification were analyzed and are presented in Figure 22 A. *E.coli* strains carrying GST–control vectors

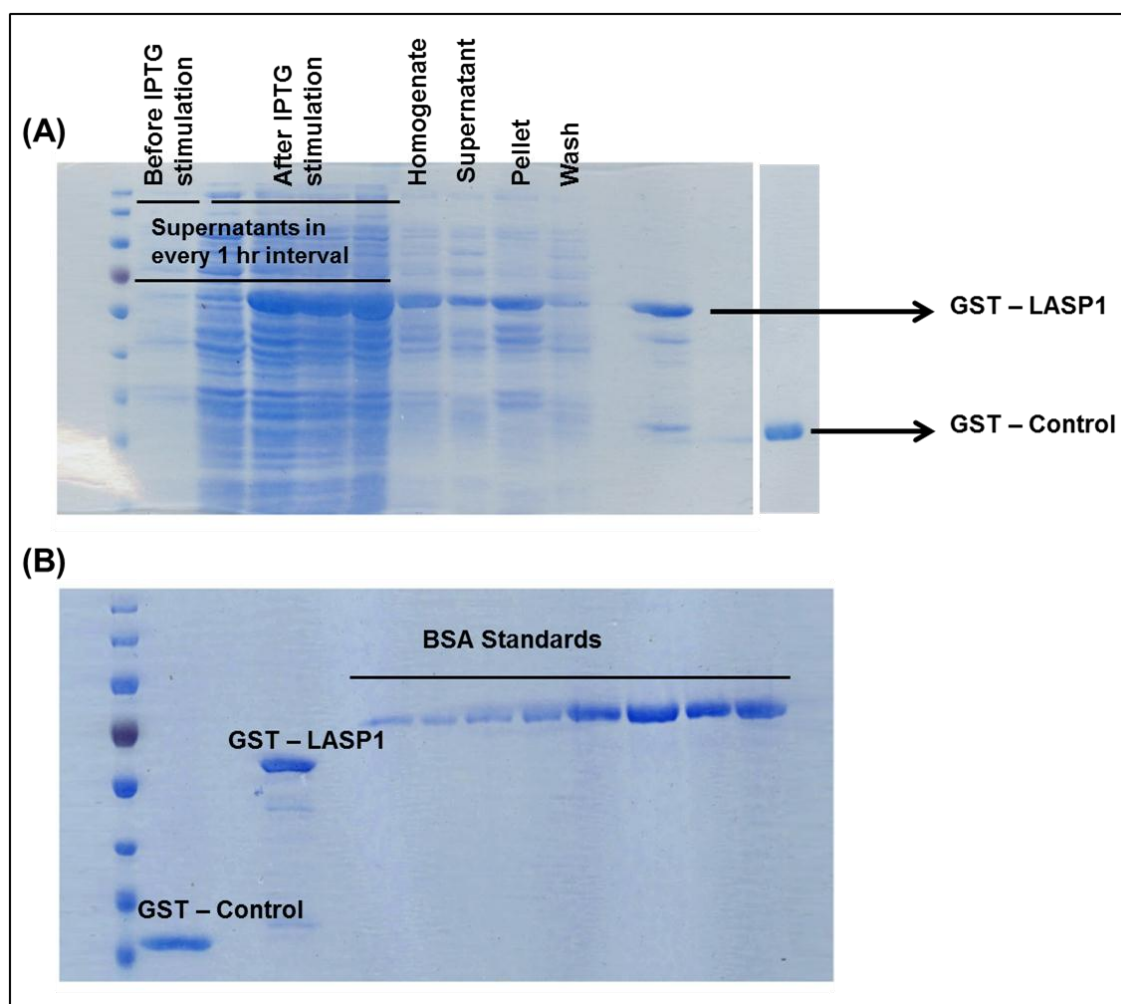


Figure 22: Screening of the expression level of proteins in GST overexpression experiments. Coomassie brilliant blue staining for protein expression levels at the expected molecular weight for (A) GST– LASP1 and control beads (protocol detailed in methods section) (B) Concentration check using bovine serum albumin (BSA) as standard (10–1000µg).

were also processed in a similar manner and the GST–control beads are shown in Figure 22 A. In Figure 22 B depicted the concentration of the purified protein in comparison to BSA standards (10 µg–1000 µg). The GST– control and LASP1 beads thus produced were used for the subsequent pull-down assays.

4.2. Pull-down assay

After GST–LASP1 production, pull-down assays were performed to validate the observed co-localization of LASP1 with dynamin and tyrosinase. MaMel2 cell lysate incubated with GST– control and LASP1 beads was analyzed for specific protein binding

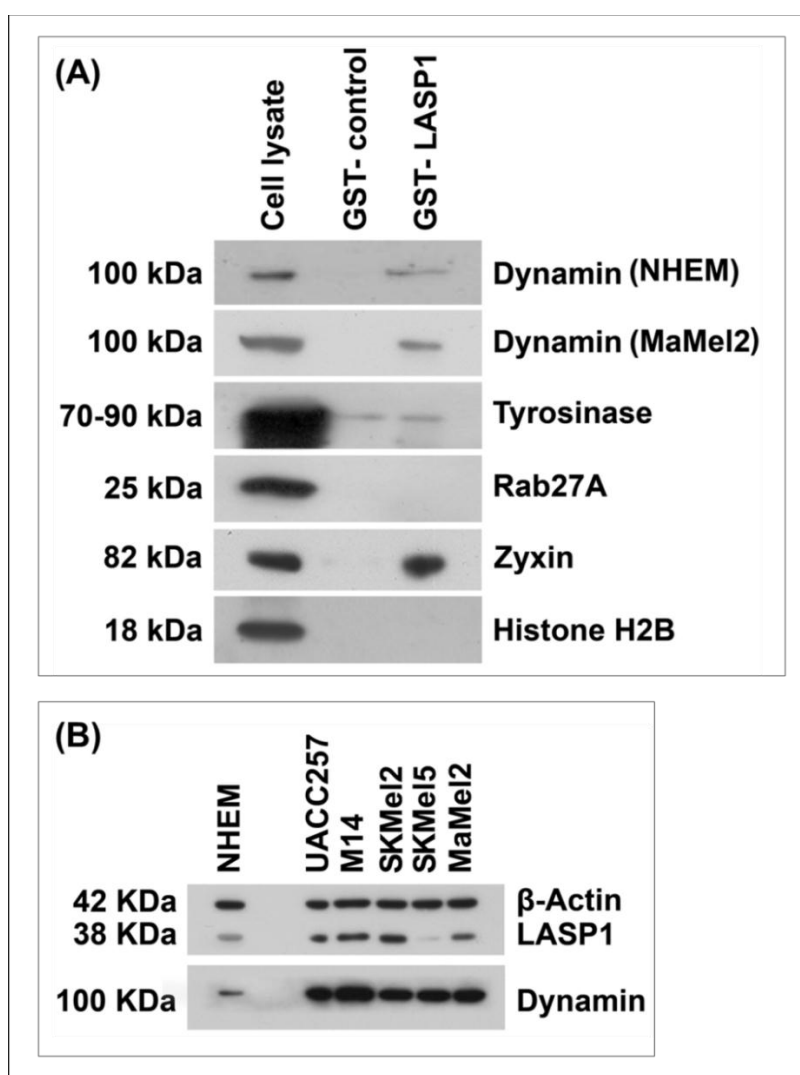


Figure 23: Dynamin a novel binding partner of LASP1 in melanocytes. (A) Pull-down studies demonstrate binding of dynamin to GST–LASP1 beads in NHEM and MaMel2 cell homogenates. But no binding of tyrosinase and Rab27A to GST–LASP1 was observed. Zyxin (positive control, known binding partner of LASP1) and histone H2B (negative control) served as controls for the experiment. (B) Western blot analysis of dynamin protein expression in NHEM and in melanoma cell lines, along with LASP1, β –Actin as loading control.

and data are shown in Figure 23 A. A concrete binding of dynamin to GST–LASP1 was detected while no binding to tyrosinase or Rab27A (a second melanosome marker that regulates the peripheral distribution of melanosomes in melanocytes) (Bruder, Pfeiffer et al. 2012) could be observed. Binding of zyxin, a known LASP1 interacting partner (Li, Zhuang et al. 2004) to GST–LASP1 beads served as positive control and histone H2B (a nuclear protein) acted as negative control for the experiment. Similar results were also achieved with UACC257 and NHEM cells. These results identified dynamin as a novel binding partner of LASP1 in melanocytes while LASP1 only co-localizes with tyrosinase, most likely at melanocytes.

Figure 23 B furnishes the expression pattern of dynamin in different melanoma cell lines and in NHEMs. All analyzed melanoma cells show a higher expression of dynamin than NHEMs. However, no correlation is observed between the pigmentation status and dynamin expression in these tested cells. The high dynamin level in amelanotic cells, for instance SKMel5, is explained by protein involvement in melanosome vesicle formation at the Golgi complex.

5. LASP1 and dynamin – two novel proteins associated with mature late stage melanosomes

To prove that LASP1 is associated with late stage melanosomes or stage IV melanosomes, the different stages of melanosomes were separated, purified and analyzed by sucrose density gradient centrifugation. Basically, the experiment takes advantage of density differences of melanosomes in various stages to purify these organelles over stepwise density gradients from 1.0 to 2.0 M sucrose (Watabe, Kushimoto et al. 2005).

5.1. Isolation and purification of melanosomal fractions by sucrose density gradient centrifugation

Melanosomes mature within the melanocyte through four morphologically distinct stages (Raposo and Marks 2007) which are dispersed in 1.0 M–1.8 M sucrose density gradients during ultracentrifugation. Early melanosomes or pre-melanosomes are detected in the 1.0 M and 1.2 M fractions while 1.6 and 1.8 M sucrose fractions contains late or matured melanosomes (Kushimoto, Basrur et al. 2001). Figure 24 shows a schematic representation of the procedure used to purify and characterize melanosomal proteins. Homogenate from pigmented MaMel2 cells were subjected to sucrose density gradient ultracentrifugation and the fractions obtained were further purified and analyzed by immunoblotting.

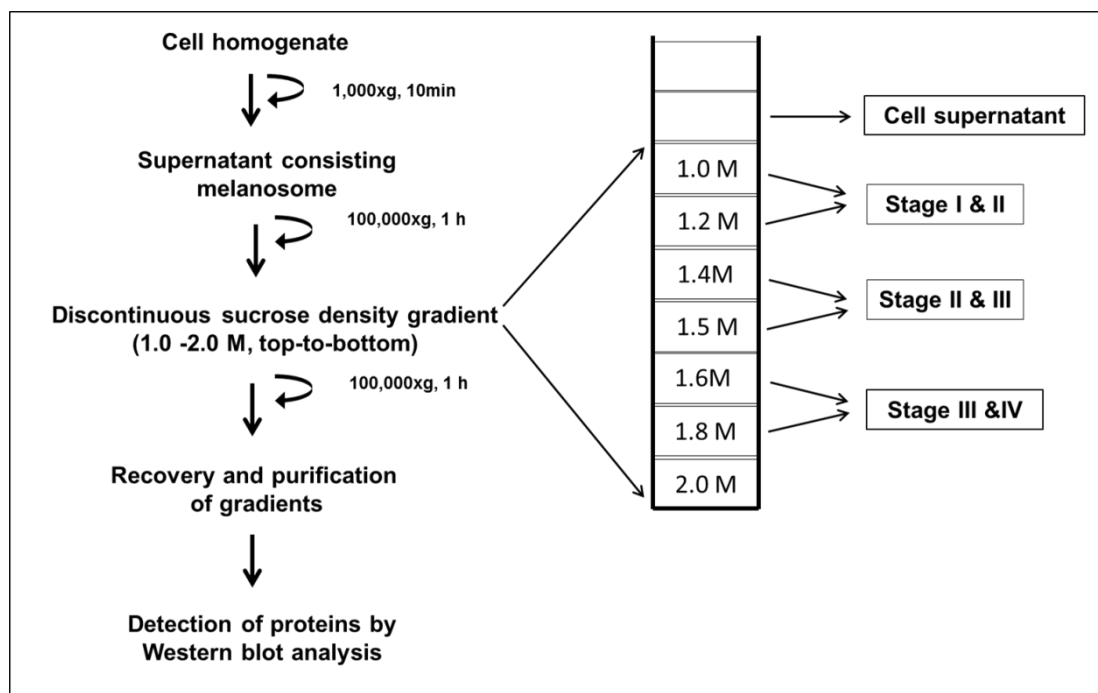


Figure 24: Layout of sucrose density gradient centrifugation protocol for melanosome isolation. Flowchart describes the method used to isolate melanosomes at various stages of maturation from pigmented MaMel2 cells. The ultracentrifuge tube illustrates fractions containing different stages of melanosomes. Stage I and II (1.0 and 1.2 M), stage II and III (1.4 M) and stage III and IV (1.6 and 1.8 M) are present in the fractions of sucrose gradient.

5.2. Distribution of melanosomal proteins by immunoblotting

The bulk of proteins, separated at very distinct and discrete parts of the sucrose density gradient, were subjected to Western blot analysis to illustrate LASP1 and dynamin being genuine melanosome vesicle associated proteins. Fractions examined included cytosol before and after centrifugation in 0.25 M sucrose solution and the 1.0, 1.2, 1.4, 1.5, 1.6 and 1.8 M sucrose fractions. Immunoblotting of the fractions demonstrated the highest protein concentration in the low density 1.0 M and 1.2 M sucrose fractions and substantiates the existence of the two most stringent markers of melanosomes – tyrosinase and TRP1 in these fractions.

Immunoblotting data shown in Figure 25 revealed that LASP1 and dynamin are present in the late stage of melanosomes. The high level of LASP1 in the low density fractions is due to smeared soluble protein from the loading sample as can be seen by high LASP1 in the “cytosol after” centrifugation fraction (Figure 25). Likewise, the presence of LASP1 in the initial fractions is not consistent with the immunofluorescence images as there is no co-localization of LASP1 with tyrosinase and dynamin around the nucleus in stage I/II (Figure 20). Accordingly, the high level of dynamin in the initial gradient indicates the possible involvement of the protein in pre-melanosome formation from the Golgi

complex, as shown in the immunofluorescence of Figure 20 B. As depicted in Figure 25, tyrosinase is present nearly in all fractions while TRP1 is more abundant in fractions containing earlier stage melanosomes.

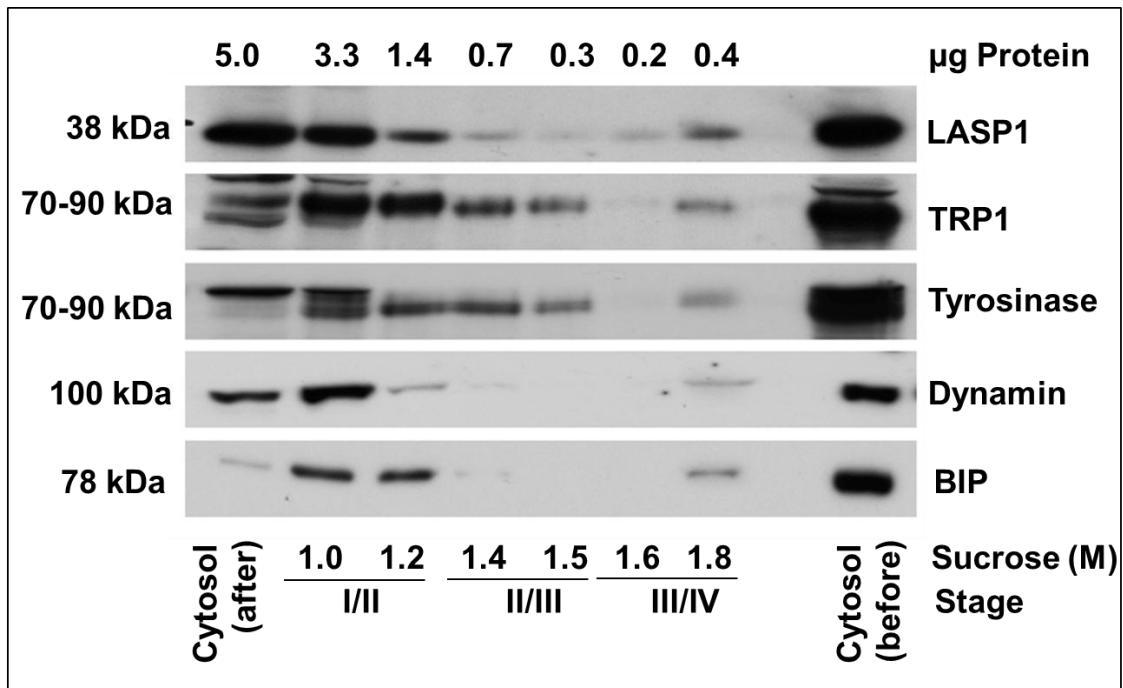


Figure 25: Immunoblot analysis of sucrose density gradient purified fractions. MaMel2 cell cytosol was subjected to sucrose density gradient centrifugation. Purified fractions were blotted against LASP1, TRP1, tyrosinase and dynamin. Lanes correspond to cell cytosol (before and after centrifugation) and the different sucrose gradient fractions. The protein concentration of the fractions and the corresponding melanosome stages are stated. All four proteins exhibited a peak in 1.8 M fraction.

As mentioned in previous study, in order to check the presence of other organelles, endoplasmic reticulum marker protein BIP (Binding Immunoglobulin Protein) was analyzed in different sucrose fractions. BIP is a molecular chaperone located in the lumen of the endoplasmic reticulum (Gething 1999) and was identified in the earlier protein rich fractions and in the 1.8 M fraction, which is in consonance with earlier finding (Kushimoto, Basrur et al. 2001). Table 10 represents the distribution pattern obtained by Western blotting of isolated melanosomal marker proteins and of the endoplasmic reticulum marker.

In two out of four experiments, even dark melanosomes were visible in 1.8 M fraction (Figure 26). The evidence of LASP1 and dynamin in the final fraction of the gradient, along with tyrosinase and TRP1, confirms the association of these proteins with late stage melanosomes (stage IV) and is in agreement with the immunofluorescence data.

Interestingly, all four proteins show a second peak of increase in the 1.8 M sucrose fraction that corresponds to the stage IV melanosomes.

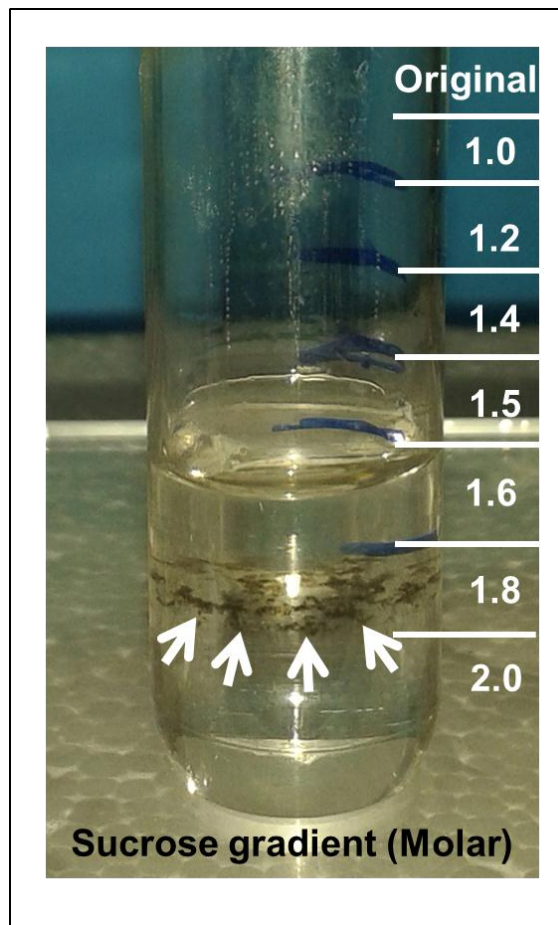


Figure 26: Ultracentrifuge tube with dark melanosomes in 1.8 M sucrose fraction. Arrowheads shows dark pigmented melanosomes in the 1.8 M fraction of sucrose, after ultracentrifugation of MaMel2 supernatant on a discontinuous sucrose gradient.

Table 10: Distribution of marker proteins by Western blotting

Fraction	Stage	Tyrosinase	TRP1	ER (BIP)
1.0 M sucrose	I, II	++	++	+
1.2 M sucrose	I, II	++	++	+
1.4 M sucrose	II, III	++	+	±
1.5 M sucrose	II, III	+	+	±
1.6 M sucrose	III, IV	±	±	±
1.8 M sucrose	III, IV	+	+	+

5.3. LASP1 and dynamin co-localizes with tyrosinase in peripheral melanosomes

As shown in Figure 27 LASP1 co-localizes with dynamin along the long dendrite of MaMel2 cells. The merged protein spots perfectly match with mature melanosomes in the bright-field. Similarly, at the periphery of NHEM cells, co-localization of LASP1 with tyrosinase is observed in accordance with the dark peripheral melanosomes visualized in the bright field (Figure 28).

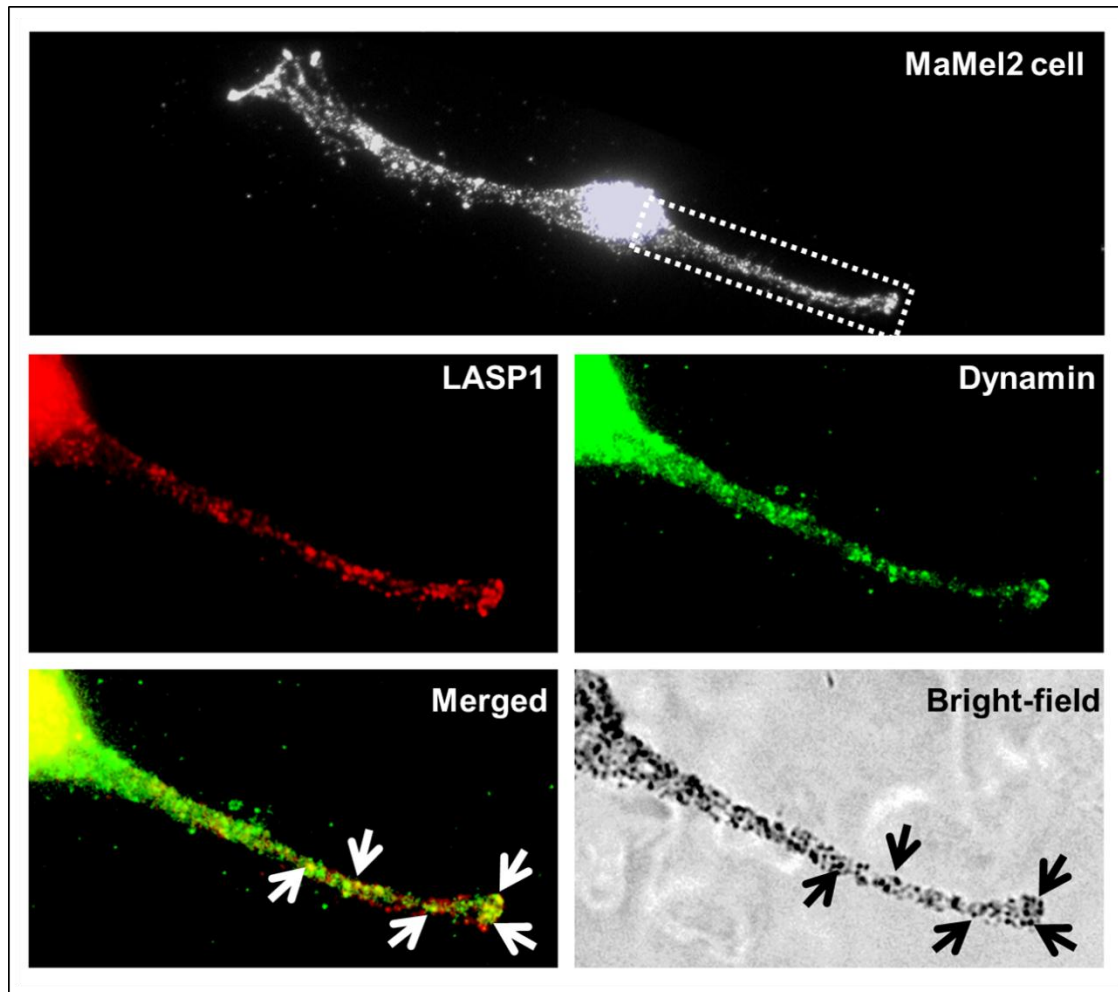


Figure 27: Co-localization of LASP1 and dynamin with peripheral melanosomes in MaMel2 cells. MaMel2 dendrite showing immunostaining for LASP1 (red) and dynamin (green). LASP1–dynamin co-localization (yellow) perfectly matches with the peripheral melanosomes in the bright–field. Arrowheads are pointing the co-localization spots.

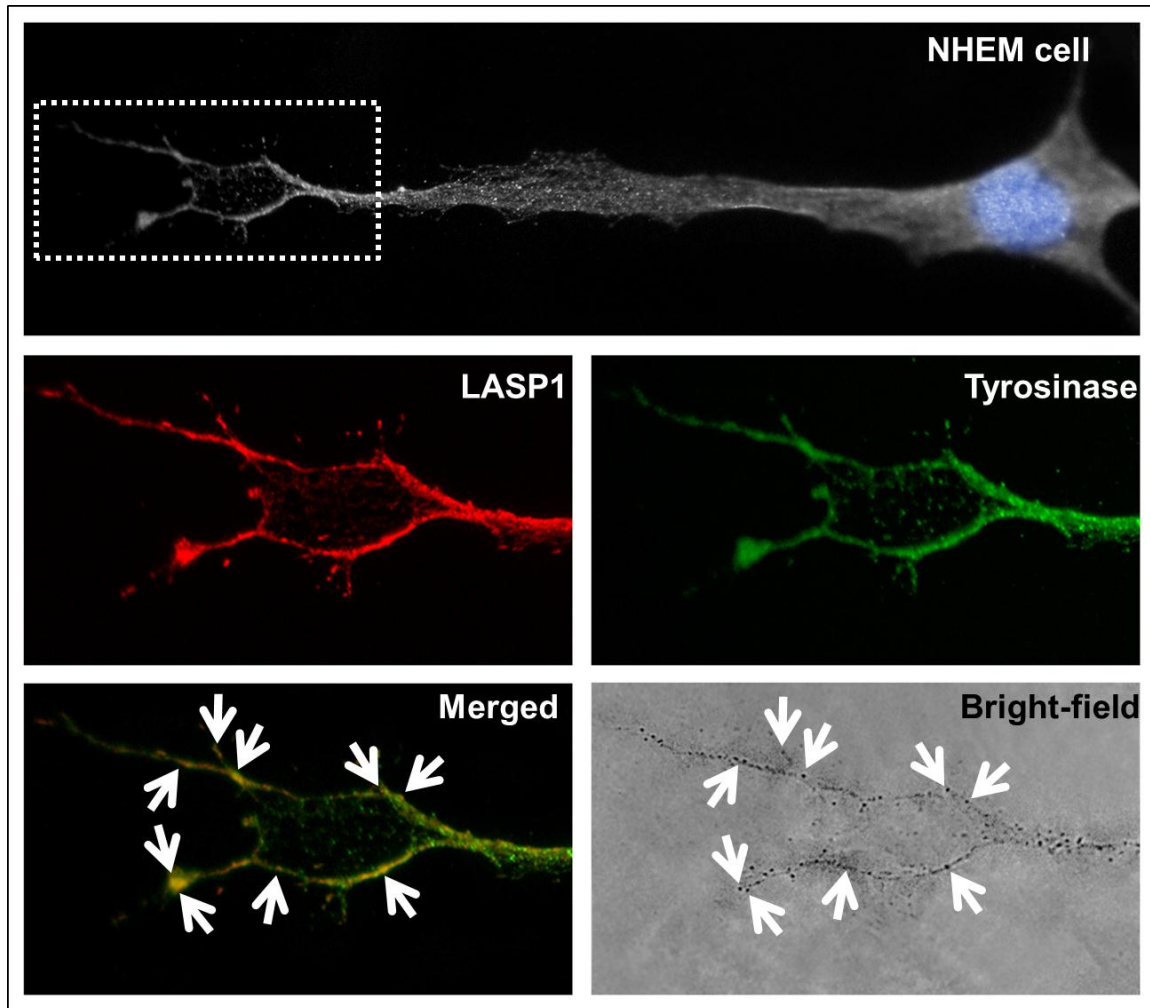


Figure 28: LASP1 co-localization with tyrosinase (melanosomes) in NHEM dendrite tips. A NHEM cell presenting the dendrite tip immunostained for LASP1 and tyrosinase. LASP1 (red) and tyrosinase (green) co-localizes (yellow) along the cell dendrites. Bright-field illumination of the dendrite tips displaying melanosomes corresponding to the co-localization (arrowheads).

As mentioned previously, melanosome biogenesis starts with pre-melanosome formation from the perinuclear region and ends with release of mature melanosomes at the plasma membrane. Dynamin, a novel protein in melanocytes displays a characteristic distribution in the cells along with the melanosomal protein tyrosinase, where it is present on a population of vesicular structures in the perinuclear region and at the peripheral region (Figure 29). These results verified the involvement of dynamin in melanosomes vesicle formation at the Golgi and in the release at the dendrite tips of cells.

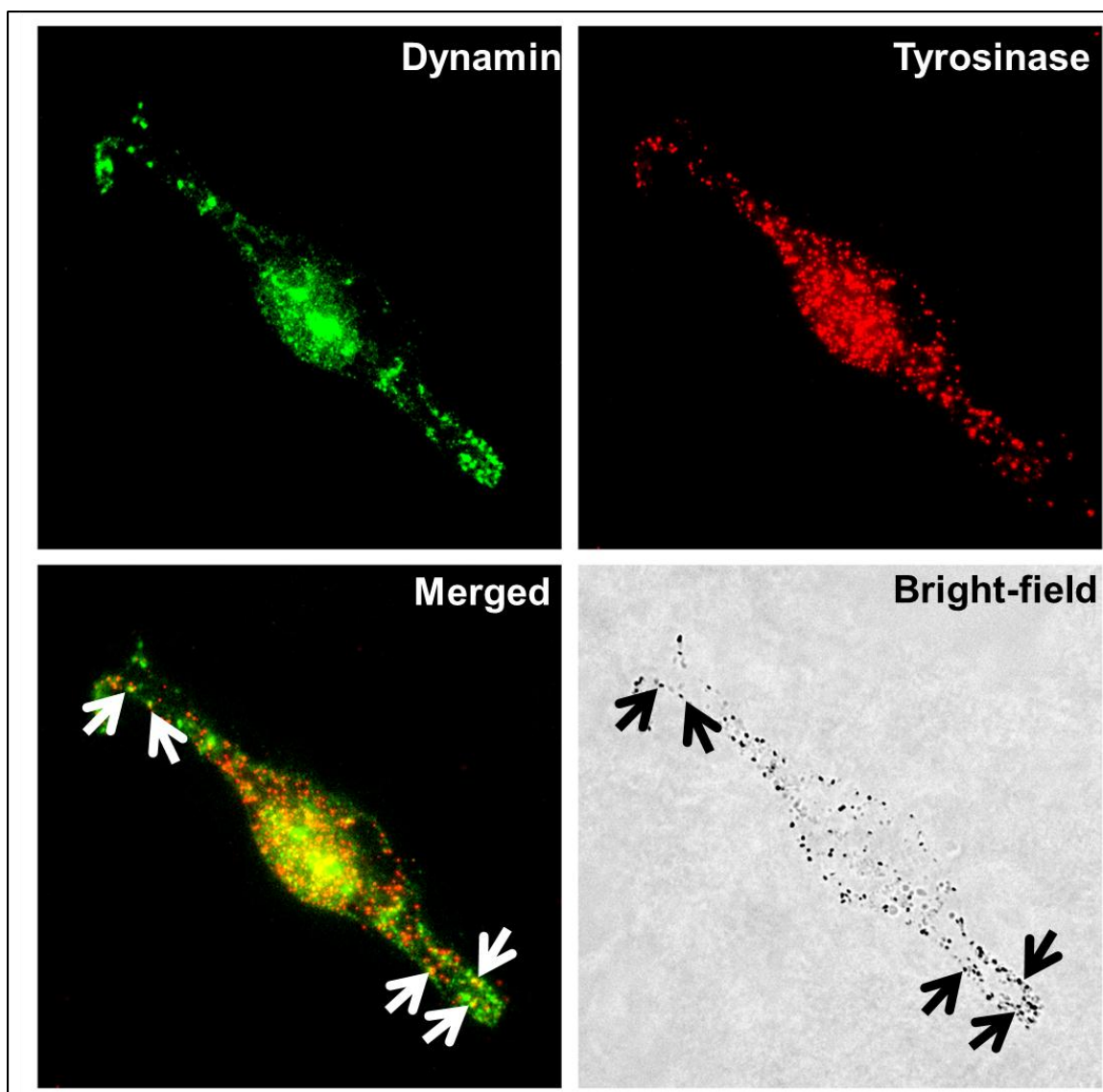


Figure 29: Subcellular distribution of dynamin and tyrosinase. Dynamin co-localizes with tyrosinase in the perinuclear and peripheral melanosomes. Dynamin (red), tyrosinase (green) and co-localization (yellow). Arrowheads represent co-localization with melanosomes.

The merged images of all three proteins– LASP1, dynamin and tyrosinase perfectly co-localizes with the representative dark melanosomes and the data substantiate the sucrose density gradient result, identifying LASP1 and dynamin in the 1.8 M fractions, along with the melanosomal proteins tyrosinase and TRP1.

Summing up all results obtained thus far, the data revealed that LASP1, a newly identified scaffolding protein in melanocytes, is associated with late stage melanosomes and is involved in melanosome vesicle release at the dendrite tips along with the binding partner dynamin.

B. LASP1 protein impact on human melanoma cancer

1. LASP1 protein expression pattern in melanoma

The malignant transformation of melanocytes into cutaneous melanoma is considered to be the most aggressive form of skin cancer and has a high risk of metastases susceptibility (Bastian 2014). Melanoma can also develop from pre-existing melanocytic nevi. Considering the very high expression of LASP1 in melanocytic nevi and since an elevated level of LASP1 have been observed in almost all tested cancer entities and were found to be involved in tumor progression [reviewed in (Orth, Cazes et al. 2015)] the investigator hypothesized that LASP1 might also be involved in melanoma tumor progression.

1.1. LASP1 expression decreases with melanoma cancer progression

LASP1 protein expression pattern was examined in 29 melanocytic nevi, 58 primary melanoma and 20 metastatic melanoma specimens. For semi-quantitative Immunoreactive Score (IRS) assessment, immunohistological samples stained for LASP1 and MART1 were scored by two independent experts, based on the evaluation criteria explained in the method's section (Remmele and Stegner 1987; Grunewald, Kammerer et al. 2007), and the data were kindly provided. Figure 30 illustrates representatives from each group for the detected LASP1 and MART1 immunoreactivity along with the normal skin specimen. Considering staining intensity and LASP1-positivity, IRS for normal skin is calculated as 1 (Figure 30).

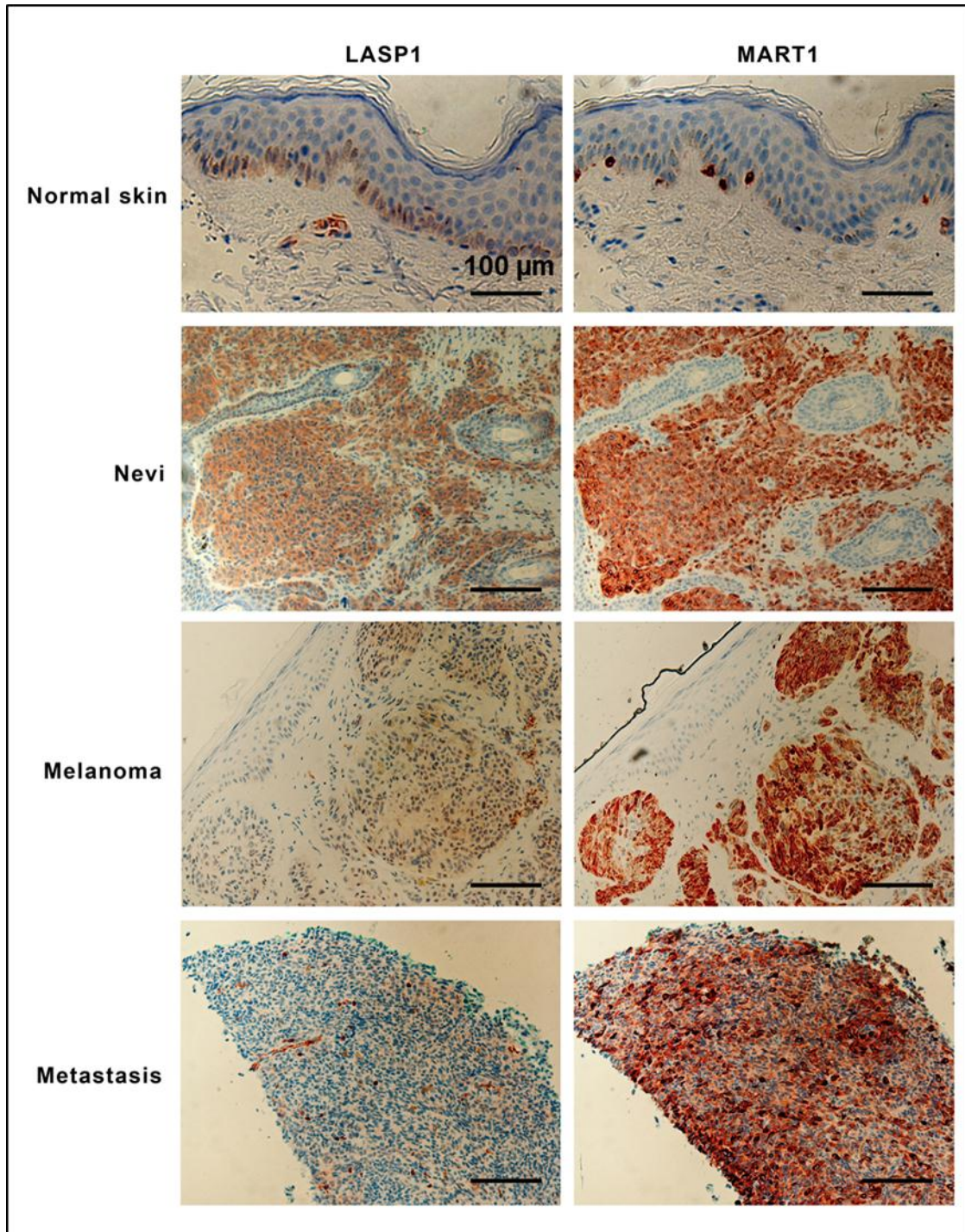


Figure 30: Immunohistochemical staining of LASP1 in normal skin, melanocytic nevi, primary and metastatic melanoma. Depicted consecutive sections from normal skin, melanocytic nevi, primary melanoma and metastatic melanoma immunostained against LASP1 (left panel) and MART1 (right panel). The sections were counterstained with haematoxylin and eosin (magnification 20X; Scale bar = 100 μm).

For statistical determination of tumors, samples scored with cytosolic LASP1–IRS ≥ 3 were classified as LASP1–positive. Surprisingly, analysis of the IRS revealed a very low expression of LASP1 in primary melanoma (13.8%) and in metastases (4.7%) in comparison to the analyzed nevi (62.0%). These data revealed that LASP1–positivity decreases with increased malignancy. In none of the samples a nuclear staining, characteristic for many aggressive LASP1–positive tumors, was observed. The assessed cytosolic and nuclear LASP1–positivity is depicted in Table 11.

Table 11: LASP1 expression in melanocytic nevi, primary melanoma, and melanoma metastases specimens

Specimens	No. of patients (n)	LASP1 positive cells, (IRS>2)	LASP1 positive nuclei, ($\geq 10\%$)
Nevi	29	18 (62.0%)	0 (100%)
Melanoma	58	8 (13.8%)	0 (100%)
Metastasis	20	1 (4.7%)	0 (100%)

1.2. No correlation of LASP1 to the clinicopathological features in melanoma patients

Provided data were further analyzed to determine a possible role of LASP1 in melanoma. Correlation of LASP1 expression to the clinicopathological characteristics in 58 melanoma patients' samples is listed in Table 12. There was no significant correlation observed between LASP1 expression and the parameters– gender, age, tumor stage (T2–T4), tumor depth or metastases. Nevertheless, a slight significant correlation (p value of 0.05) to the cancer related death (CRD) was noticed. 75% of the LASP1–positive patients died (6 out of 8) compared to 38% of LASP1–negative patients (19 out of 50), suggesting a poor survival of melanoma patients with observed LASP1 expression. However, the overall number of deceased LASP1–positive individuals (n=8) is too low for a statistically robust conclusion on CRD.

Table 12: Correlation of LASP1 expression to clinicopathological characteristics in 58 melanoma patients

Parameter	Melanoma	LASP1 Positive	LASP1 Negative	<i>p</i>
Number of patients	58	8	50	
Sex				0.81
male	34	3	29	
female	24	5	21	
Age at primary diagnosis				0.13
≤ 60	22	1	21	
> 60	36	7	29	
Lymph node metastases *	30	6	24	0.18
Distant metastases *	28	6	22	0.11
Tumor depth * (AJCC)				0.1
1–2 mm (T2)	26	3	23	
2.1–4 mm (T3)	13	4	9	
>4 mm (T4)	19	1	18	
Cancer-related death **	25	6	19	0.05

* Tumor depth after AJCC guidelines. ** Within 5 years follow-up. Values of *p* were calculated by Chi-Square test; statistical significance is assumed when $p < 0.05$.

2. LASP1 nuclear localization is absent in melanoma cell lines and NHEM

Previous studies demonstrated a predominant nuclear localization of LASP1 in several cancer entities and were reported to correlate with worse long-time survival of patients in breast cancer (Frietsch, Grunewald et al. 2010). Although melanoma tissues show no nuclear LASP1 staining, the possibility of LASP1 to localize to the nucleus in melanoma cells was assessed.

2.1. LASP1 is not localized within the nucleus in melanoma cell lines

Stimulation with forskolin, results in an intracellular elevation of cAMP levels and concomitant activation of PKA, which leads to the downstream phosphorylation of LASP1 at Ser-146 and nuclear trans-localization of the protein (Mihlan, Reiss et al. 2013). To investigate nuclear localization of LASP1, cytosolic and nuclear fractions were prepared from control- and forskolin-treated cells of NHEMs and melanoma cell lines- MaMel2 and UACC257. Similarly and as a positive control, fractions were obtained from the breast cancer cell line- MDAMB231 and were analyzed in parallel. As shown in Figure 31, LASP1 and pLASP1-S146 were localized exclusively in the cytosol of melanoma cell lines and NHEM, while in breast cancer cells a distinct nuclear LASP1 signal was noticed. The purity of the cytosolic and nuclear preparations was controlled by the detection of lamin A/C or histone H2B (nucleus) and GAPDH (cytosol). The results confirmed the immunohistochemical data showing no nuclear LASP1 localization in melanocytic nevi, primary melanoma and melanoma metastases (Figure 30).

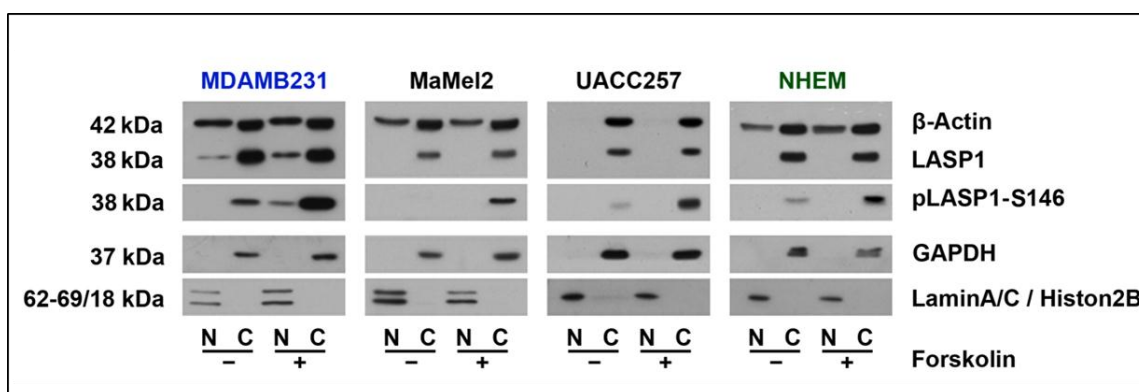


Figure 31: Immunoblot analysis of nuclear and cytosolic fractions for LASP1 distribution.

Cytosolic and nuclear fractions isolated from control and forskolin-stimulated cells were analyzed by Western blotting. Fractions from melanoma cell lines: MaMel2, UACC257, normal human epidermal melanocyte (NHEM) and breast cancer cell line: MDAMB231 were blotted with antibodies for LASP1, pSer-146 LASP1 (nuclear translocalisation), β-Actin (loading control), GAPDH (cytosolic marker), Lamin A/C or histone H2B (nuclear markers). Nuclear trans-localization is absent in melanoma and melanocyte (NHEM) cells.

2.2. LASP1 interacting partners assisting in nuclear shuttling are absent in melanocytes

It has been shown that LASP1 protein shuttles between the cytosol and the nucleus in a phosphorylation-dependent manner by binding to zonula occludens protein 2 (ZO2) (Mihlan, Reiss et al. 2013). To investigate the reason for the absence of nuclear LASP1 trans-localization, the expression of proteins involved in cytoplasmic-nuclear shuttling was analysed. As seen in Figure 32, the tested melanoma cell lines MaMel2, SKMel5 and NHEM do not express the LASP1 binding shuttle partner ZO2, as does the breast cancer cell line MDAMB231 (Figure 32). Unexpectedly, UACC257 cells express ZO2, though LASP1 is not detected in the nucleus. Protein kinase A (PKA) is expressed in all verified cell lines as shown in Figure 32.

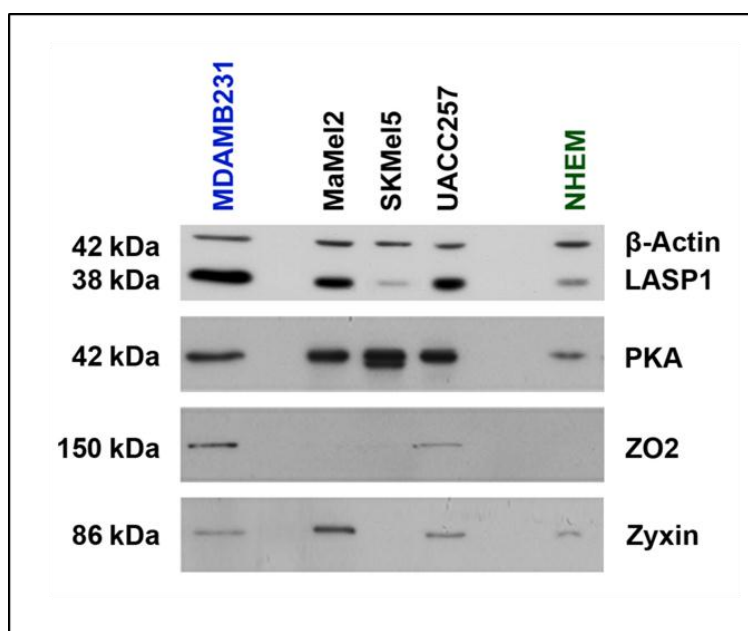


Figure 32: Western blot analysis of binding partners of LASP1 in cell lines. Expression pattern of ZO2, PKA and zyxin along with LASP1 was verified in melanoma cell lines and NHEMs and were compared with breast cancer cells– MDAMB231. Equal loading was adjusted using β-Actin.

Concluding the section, cutaneous melanoma is considered as the first tumor tested hitherto, showing no LASP1 overexpression. The protein is not involved in the development and progression of melanoma.

V. Chapter – Discussion

Discussion

Skin is the body's largest organ giving protection from ultraviolet radiation induced DNA damage and hence plays an essential role in human survival. As illustrated in Figure 33, skin has a complex structure and the most important layer is the highly proliferative and migrating stratum basale of epidermis. This is the first study demonstrating the existence of the scaffolding cytoskeletal protein, LASP1 in the pigment producing melanocytes of the skin.

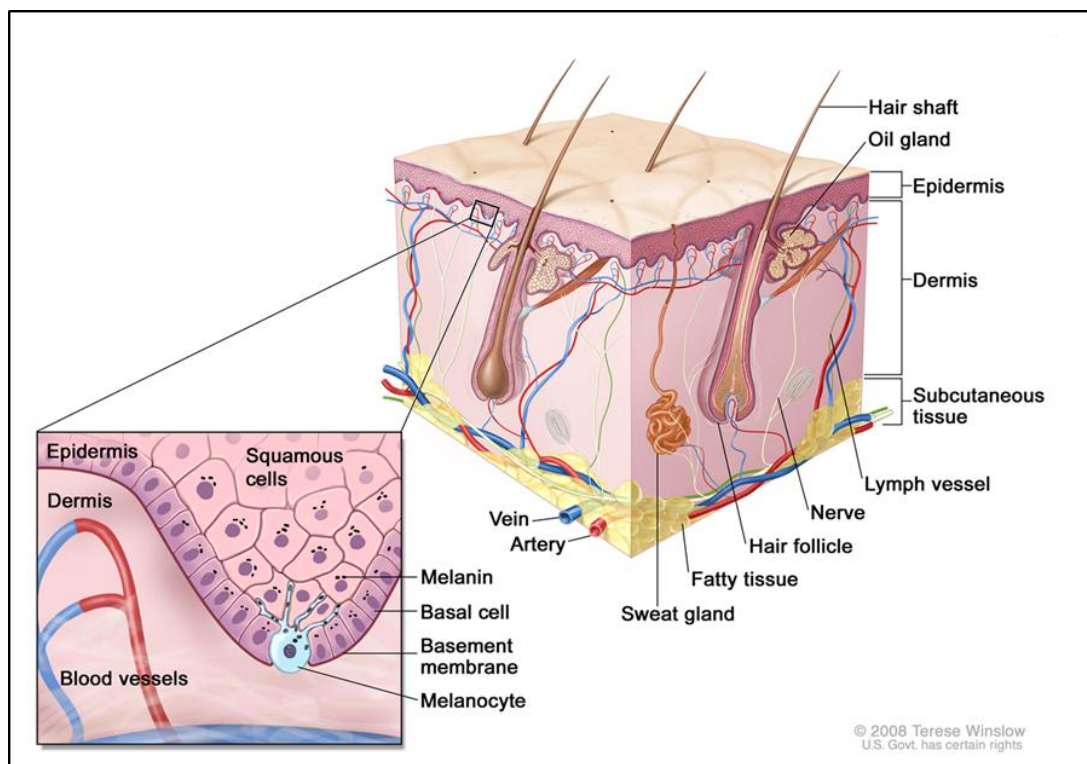


Figure 33: Schematic presentation of skin structure. Illustrated the complex structure of skin and inset a small portion of epidermal basal layer is depicted demonstrating basal cells and melanocytes.

Source: <http://www.uchospitals.edu/online-library/content=CDR552637>

In immunohistochemistry, LASP1 displays a positive staining in the highly proliferating stratum basale (Figure 9 B) while cells of superficial layers (stratum spinosum and stratum granulosum) exhibit no LASP1 expression (Figures 9 & 10). This finding resembles to the previous report showing LASP1 existence in human breast epidermal basal cells (Grunewald, Kammerer et al. 2007). Interestingly, a distinct nuclear localization is also detected in these basal cells (Figure 11). Previously it has been shown that the nuclear localization of LASP1 is associated with proliferation as well as cell cycle mechanism of the cells (Frietsch, Grunewald et al. 2010; Traenka, Remke et al. 2010) and the data also suggested a possible, but not yet proven, transcriptional

function. As the basal cells of the epidermis are highly proliferative, LASP1 is presumed to participate in the proliferation and also migration of these cells towards the upper layer of the skin.

Since the knockdown experiments in normal human epidermal melanocytes were not successful, cell based assays were performed in human melanoma cell lines. *In vitro* experiments exploiting RNA interference strategy were carried out to analyze LASP1 protein influence on proliferation, adhesion and migration. Proliferation rates of the cells decreased significantly at 10% upon LASP1 depletion and a distinct reduction in the migratory processes by more than 25% was observed (Figure 18). These data justify the noted presence of LASP1 in the highly proliferating and migrating basal cells of the epidermis (Figure 11).

LASP1 protein has been bespoken to have an elevated level of expression in several cancer entities and participates in the development of tumor metastases (Grunewald, Kammerer et al. 2007; Frietsch, Grunewald et al. 2010; Wang, Zheng et al. 2012; Wang, Li et al. 2013) and is also documented to serve as a prognostic tumor marker for cancer detection, for example in medulloblastoma (Traenka, Remke et al. 2010) and hepatocellular carcinoma (Wang, Li et al. 2013).

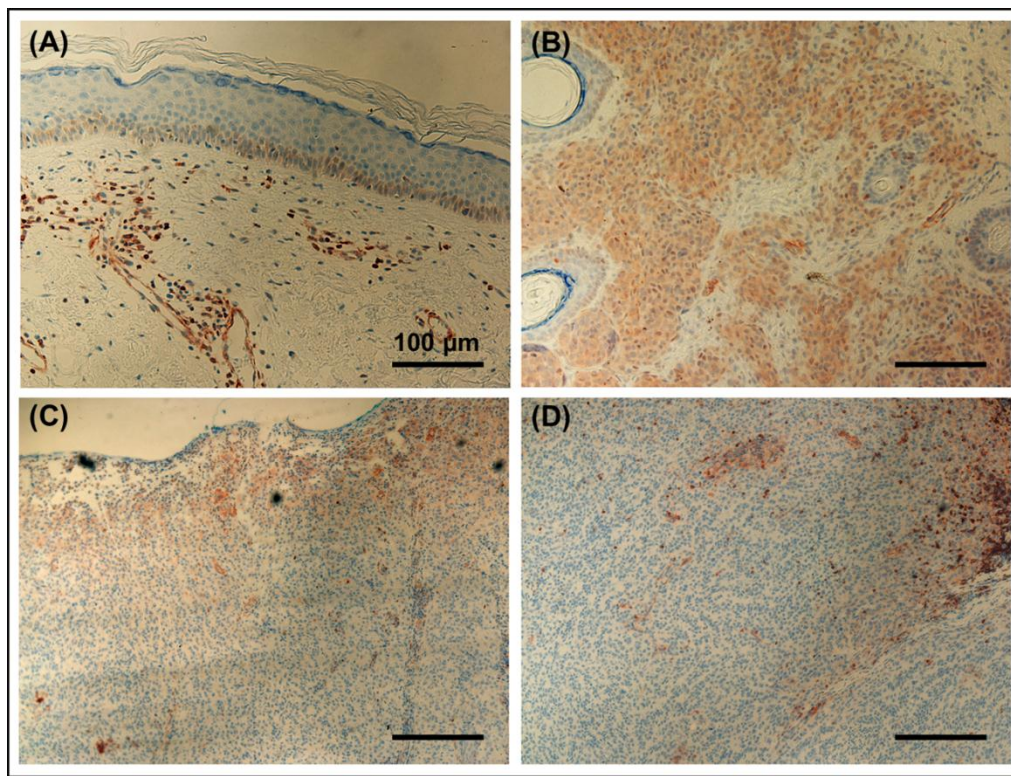


Figure 34: LASP1 immunostaining in tissue samples. (A) Normal skin (B) Melanocytic nevi (C) primary melanoma (D) melanoma metastases.

Intriguingly a very high expression of LASP1 is detected in benign melanocyte (Figures 12 & 34 B). Surprisingly and in contradiction to the tested tumor entities to date, immunohistostaining of primary melanoma revealed a very low LASP1 expression pattern and an even reduced level in metastases (Figures 30 & 34 C-D). Besides, the minor effects observed in melanoma cell lines on proliferation (~10%) and migratory processes (~25%) after 75% depletion of the protein are not that impressive when compared to other studied tumors. Knockdown of LASP1 in breast and gastric cancer, for example, led to more than 50% reduction in migration (Grunewald, Kammerer et al. 2006; Zheng, Yu et al. 2014). Furthermore, no significant correlation between LASP1 expressions to clinicopathological parameters in melanoma patients is observed (Table 12). Although, no obvious correlation is noted to the melanoma prognostic factors like gender, age, tumor depth and metastases, a significance of $p=0.05$ is noticed to cancer related death (CRD) in LASP1-positive patients. Nevertheless, an overt decision on CRD is impossible due to the lack of considerable number of LASP1-positive patients (n=8).

As explained in the Review of literature, various studies demonstrated that LASP1 overexpression and nuclear localization are positively correlated with malignancy, tumor grade and metastatic lymph node status (Grunewald, Kammerer et al. 2007; Frietsch, Grunewald et al. 2010; Wang, Zheng et al. 2012; Wang, Li et al. 2013). However, a positive nuclear localization is absent in benign tumor – melanocytic nevi (Figure 13) and also in primary melanoma and melanoma metastases. The data are also supported by the *in vitro* LASP1 nuclear localization experiments, revealing no LASP1 nuclear localization in melanoma cell lines.

Upon forskolin stimulation, LASP1 get phosphorylated at Ser-146 by PKA and translocated into the nucleus by binding to zonula occludens 2 (ZO2) in breast cancer cell line – MDAMB231 (Mihlan, Reiss et al. 2013). Similar study in the melanoma cell lines – MaMel2 and UACC257 did not reveal any nuclear trans-localization of LASP1 after forskolin stimulation. The absence of LASP1 nuclear localization is also detected in chronic myeloid leukemia (CML), however, no mechanism is discussed (Frietsch, Kastner et al. 2014). Unexpectedly, NHEMs also showed no nuclear trans-localization of LASP1, which is contradictory to the observed nuclear expression of LASP1 in the basal cells of normal skin.

A possible explanation for this discrepancy could be that LASP1 might have a melanocyte specific function rather than being involved in the human melanoma development and progression. Earlier researches have illustrated LASP1 participation in

various physiological activities in different cells, for instance, gastric parietal cells HCl secretion (Chew, Chen et al. 2008) and kidney ductal cell function (Chew, Parente et al. 2000).

The most striking and interesting fact is the very high LASP1 expression in melanocytes – both, in stratum basale of normal skin (Figure 9 B) and in melanocytic nevi (Figure 11) assuming a novel role of LASP1 protein in melanocyte function.

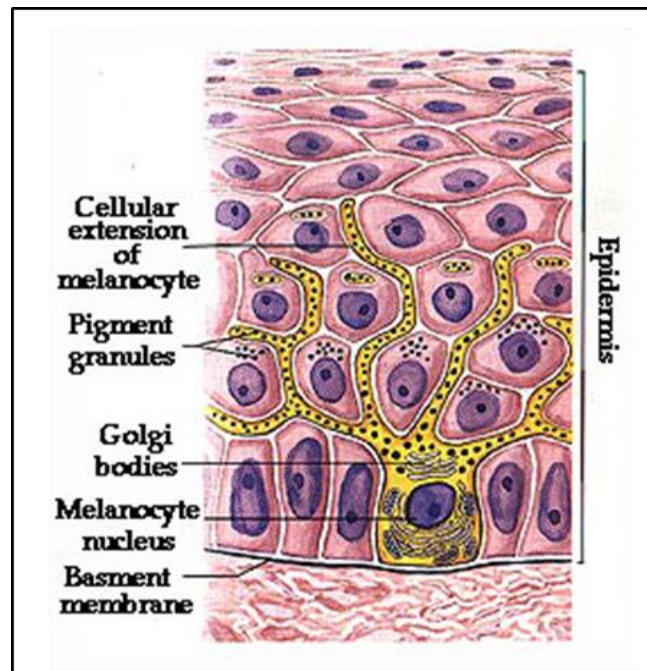


Figure 35: Illustrated the epidermal melanin unit of skin. Melanocyte reside between the basal layer cells and through dendritic processes communicates with about 30–40 keratinocytes in the epidermal melanin unit. Melanocyte synthesizes melanin in melanosomes and delivered to keratinocytes to protect cells from UV radiation.

Source: <http://www.bloggang.com/mainblog.php?id=pupesosweet&month=19-02-2012&group=6&gblog=26>

The epidermal melanin unit of skin consists of a minority population of melanocytes and a majority of keratinocytes in proportion to 1:~40 (Hume and Seabra 2011) – as it is represented in Figure 35. The melanocytes and keratinocytes function in a symbiotic manner – melanocytes synthesize the coloring pigment melanin in specific organelles, termed melanosomes, and release these into the extracellular matrix where keratinocytes phagocytose these organelles, thereby forming a melanin nuclear cap and protecting the cells from UV irradiation [reviewed in (Cichorek, Wachulska et al. 2013)].

The principal function of melanocytes is the production of the coloring pigment melanin, thence the existence of LASP1 in melanocytes, strongly suggests an involvement of this protein in melanogenesis pathway comprising of melanosome formation at the Golgi

complex around the nucleus [reviewed in (Sitaram and Marks 2012)], maturation of the organelle, followed by melanin synthesis and deposition [reviewed in (Cichorek, Wachulska et al. 2013)], and finally transport of the melanosome organelle towards the dendrite tips of melanocytes and melanosome vesicle release at the plasma membrane (Hume and Seabra 2011).

An elevated intracellular melanin level (10%) in LASP1 depleted cells despite an unaltered expression of the two melanogenesis regulator proteins tyrosinase and TRP1, suggests a partial hindrance in melanin release. Prior studies have proven that LASP1 can bind to various melanosome trafficking proteins e.g. F-Actin (Chew, Chen et al. 2002; Watabe, Valencia et al. 2008) and dynamin (Chi, Valencia et al. 2006; Mihlan, Reiss et al. 2013). These facts put forward strong reasons to examine the subcellular distribution of LASP1 in melanocytes and to analyze protein contribution in the steps of melanogenesis.

Tyrosinase, a glycoprotein located in the melanosomal membrane, is defined as a melanosome specific marker as well as considered as the rate limiting enzyme for melanin synthesis [reviewed in (Raposo and Marks 2007; Park, Kosmadaki et al. 2009)]. Immunofluorescence images, illustrating LASP1 co-localization with tyrosinase at the dendrite tips of cells, confirmed the existence of LASP1 in the pigment producing vesicles, and especially in late melanosomes (Figure 20 & 28). Dynamin is a well-known protein involved in clathrin-mediated vesicle trafficking and in membrane fission [reviewed in (Praefcke and McMahon 2004; Faelber, Held et al. 2012; Morlot and Roux 2013)]. Additionally, LASP1 co-localization with dynamin along the melanocyte dendrites and at the cell tips (Figures 21 & 27), suggests a possible participation of LASP1 in late melanosome vesicle release at the plasma membrane. GST-pull-down studies confirmed the perceived co-localization of dynamin with LASP1 (Figure 23).

In 2006, *Chi et al.* characterized melanosome proteomics by liquid chromatography / mass spectrometry and listed ~1500 proteins, amongst them LASP1 and dynamin as putative proteins in melanosomes, albeit the data had not yet been validated by any method (Chi, Valencia et al. 2006). This is the first study confirming now the presence of LASP1 and dynamin in melanocytes and in melanosomes in *in vitro* experiments.

It has been demonstrated previously that melanosomes mature through four morphologically distinct stages I – IV. Melanosome isolation by sucrose density gradient and examination of the fractions by Western blot revealed the presence of LASP1 and dynamin in the 1.8 M sucrose fraction which comprises of late melanosomes in stage III

and IV (Figure 25). The detected band for dynamin in the early 1.0 M fraction explains its role in pre-melanosome (stage I) formation and is also supported by the IF images displaying dynamin staining around the nucleus (Figure 21). Moreover, co-localization of dynamin with tyrosinase further confirms its presence in perinuclear and peripheral melanosomes (Figure 29). Besides, dynamin is determined as a novel binding partner of LASP1 in melanocytes (Figure 23).

The major melanosomal proteins of tyrosinase gene family—tyrosinase and tyrosinase related proteins 1 and 2 (TRP1 and TRP2) get glycosylated at the trans-Golgi network and are then directed to the ellipsoidal pre-melanosomes to modulate tyrosinase activity [reviewed in (Ghanem and Fabrice 2011)]. Researches have evidenced that both proteins are predominately present at stage III and IV of melanosomes (Raposo and Marks 2007). Concordant with the previous reports, the immunoblot analysis in this study revealed the distinct presence of TRP1 in the initial fractions of the sucrose gradient and the presence of tyrosinase in almost all fractions (Kushimoto, Basrur et al. 2001). Besides, all proteins unveiled a second peak in the 1.8 M fraction of the sucrose gradient which corresponds to stage IV or late stage melanosome (Figure 25). The data delineated in Table 10 are in agreement with a previous publication (Kushimoto, Basrur et al. 2001) for organelle markers.

Piling up all evidences, the data firmly suggest that LASP1 is associated to the late stage melanosomes and is involved in melanosome vesicle release at the plasma membrane. Evident mechanisms by which melanocytes transfer melanin to keratinocytes is, thus far, unknown, but are explained in view of exocytosis processes in neuronal cells and cells of hematopoietic lineage which are analogues to melanocytes (Van Den Bossche, Naeyaert et al. 2006). LASP1 expression has been reported previously in neurons and has shown to concentrate at the synaptic terminals, where the release of neurotransmitters occurs (Phillips, Anderson et al. 2004). These data recommend a potential role of LASP1 in the complex release mechanisms taking place at the dendrite tips of the melanocyte cells.

A diagrammatic model based on the previously explained mechanisms (Orth and McNiven 2003; Anitei and Hoflack 2012) illustrates a possible involvement of LASP1 in the F-Actin – dynamin mediated vesicle fission processes at the melanocyte dendrite tips (Figure 36). In 1992, *Cerdan et al.* identified first time the release of melanin occurs in specific melanocytic vesicles (Cerdan, Redziniak et al. 1992). Later *Ando et al.* confirmed that melanosomes are shed in membrane bound pigment globules, containing multiple melanosome vesicles (Ando, Niki et al. 2011; Ando, Niki et al. 2012).

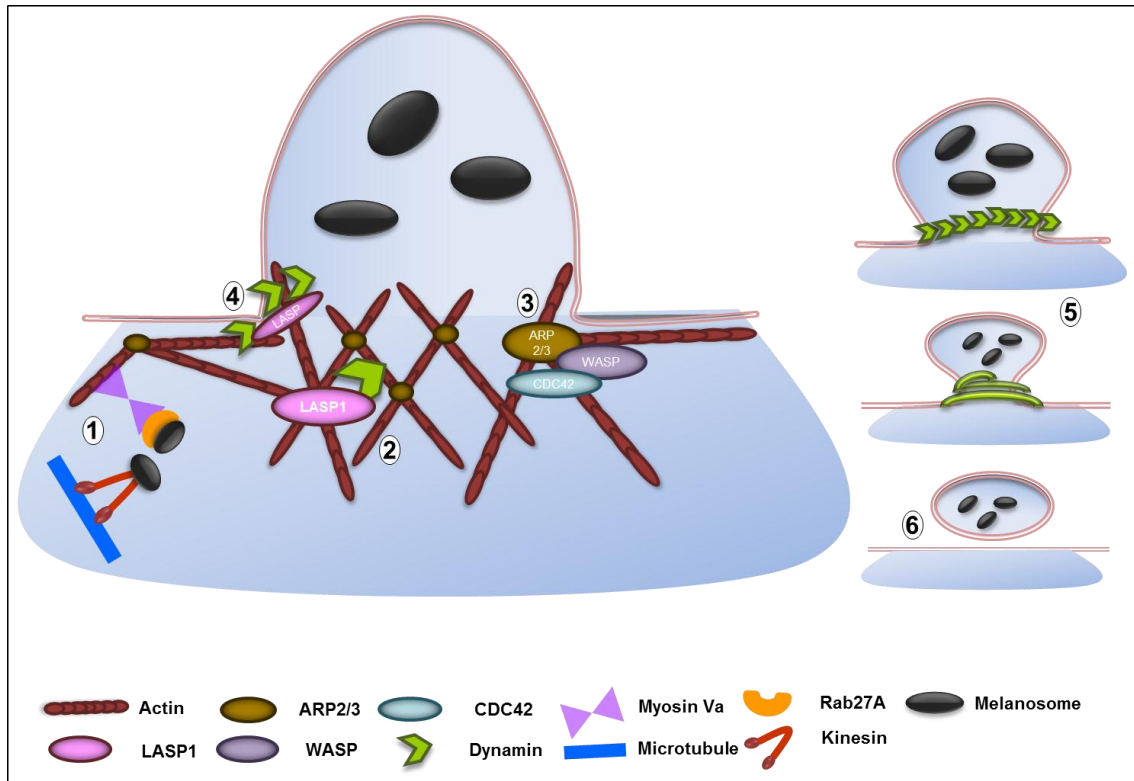


Figure 36: Proposed model for LASP1 involved actin – dynamin mediated melanosome vesicle scission at melanocyte dendrite tips. In anterograde melanosomal transport mature melanosomes move along microtubules by means of the motor protein kinesin and were transferred towards the cell periphery. Once at the periphery, track switching from microtubules to actin filaments occurs which is mediated by Rab27A and myosin Va, a molecular motor protein and thus the complex gets coupled to the actin (1). In this fashion microtubule, actin filaments and motor systems co-operate to promote melanosome transport and to retain the organelle in peripheral dendrites. LASP1 and dynamin are present at actin mesh at the plasma membrane. LASP1 binds to actin and dynamin through its nebulin repeat and SH3 domain, respectively. Dynamin exits as a dimer and binds to actin through the stalk region (2). WASP and CDC42 mediated activation of ARP2/3 lead to the branched polymerization of actin filaments towards the release site. Actin, together with other motor proteins, pushes the plasma membrane and enhances membrane invagination (3). As an adaptor/scaffolding protein, LASP1 recruits and positions dynamin at the tubular membrane (4). Subsequent polymerization of dynamin around the membrane in a helical manner together with GTP hydrolysis results in membrane constriction and melanosome vesicle scission at dendrite tips (5 and 6).

The stage IV mature melanosomes are transported towards the periphery of the melanocytes along microtubules by kinesin and then track switching from microtubules to the actin mesh occurs. Later, melanosome complexes get coupled to the actin filaments via Rab27A and myosin Va motor proteins and then get driven centrifugally to the scission sites at dendrite tips (Hume and Seabra 2011). A first step in vesicle budding is the induction of membrane curvature and membrane tubulation at scission site. F-Actin polymerization mediated by ARP2/3, N-WASP and CDC42, supports the

processes of curvature formation and tubulation of the site (Orth and McNiven 2003; Anitei and Hoflack 2012)

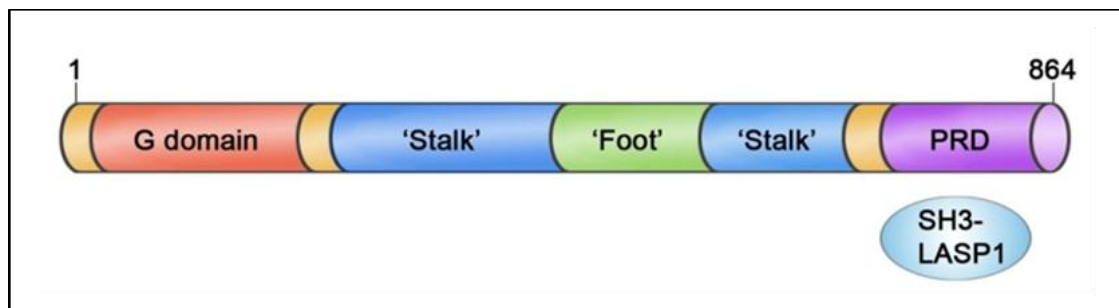


Figure 37: Representation of the domain organization of Dynamin. Linear representation of the dynamin structure as revealed by crystallographic studies (numbers indicate amino acid position within the primary sequence). The proline rich motif of dynamin (PRD) interacts with the SH3 – domain of LASP1.

Dynamin is a 100 kDa protein comprising of an amino-terminal G domain; a 'middle' or 'stalk' region; a pleckstrin homology domain (PH domain); a GTPase effector domain (GED) and a proline-rich carboxy-terminal region (Praefcke and McMahon 2004; Ferguson and De Camilli 2012; Morlot and Roux 2013). The domain structure of dynamin is illustrated in Figure 37, and it has been mentioned previously that the proline rich motif of dynamin interacts with the SH3 domain of LASP1 (Okamoto, Li et al. 2002). Dynamin has previously been characterized as a phosphoprotein in nerve terminals at the position of neurotransmitters release. Several researches demonstrated the involvement of dynamin in vesicle fission, both in endocytosis and in exocytosis. Dynamin functions by the oligomerization-dependent GTPase activation and also shows affinity to interact with lipid membranes (Praefcke and McMahon 2004).

The possible actin-dynamin mediated vesicle budding at the plasma membrane is comprised of a series of steps – attachment of the melanosome to the actin mesh, membrane curvature and tubulation via tension generated by actin polymerization, followed by dynamin positioning at the tubular membrane as well as dynamin mediated-membrane constriction and finally melanosome vesicle fission. The involvement of actin in the membrane curvature and the membrane constriction by dynamin have been mentioned in many studies (Orth and McNiven 2003; Heymann and Hinshaw 2009; Anitei and Hoflack 2012).

The model hypothesizes LASP1 being a scaffolding/adaptor protein, interacting with dynamin through the SH3 domain and later recruiting dynamin from the actin mesh to the tubular edges of the plasma membrane. Afterwards, dynamin binds via the PH domain to the phospholipids of the plasma membrane, and subsequent, GTPase

dependent oligomerization results in the formation of a helical ring around the tubular membrane. Eventually conformational changes in the dynamin oligomer leads to membrane constriction and ultimately results in vesicle fission [reviewed in (Praefcke and McMahon 2004; Faelber, Held et al. 2012; Ferguson and De Camilli 2012)]. The functioning of dynamin by GTP hydrolysis and membrane twisting of vesicle neck during vesicle scission has been demonstrated through live microscopy based assays and *in vitro* immunogold assay (Jakobsson, Ackermann et al. 2011; Faelber, Held et al. 2012).

As quoted before, participation of LASP1 in a similar mechanism has also been denoted in gastric parietal cells. A cAMP-dependent phosphorylation of LASP1 alters interaction with F-Actin and/or endocytic proteins and redistribution of LASP1 led to translocation of the protein to canalicular region. The authors also suggested the possibility that LASP1 can serve as a vehicle for translocation of transport associated proteins to different functional regions within cell (Chew, Parente et al. 2000; Okamoto, Li et al. 2002).

Though other factors may also assist for the action of dynamin, the present study illustrates that LASP1 and dynamin are newly identified proteins in melanosomes and that LASP1 is involved in the process of recruiting dynamin at the scission site for melanosome release.

Since melanocytes constitute a minority population in the stratum basale of epidermis, an efficient transfer of melanosomes (melanin laden) to keratinocytes is crucial in the process of skin photoprotection. Numerous researches exemplified defects in melanosome transfer that lead to multifarious disorders. Therefore, understanding the nature of this process has great importance in clinical implications. The proposed model is likely to be helpful to enlighten two newly identified partners in the mechanism of melanosome vesicle release and might have some hints for the underway researches.

References

- Abdel-Naser, M. B., K. Krasagakis, et al. (2003). "Direct effects on proliferation, antigen expression and melanin synthesis of cultured normal human melanocytes in response to UVB and UVA light." Photodermatology, photoimmunology & photomedicine **19**(3): 122-127.
- Ando, H., Y. Niki, et al. (2012). "Melanosomes are transferred from melanocytes to keratinocytes through the processes of packaging, release, uptake, and dispersion." The Journal of investigative dermatology **132**(4): 1222-1229.
- Ando, H., Y. Niki, et al. (2011). "Involvement of pigment globules containing multiple melanosomes in the transfer of melanosomes from melanocytes to keratinocytes." Cellular logistics **1**(1): 12-20.
- Anitei, M. and B. Hoflack (2012). "Bridging membrane and cytoskeleton dynamics in the secretory and endocytic pathways." Nature cell biology **14**(1): 11-19.
- Basrur, V., F. Yang, et al. (2003). "Proteomic analysis of early melanosomes: identification of novel melanosomal proteins." Journal of proteome research **2**(1): 69-79.
- Bastian, B. C. (2014). "The molecular pathology of melanoma: an integrated taxonomy of melanocytic neoplasia." Annual review of pathology **9**: 239-271.
- Besaratinia, A. and S. Tommasi (2014). "Epigenetics of human melanoma: promises and challenges." Journal of molecular cell biology **6**(5): 356-367.
- Brito, F. C. and L. Kos (2008). "Timeline and distribution of melanocyte precursors in the mouse heart." Pigment cell & melanoma research **21**(4): 464-470.
- Bruder, J. M., Z. A. Pfeiffer, et al. (2012). "Melanosomal dynamics assessed with a live-cell fluorescent melanosomal marker." PloS one **7**(8): e43465.
- Busam, K. J. (2013). "Molecular pathology of melanocytic tumors." Seminars in diagnostic pathology **30**(4): 362-374.
- Butt, E., S. Gambaryan, et al. (2003). "Actin binding of human LIM and SH3 protein is regulated by cGMP- and cAMP-dependent protein kinase phosphorylation on serine 146." The Journal of biological chemistry **278**(18): 15601-15607.
- Byers, H. R., M. Yaar, et al. (2000). "Role of cytoplasmic dynein in melanosome transport in human melanocytes." The Journal of investigative dermatology **114**(5): 990-997.
- Cerdan, D., G. Redziniak, et al. (1992). "C32 human melanoma cell endogenous lectins: characterization and implication in vesicle-mediated melanin transfer to keratinocytes." Experimental cell research **203**(1): 164-173.
- Chew, C. S. and M. R. Brown (1987). "Histamine increases phosphorylation of 27- and 40-kDa parietal cell proteins." The American journal of physiology **253**(6 Pt 1): G823-829.

- Chew, C. S., X. Chen, et al. (2008). "Targeted disruption of the Lasp-1 gene is linked to increases in histamine-stimulated gastric HCl secretion." American journal of physiology. Gastrointestinal and liver physiology **295**(1): G37-G44.
- Chew, C. S., X. Chen, et al. (2002). "Lasp-1 binds to non-muscle F-actin in vitro and is localized within multiple sites of dynamic actin assembly in vivo." Journal of cell science **115**(Pt 24): 4787-4799.
- Chew, C. S., J. A. Parente, Jr., et al. (2000). "The LIM and SH3 domain-containing protein, lasp-1, may link the cAMP signaling pathway with dynamic membrane restructuring activities in ion transporting epithelia." Journal of cell science **113 (Pt 11)**: 2035-2045.
- Chi, A., J. C. Valencia, et al. (2006). "Proteomic and bioinformatic characterization of the biogenesis and function of melanosomes." Journal of proteome research **5**(11): 3135-3144.
- Cichorek, M., M. Wachulska, et al. (2013). "Skin melanocytes: biology and development." Postepy dermatologii i alergologii **30**(1): 30-41.
- Costin, G. E. and V. J. Hearing (2007). "Human skin pigmentation: melanocytes modulate skin color in response to stress." FASEB journal : official publication of the Federation of American Societies for Experimental Biology **21**(4): 976-994.
- d'Ischia, M., K. Wakamatsu, et al. (2013). "Melanins and melanogenesis: methods, standards, protocols." Pigment cell & melanoma research **26**(5): 616-633.
- Damsky, W. E., L. E. Rosenbaum, et al. (2010). "Decoding melanoma metastasis." Cancers **3**(1): 126-163.
- Eller, M. S., T. Maeda, et al. (1997). "Enhancement of DNA repair in human skin cells by thymidine dinucleotides: evidence for a p53-mediated mammalian SOS response." Proceedings of the National Academy of Sciences of the United States of America **94**(23): 12627-12632.
- Faelber, K., M. Held, et al. (2012). "Structural insights into dynamin-mediated membrane fission." Structure **20**(10): 1621-1628.
- Fecher, L. A., R. K. Amaravadi, et al. (2008). "The MAPK pathway in melanoma." Current opinion in oncology **20**(2): 183-189.
- Ferguson, S. M. and P. De Camilli (2012). "Dynamin, a membrane-remodelling GTPase." Nature reviews. Molecular cell biology **13**(2): 75-88.
- Fistarol, S. K. and P. H. Itin (2010). "Disorders of pigmentation." Journal der Deutschen Dermatologischen Gesellschaft = Journal of the German Society of Dermatology : JDDG **8**(3): 187-201; quiz 201-182.

- Frietsch, J. J., T. G. Grunewald, et al. (2010). "Nuclear localisation of LASP-1 correlates with poor long-term survival in female breast cancer." British journal of cancer **102**(11): 1645-1653.
- Frietsch, J. J., C. Kastner, et al. (2014). "LASP1 is a novel BCR-ABL substrate and a phosphorylation-dependent binding partner of CRKL in chronic myeloid leukemia." Oncotarget **5**(14): 5257-5271.
- Garcia-Borron, J. C., B. L. Sanchez-Laorden, et al. (2005). "Melanocortin-1 receptor structure and functional regulation." Pigment cell research / sponsored by the European Society for Pigment Cell Research and the International Pigment Cell Society **18**(6): 393-410.
- Gething, M. J. (1999). "Role and regulation of the ER chaperone BiP." Seminars in cell & developmental biology **10**(5): 465-472.
- Ghanem, G. and J. Fabrice (2011). "Tyrosinase related protein 1 (TYRP1/gp75) in human cutaneous melanoma." Molecular oncology **5**(2): 150-155.
- Goding, C. R. (2007). "Melanocytes: the new Black." The international journal of biochemistry & cell biology **39**(2): 275-279.
- Gonzalez-Mariscal, L., P. Bautista, et al. (2012). "ZO-2, a tight junction scaffold protein involved in the regulation of cell proliferation and apoptosis." Annals of the New York Academy of Sciences **1257**: 133-141.
- Gray, C. H., L. C. McGarry, et al. (2009). "Novel beta-propeller of the BTB-Kelch protein Krp1 provides a binding site for Lasp-1 that is necessary for pseudopodial extension." The Journal of biological chemistry **284**(44): 30498-30507.
- Grunewald, T. G. and E. Butt (2008). "The LIM and SH3 domain protein family: structural proteins or signal transducers or both?" Molecular cancer **7**: 31.
- Grunewald, T. G., U. Kammerer, et al. (2007). "Nuclear localization and cytosolic overexpression of LASP-1 correlates with tumor size and nodal-positivity of human breast carcinoma." BMC cancer **7**: 198.
- Grunewald, T. G., U. Kammerer, et al. (2006). "Silencing of LASP-1 influences zyxin localization, inhibits proliferation and reduces migration in breast cancer cells." Experimental cell research **312**(7): 974-982.
- Grunewald, T. G., U. Kammerer, et al. (2007). "Overexpression of LASP-1 mediates migration and proliferation of human ovarian cancer cells and influences zyxin localisation." British journal of cancer **96**(2): 296-305.
- Grunewald, T. G., S. M. Pasedag, et al. (2009). "Cell Adhesion and Transcriptional Activity - Defining the Role of the Novel Protooncogene LPP." Translational oncology **2**(3): 107-116.

- Hara, M., M. Yaar, et al. (2000). "Kinesin participates in melanosomal movement along melanocyte dendrites." The Journal of investigative dermatology **114**(3): 438-443.
- He, B., B. Yin, et al. (2013). "Overexpression of LASP1 is associated with proliferation, migration and invasion in esophageal squamous cell carcinoma." Oncology reports **29**(3): 1115-1123.
- Heymann, J. A. and J. E. Hinshaw (2009). "Dynamins at a glance." Journal of cell science **122**(Pt 19): 3427-3431.
- Homsji, J., M. Kashani-Sabet, et al. (2005). "Cutaneous melanoma: prognostic factors." Cancer control : journal of the Moffitt Cancer Center **12**(4): 223-229.
- Hu, D. N. (2008). "Methodology for evaluation of melanin content and production of pigment cells in vitro." Photochemistry and photobiology **84**(3): 645-649.
- Hume, A. N. and M. C. Seabra (2011). "Melanosomes on the move: a model to understand organelle dynamics." Biochemical Society transactions **39**(5): 1191-1196.
- Jakobsson, J., F. Ackermann, et al. (2011). "Regulation of synaptic vesicle budding and dynamin function by an EHD ATPase." The Journal of neuroscience : the official journal of the Society for Neuroscience **31**(39): 13972-13980.
- Jordens, I., W. Westbroek, et al. (2006). "Rab7 and Rab27a control two motor protein activities involved in melanosomal transport." Pigment cell research / sponsored by the European Society for Pigment Cell Research and the International Pigment Cell Society **19**(5): 412-423.
- Kadrmaz, J. L. and M. C. Beckerle (2004). "The LIM domain: from the cytoskeleton to the nucleus." Nature reviews. Molecular cell biology **5**(11): 920-931.
- Keicher, C., S. Gambaryan, et al. (2004). "Phosphorylation of mouse LASP-1 on threonine 156 by cAMP- and cGMP-dependent protein kinase." Biochemical and biophysical research communications **324**(1): 308-316.
- Krengel, S., A. Hauschild, et al. (2006). "Melanoma risk in congenital melanocytic naevi: a systematic review." The British journal of dermatology **155**(1): 1-8.
- Kushimoto, T., V. Basrur, et al. (2001). "A model for melanosome biogenesis based on the purification and analysis of early melanosomes." Proceedings of the National Academy of Sciences of the United States of America **98**(19): 10698-10703.
- Li, B., L. Zhuang, et al. (2004). "Zyxin interacts with the SH3 domains of the cytoskeletal proteins LIM-nebulette and Lasp-1." The Journal of biological chemistry **279**(19): 20401-20410.
- Lin, W. M., S. Luo, et al. (2015). "Outcome of patients with de novo versus nevus-associated melanoma." Journal of the American Academy of Dermatology **72**(1): 54-58.

- Lohmann, S. M., U. Walter, et al. (1980). "Identification of endogenous substrate proteins for cAMP-dependent protein kinase in bovine brain." The Journal of biological chemistry **255**(20): 9985-9992.
- Meyskens, F. L., Jr., P. J. Farmer, et al. (2004). "Etiologic pathogenesis of melanoma: a unifying hypothesis for the missing attributable risk." Clinical cancer research : an official journal of the American Association for Cancer Research **10**(8): 2581-2583.
- Mihlan, S., C. Reiss, et al. (2013). "Nuclear import of LASP-1 is regulated by phosphorylation and dynamic protein-protein interactions." Oncogene **32**(16): 2107-2113.
- Morlot, S. and A. Roux (2013). "Mechanics of dynamin-mediated membrane fission." Annual review of biophysics **42**: 629-649.
- Nishikawa, R., Y. Goto, et al. (2014). "Tumor-suppressive microRNA-218 inhibits cancer cell migration and invasion via targeting of LASP1 in prostate cancer." Cancer science **105**(7): 802-811.
- Okamoto, C. T., R. Li, et al. (2002). "Regulation of protein and vesicle trafficking at the apical membrane of epithelial cells." Journal of controlled release : official journal of the Controlled Release Society **78**(1-3): 35-41.
- Orth, J. D. and M. A. McNiven (2003). "Dynamin at the actin-membrane interface." Current opinion in cell biology **15**(1): 31-39.
- Orth, M. F., A. Cazes, et al. (2015). "An update on the LIM and SH3 domain protein 1 (LASP1): a versatile structural, signaling, and biomarker protein." Oncotarget **6**(1): 26-42.
- Park, H. Y., M. Kosmadaki, et al. (2009). "Cellular mechanisms regulating human melanogenesis." Cellular and molecular life sciences : CMLS **66**(9): 1493-1506.
- Phillips, G. R., T. R. Anderson, et al. (2004). "Actin-binding proteins in a postsynaptic preparation: Lasp-1 is a component of central nervous system synapses and dendritic spines." Journal of neuroscience research **78**(1): 38-48.
- Praefcke, G. J. and H. T. McMahon (2004). "The dynamin superfamily: universal membrane tubulation and fission molecules?" Nature reviews. Molecular cell biology **5**(2): 133-147.
- Prieto, V. G. and C. R. Shea (2011). "Immunohistochemistry of melanocytic proliferations." Archives of pathology & laboratory medicine **135**(7): 853-859.
- Rachlin, A. S. and C. A. Otey (2006). "Identification of palladin isoforms and characterization of an isoform-specific interaction between Lasp-1 and palladin." Journal of cell science **119**(Pt 6): 995-1004.

- Raman, D., J. Sai, et al. (2010). "LIM and SH3 protein-1 modulates CXCR2-mediated cell migration." *PloS one* **5**(4): e10050.
- Raposo, G. and M. S. Marks (2007). "Melanosomes--dark organelles enlighten endosomal membrane transport." *Nature reviews. Molecular cell biology* **8**(10): 786-797.
- Remmele, W. and H. E. Stegner (1987). "[Recommendation for uniform definition of an immunoreactive score (IRS) for immunohistochemical estrogen receptor detection (ER-ICA) in breast cancer tissue]." *Der Pathologe* **8**(3): 138-140.
- Schreiber, V., R. Masson, et al. (1998). "Chromosomal assignment and expression pattern of the murine Lasp-1 gene." *Gene* **207**(2): 171-175.
- Sheffield, M. V., H. Yee, et al. (2002). "Comparison of five antibodies as markers in the diagnosis of melanoma in cytologic preparations." *American journal of clinical pathology* **118**(6): 930-936.
- Shenenberger, D. W. (2012). "Cutaneous malignant melanoma: a primary care perspective." *American family physician* **85**(2): 161-168.
- Shimizu, F., M. Shiiba, et al. (2013). "Overexpression of LIM and SH3 Protein 1 leading to accelerated G2/M phase transition contributes to enhanced tumourigenesis in oral cancer." *PloS one* **8**(12): e83187.
- Sitaram, A. and M. S. Marks (2012). "Mechanisms of protein delivery to melanosomes in pigment cells." *Physiology* **27**(2): 85-99.
- Slominski, A., J. Wortsman, et al. (2001). "Malignant melanoma." *Archives of pathology & laboratory medicine* **125**(10): 1295-1306.
- Spence, H. J., L. McGarry, et al. (2006). "AP-1 differentially expressed proteins Krp1 and fibronectin cooperatively enhance Rho-ROCK-independent mesenchymal invasion by altering the function, localization, and activity of nondifferentially expressed proteins." *Molecular and cellular biology* **26**(4): 1480-1495.
- Steel, K. P. and C. Barkway (1989). "Another role for melanocytes: their importance for normal stria vascularis development in the mammalian inner ear." *Development* **107**(3): 453-463.
- Stolting, M., C. Wiesner, et al. (2012). "Lasp-1 regulates podosome function." *PloS one* **7**(4): e35340.
- Tachibana, M. (1999). "Sound needs sound melanocytes to be heard." *Pigment cell research / sponsored by the European Society for Pigment Cell Research and the International Pigment Cell Society* **12**(6): 344-354.
- Takeshita, N., M. Mori, et al. (2012). "miR-203 inhibits the migration and invasion of esophageal squamous cell carcinoma by regulating LASP1." *International journal of oncology* **41**(5): 1653-1661.

- Tang, R., F. Kong, et al. (2012). "Role of hepatitis B virus X protein in regulating LIM and SH3 protein 1 (LASP-1) expression to mediate proliferation and migration of hepatoma cells." Virology journal **9**: 163.
- Thompson, J. F., R. A. Scolyer, et al. (2005). "Cutaneous melanoma." Lancet **365**(9460): 687-701.
- Tomasetto, C., C. Moog-Lutz, et al. (1995). "Lasp-1 (MLN 50) defines a new LIM protein subfamily characterized by the association of LIM and SH3 domains." FEBS letters **373**(3): 245-249.
- Traenka, C., M. Remke, et al. (2010). "Role of LIM and SH3 protein 1 (LASP1) in the metastatic dissemination of medulloblastoma." Cancer research **70**(20): 8003-8014.
- Tronnier, M. and C. Mitteldorf (2014). "Treating advanced melanoma: current insights and opportunities." Cancer management and research **6**: 349-356.
- Tsao, H., L. Chin, et al. (2012). "Melanoma: from mutations to medicine." Genes & development **26**(11): 1131-1155.
- Van Den Bossche, K., J. M. Naeyaert, et al. (2006). "The quest for the mechanism of melanin transfer." Traffic **7**(7): 769-778.
- Van Engen-van Grunsven, A. C., H. Kusters-Vandeveld, et al. (2014). "Update on Molecular Pathology of Cutaneous Melanocytic Lesions: What is New in Diagnosis and Molecular Testing for Treatment?" Front Med **1**(39).
- Vance, K. W. and C. R. Goding (2004). "The transcription network regulating melanocyte development and melanoma." Pigment cell research / sponsored by the European Society for Pigment Cell Research and the International Pigment Cell Society **17**(4): 318-325.
- Videira, I. F., D. F. Moura, et al. (2013). "Mechanisms regulating melanogenesis." Anais brasileiros de dermatologia **88**(1): 76-83.
- Wang, B., P. Feng, et al. (2009). "LIM and SH3 protein 1 (Lasp1) is a novel p53 transcriptional target involved in hepatocellular carcinoma." Journal of hepatology **50**(3): 528-537.
- Wang, C., X. Zheng, et al. (2012). "MicroRNA-203 suppresses cell proliferation and migration by targeting BIRC5 and LASP1 in human triple-negative breast cancer cells." Journal of experimental & clinical cancer research : CR **31**: 58.
- Wang, H., H. An, et al. (2013). "miR-133a represses tumour growth and metastasis in colorectal cancer by targeting LIM and SH3 protein 1 and inhibiting the MAPK pathway." European journal of cancer **49**(18): 3924-3935.

- Wang, H., W. Li, et al. (2013). "LIM and SH3 protein 1, a promoter of cell proliferation and migration, is a novel independent prognostic indicator in hepatocellular carcinoma." European journal of cancer **49**(4): 974-983.
- Wang, L., X. Li, et al. (2014). "Downregulation of miR-133 via MAPK/ERK signaling pathway involved in nicotine-induced cardiomyocyte apoptosis." Naunyn-Schmiedeberg's archives of pharmacology **387**(2): 197-206.
- Watabe, H., T. Kushimoto, et al. (2005). "Isolation of melanosomes." Current protocols in cell biology / editorial board, Juan S. Bonifacino ... [et al.] **Chapter 3**: Unit 3 14.
- Watabe, H., J. C. Valencia, et al. (2008). "Involvement of dynein and spectrin with early melanosome transport and melanosomal protein trafficking." The Journal of investigative dermatology **128**(1): 162-174.
- Wu, X. and J. A. Hammer (2014). "Melanosome transfer: it is best to give and receive." Current opinion in cell biology **29**: 1-7.
- Yajima, I., M. Y. Kumasaka, et al. (2012). "RAS/RAF/MEK/ERK and PI3K/PTEN/AKT Signaling in Malignant Melanoma Progression and Therapy." Dermatology research and practice **2012**: 354191.
- Yamaguchi, Y. and V. J. Hearing (2006). Melanocyte Distribution and Function in Human Skin.
- Yang, F., X. Zhou, et al. (2014). "LIM and SH3 domain protein 1 (LASP-1) overexpression was associated with aggressive phenotype and poor prognosis in clear cell renal cell cancer." PloS one **9**(6): e100557.
- Zalaudek, I., M. Manzo, et al. (2009). "The morphologic universe of melanocytic nevi." Seminars in cutaneous medicine and surgery **28**(3): 149-156.
- Zhang, H., X. Chen, et al. (2009). "Lasp1 gene disruption is linked to enhanced cell migration and tumor formation." Physiological genomics **38**(3): 372-385.
- Zhao, L., H. Wang, et al. (2010). "Promotion of colorectal cancer growth and metastasis by the LIM and SH3 domain protein 1." Gut **59**(9): 1226-1235.
- Zhao, T., H. Ren, et al. (2015). "LASP1 is a HIF1alpha target gene critical for metastasis of pancreatic cancer." Cancer research **75**(1): 111-119.
- Zheng, J., S. Yu, et al. (2014). "LASP-1 promotes tumor proliferation and metastasis and is an independent unfavorable prognostic factor in gastric cancer." Journal of cancer research and clinical oncology **140**(11): 1891-1899.

Annexure**List of Units**

Symbols	Units
A	Ampere
~	Approximate
°C	Degree Celsius
DC	Direct current
g	Gram
hr	Hour
kDa	Kilodalton
l	Liter
μl	Microliter
μm	Micrometer
μM	Micromolar
mg	Milligram
ml	Milliliter
mM	Millimolar
min	Minute
M	Molar
nm	Nanometer
OD	Optical density
%	Percentage
<i>g</i>	Relative centrifugal force
sec	Second
V	Voltage

Publication and Posters

- **Anjana Vaman VS**, Heiko Poppe, Roland Houben, Thomas G. P. Grunewald, Matthias Goebeler and Elke Butt. LASP1, a newly identified melanocytic protein with a possible role in melanin release, but not in melanoma progression. PLoS One. (Accepted).
- **Anjana Vaman V S**, Heiko Poppe, Roland Houben, Matthias Goebeler and Elke Butt. "LASP-1 in melanoma – no tumor marker but melanin regulator". Poster presented at 2nd International Symposium (Trends in Melanoma Research), Regensburg, Germany, 2014.
- **Anjana Vaman V S**, Heiko Poppe and Elke Butt. "Role of LASP-1 in melanoma". Poster presented at 9th International GSLS symposium (Eureka), Würzburg, Germany, 2014.
- **Anjana Vaman V S**, Sandra Vorlova, Susanne Kneitz, Sabine Gätzner and Elke Butt. "Regulatory function of LASP-1 in the nucleus of cells". Poster presented at 8th International GSLS symposium (Scientific crosstalk), Würzburg, Germany, 2013.
- **Anjana Vaman V S**, Sandra Vorlova and Elke Butt. "Role of LASP 1 in the nucleus of breast cancer cells". Poster presented at 7th International GSLS symposium (Scientific crosstalk), Würzburg, Germany, 2012

Funding Agency

- Minister of Social Justice and Empowerment. Government of India.

Curriculum Vitae

List of Publications_

- LASP1, a newly identified melanocytic protein with a possible role in melanin release, but not in melanoma progression. **Anjana Vaman VS**, Heiko Poppe, Roland Houben, Thomas GP Grunewald, Mathias Goebeler and Elke Butt. – Journal: Plos One – Accepted.
- Effect of fibrin glue on antioxidant defense mechanism, oxidative DNA damage and chromosomal aberrations. Toxicology mechanisms and methods, 23(7):500–8. (2013). **VS Anjana Vaman**, SK Tinu, CS Geetha, KK Lissy and PV. Mohanan.
- Effect of Hydroxyapatite Coated Bioactive Glass and Ethyl Vinyl Acetate on Antioxidant Defense Mechanism, Oxidative DNA Damage and Chromosomal Anomalies, Trends Biomater. Artif. Organs, 26(2), 64–73. (2012). **Anjana Vaman VS**, Tinu SK, Geetha CS, Mohanan PV.
- Assessment of micronuclei and chromosomal anomalies of five biocompatible materials in mice. Toxicological & Environmental Chemistry Volume 94, Issue 6. (2012). **V.S. Anjana Vaman**, S.K. Tinu, C.S. Geetha & P.V. Mohanan.
- Analysis of mitochondrial DNA damage using 8–hydroxy 2’deoxyguanosine on in vitro and in vivo exposure of biomaterials. Toxicology Mechanisms and Methods, UTXM–2012–0106. (2012). Tinu SK, **Anjana Vaman VS**, Geetha CS, Mohanan, PV.
- Effect of latex material on antioxidant enzymes, lipid peroxidation, DNA damage, and chromosomal aberration. Toxicological & Environmental Chemistry, 01/2012; DOI: 10.1080/02772248.2012.655990. S. K. Tinu, **V. S. Anjana Vaman**, M. Arun, C. S. Geetha, P. V. Mohanan.

Research Experiences_

Ph. D Researcher

Project: LASP1, a newly identified melanocytic protein with a possible role in melanin release, but not in melanoma progression.

Junior Research Fellow

Project: Evaluation of molecular toxicity of newly developed materials intended for biomedical applications.

Institute: Department of Toxicology, Sree Chitra Tirunal Institute of Science and Technology (a Cofrac Accredited laboratory), Biomedical Wing, Trivandrum, India.

Period: 29th December 2010 – 30th November 2011

Junior Research Fellow

Project: DNA Barcoding of Plants

Institute: Biotechnology and Bioinformatics Division, Tropical Botanic Garden and Research Institute, Trivandrum, India.

Period: 3rd December 2008 – 30th November 2009

Technical Expertise_

Animal cell culture and transfection experiments, Cell based assays – proliferation, adhesion, migration, Protein expression, Pull-down assay, Immunoprecipitation methods, Western blotting, Immunofluorescence, Nucleic acid isolation from cell lines and plant cells, Polymerase Chain Reactions, Electrophoresis (PAGE and AGE), Chromatography Thin Layer and Paper chromatography, Biochemical assays, and microscopic techniques.

Honors/Awards/Scholarship

- Qualified National Overseas Scholarship given by Ministry of Social Justice and Empowerment, Government of India (2011).
- Qualified Graduate aptitude Test in Engineering conducted jointly by the Indian Institute of Science and seven Indian Institutes of Technology on behalf of the National Coordination Board – GATE, Department of Higher Education, Ministry of Human Resource Development (MHRD), Government of India (2010).
- Qualified National Eligibility Test for Lectureship conducted jointly by Council of Scientific Research and Industrial Research and University Grant Commission, Government of India (2008).
- 3rd rank in M. Sc. Biotechnology, University of Kerala (2008).

Projects and training

- A three month project entitled “Therapeutic intervention of the cell cycle machinery of cervical cancer cells by a selective serotonin reuptake inhibitor” at the Department of Molecular Medicine, Rajiv Gandhi Centre for Biotechnology, Kerala as a part of post-graduation.
- A six month project entitled “Invitropropagation of *Datura fastuosa*, its detailed study based on biochemical, antifungal and antibacterial activities followed by the use of animal model to analyze , its effect on intestinal motility” at the Department of Ethanomedicine and Ethanopharmacology, Tropical Botanic Garden and

Research Institute, and Department of Biotechnology, Government College, Kariavattom as a part of under graduation.

- Undergone a training program on “Analysis of packaged drinking water” at the Cashew Export and Promotion Council of India, Kerala as a part of under graduation.

Conferences_

- Trends in Melanoma Research. 2nd International Symposium, Regensburg, Germany, 2014.
- Eureka, 9th International GSLS symposium, Würzburg, Germany, 2014.
- 8th International GSLS symposium (Scientific crosstalk), Würzburg, Germany, 2013.
- Scientific crosstalk, 7th International GSLS symposium, Würzburg, Germany, 2012
- National Symposium on Biotechnology of 21st Century on February 2nd & 3rd 2006, by Department of Biotechnology, Fatima Matha College and KSCSTE.
- Member of organizing committee and attended a State Level Seminar on Biotechnology, “BIOQUEST KERALA 2003” on 21st October 2003, by Lifetech – A Bioscience Association of Department of Biotechnology Kariavattom Government College.
- Member of organizing committee and attended a State Level Seminar on Biotechnology, “BIOQUEST KERALA 2004” on 21st October 2004, by Lifetech – A Bioscience Association of Department of Biotechnology, Kariavattom Government College.
- Member of organizing committee and attended a State Level Seminar on Biotechnology, “BIOQUEST KERALA 2006” on 16th October 2006, by Lifetech – A Bioscience Association of Department of Biotechnology, Kariavattom Government College.

References_

Prof. Dr. rer. nat. Elke Butt

Universitätsklinikum Würzburg
Institut für Klinische Biochemie,
Grombühlstrasse. 12, 97080 Würzburg
Tel.: 0049-931-31-83174, FAX: 0049-931-3293630
Email: butt@klin-biochem.uni-wuerzburg.de

Dr. P. V. Mohanan

Scientist E, Toxicology Division,
Sree Chitra Tirunal Institute of Science and Technology,
Kerala, India.
Tel.: 0091-9446542702
Email: mohanpv10@gmail.com

Declaration

I hereby declare that the above provided informations are true to the best of my knowledge.

ANJANA VAMAN V. S.

Würzburg, Germany